Characterization of $MgCl_2$-supported Catalyst and Initial Kinetics Determination in Low-pressure Propene Polymerization

Miroslav Skoumal

Promotion Committee:

Prof. Dr. –Ing. habil. G. Weickert	University of Twente, The Netherlands
Dr. I. Cejpek	Polymer Institute Brno, Czech Republic
Prof. Dr. L. Böhm	University of Aachen, Germany
Prof. Dr. rer. nat. K.-H. Reichert	Technical University Berlin, Germany
Prof. dr. ir. W.P.M. van Swaaij	University of Twente, The Netherlands
Prof. dr. ir. J.G.E. Gardeniers	University of Twente, The Netherlands

The research presented in this work was performed at the Polymer Institute Brno spol. s r. o., Czech Republic (slurry polymerizations) and the Polymer Reactor Technology GmbH, Germany (gas-phase polymerization in fixed-bed reactor). The gas-phase reactor has been financially supported by the Dutch Polymer Institute. The catalyst used in this study was provided by the BASF Catalysts LLC, TX USA.

Ph.D. Thesis, University of Twente, Enschede 2007
ISBN 978-90-365-2522-0

CHARACTERIZATION OF $MgCl_2$-SUPPORTED CATALYST AND INITIAL KINETICS DETERMINATION IN LOW-PRESSURE PROPENE POLYMERIZATION

DISSERTATION

to obtain
the doctor's degree at the University of Twente,
on the authority of the rector magnificus,
prof. dr. W.H.M. Zijm,
on account of the decision of the graduation committee,
to be publicly defended
on Friday July 6th 2007 at 15:00

by

Miroslav Skoumal
born on March 3rd 1980
in Brno, Czech Republic

This dissertation is approved by
the promoter
Prof. Dr. –Ing. habil. G. Weickert
and the assistant promoter
Dr. I. Cejpek

ABSTRACT

The scope of the presented research was focused on the 4th generation of $MgCl_2$--supported $TiCl_4$ catalyst behavior at low temperature (30 – 40℃) and pressure (1 atm) during propene polymerization in n-heptane slurry. The influence of triethylaluminium (TEA) cocatalyst, prepolymerization and propene concentration on the catalyst and polymer properties was investigated.

Special attention was devoted to the determination of the initial polymerization kinetics. For this purpose, a new technique for the determination of initial kinetic profile in the first seconds of polymerization was developed. It is based on the accurate timing of short polymerizations resulting from the immediate start of a reaction between the catalyst separated in oil phase and the remaining components of the system upon their being mixed together. Consequent complementation with the kinetic measurements based on monomer consumption allowed the exact determination of the catalyst behavior since the first seconds of polymerization up to one hour.

Furthermore the comparison of the catalyst behavior during the initial polymerization stage in the different environments of gas-phase and *n*-heptane slurry was investigated. The initial kinetic profile in the gas-phase was determined using the special fixed-bed reactor, allowing the fast change of the gas composition and precise control of the polymerization time.

Moreover, the polymer samples obtained from the short-time experiments were utilized for the determination of their molecular weight distribution by GPC/SEC analysis. Then the number of active sites and propagation rate coefficients could be evaluated from the dependence of the number of macromolecules on polymer yield. Furthermore the microstructure of the selected samples was analyzed by ^{13}C-NMR measurement.

On the basis of the presented results, a theory based on the TEA monomer-dimer equilibrium was postulated for the interpretation of the observed kinetic profiles at low TEA concentrations. Furthermore the GPC/SEC and ^{13}C-NMR analyses revealed that the TEA influences directly the nature of the active site, probably by forming bimetallic complexes.

In the last Chapter, the difference between the polymerizations carried out in gas-phase and *n*-heptane slurry at low temperature and pressure is discussed. The obtained data indicate the significant influence of the monomer concentration in the polymer layer surrounding the catalyst particles.

TABLE OF CONTENTS

ABSTRACT VII
TABLE OF CONTENTS VIII
1 INTRODUCTION 1
2 ZIEGLER-NATTA CATALYTIC SYSTEM 3
2.1 $MgCl_2$-supported Catalysts for α-Olefin Polymerization 3
2.1.1 Polymerization Kinetics with $MgCl_2$-supported Catalysts 3
2.1.1.1 Kinetic Models 6
2.1.2 The Role of Alkylaluminium 8
2.1.3 The Influence of Internal (ID) and External (ED) Donors 9
2.1.4 The Role of Hydrogen 11
2.2 Active site models 12
2.3 Mechanism of Polymerization 15
2.3.1 Monomer Coordination to Active Site 15
2.3.2 Proposed Models of Polymerization 17
2.4 Active Sites Determination 19
2.4.1 Selective Labeling of Macromolecules 19
2.4.1.1 Labeling of Macromolecules by Radioactive Organometals 19
2.4.1.2 Labeling of Growing Chains 19
2.4.1.2.1 The Number of Macromolecules (*N*) 19
2.4.1.2.2 The Number of Metal-Polymer Bonds (MPB) 21
2.4.1.2.3 Selective Tagging of Growing Chains 22
2.4.1.2.4 Combination of Quenching and Tagging Techniques 23
2.4.2 Consumption of Effective Catalyst Poisons 24
3 OUTLINE OF THESIS 25
4 EXPERIMENTAL PART 26
4.1 Slurry Polymerizations 26
4.1.1 Chemicals 26
4.1.2 Polymerization Apparatus 26
4.1.2.1 Polymerization Reactor 28
4.1.3 Polymerization Procedure 28
4.1.4 Polymer extraction and purification 30
4.1.5 *n*-Heptane/Propene Thermodynamic Equilibrium Determination 30
4.1.6 Polymerization Kinetics Assessed via Monomer Consumption 32
4.1.7 Mathematical Function for Kinetic Profiles Description 34
4.2 Gas-phase Polymerizations 36
4.2.1 Chemicals 36
4.2.2 Gas-phase Polymerization Apparatus 36
4.2.2.1 Fixed-bed Reactor for Gas-phase Polymerizations 37
4.2.3 Polymerization Procedure 37
4.3 GPC/SEC – Molecular Mass Distribution Determination 38
4.4 ^{13}C-NMR – Isotactic Pentad Distribution Determination 38
5 RESULTS AND DISCUSSION 39
5.1 Influence of Catalyst Amount, Al/Ti Molar Ratio and Initial TEA Concentration on Polymerization Activity in Slurry 39
5.2 Alkylaluminium Cocatalyst Influence on $MgCl_2$-supported $TiCl_4$ Catalyst 40

5.2.1 Impact of Initial TEA Concentration in Slurry on Net Polymerization Rate 40
5.2.2 Impact of Initial TEA Concentration on Polymerization Kinetics 44
5.2.3 Impact of Initial TEA Concentration in Slurry on Catalyst and Polymer Properties 56
5.2.4 Effect of Catalyst Prepolymerization in Slurry at Low TEA Concentration 67
5.2.5 Influence of Propene Concentration in Slurry and Gas-phase Experiments 76
6 CONCLUSIONS 87
7 REFERENCES 90
8 LIST OF SYMBOLS AND ABBREVIATIONS 95
ACKNOWLEDGEMENTS 97
ABOUT THE AUTHOR 98

1 INTRODUCTION

The discovery of Ziegler-Natta (ZN) catalysts in the 1950s is one of the most significant inventions of the 20th century. These new catalysts based on transition metal chlorides combined with alkylaluminium cocatalysts allowed the synthesis of new polymer materials with unique properties such as linear high-density polyethene (HDPE) and isotactic polypropene (i-PP). However the first commercially applied ZN catalysts, like $TiCl_3$/DEAC, exhibited low activities and poor stereospecificities with respect to i-PP production. Hence expensive purification procedures were required to remove corrosive catalyst residues and by-products, such as low molecular weight polymer and atactic PP.

Therefore, an enormous effort of the polyolefin industry was invested during the last four decades to enhance the catalyst activities and stereospecificities. The intensive research led to the development of $MgCl_2$-supported $TiCl_4$ catalysts with about 1000 times higher activity and almost precise control of polymer stereoregularity. The stereoregularities of PP produced by the latest 1,3-diether $MgCl_2$-supported $TiCl_4$ catalysts have achieved 99 % of isotactic pentad (*mmmm*) in the polymer [1].

During recent years, along with the continuous effort in the ZN catalysts development driven by the unflagging industrial interest in their application, also has come the development of single-site catalysts with very high stereospecificity, narrow molecular mass distribution and precise polymer particle morphology. However, such resulting new catalytic systems offering a wide range of new unique polymers such as elastomeric polypropene (ELPP), high melt strength PP (HMS-PP) or hybrid polyolefin/polar polymers [1,2] have to compete with traditional applicability, good polymer particles morphology and high catalyst efficiency of widely employed commercial ZN catalysts.

A common negative feature of the majority of industrial catalysts, including the newly developed single-site based systems is intensive release of heat at the initial stage of polymerization, caused by high initial activities. The reactions proceeding within a short period of time upon contacting the activated catalyst with monomer often determine the catalyst performance exhibited during the polymer production under industrial conditions. It is obvious that these phenomena could unfavorably influence the formation and stability of active sites and the consequent polymer particle morphology. That is why the industrial polymerization processes are often preceded by catalyst prepolymerization under mild conditions [3-5]. The complete understanding of the catalyst behavior in every moment of the polymerization process is essential for the perfect adjustment of operating conditions, allowing precise control of final polymer properties.

Many authors reviewed in [3-5] contributed to the investigation of the polymerization kinetics of ZN catalysts. However, the standard experimental technique for the kinetics assessment, based on the monomer consumption during polymerization, allowed the accurate kinetics determination only after reaching steady state conditions. On the other hand, propene polymerization kinetics data for high activity Ziegler-Natta $MgCl_2$-supported catalysts have been published for periods shorter than 1 s, based on a stopped-flow method [6].

Evaluation of the kinetic profile during the initial stage of polymerization has always been a difficult piece of laboratory art. Although nice examples of such technique have been developed recently by Weickert [7], Al-haj Ali [8] (both using the isoperibolic calorimetry) and Di Martino [9,10] (modified stopped-flow technique for industrial conditions).

It is generally assumed that the future direction of the ZN catalysts will lead to a more complete understanding of the catalyst behavior during polymerization. The intensive research dedicated to elucidation of the nature of the polymerization process motivates researchers to directly address the needs of polymer producers.

The original experimental procedure employing the Diffusion Interface Method [11] in *n*-heptane slurry was developed under the framework of the present thesis. It is based on utilization of diffusion limitations within the mineral oil/heptane interface. It allows low-conversion polymer yields to be determined from precisely defined short-time runs, ranging from 1 to 600 s, with relatively simple laboratory technique. The resulting reaction kinetic profiles are not dependent on material balance calculations, the polymer samples that are obtained can be utilized for assessing the number of active sites. Furthermore this method is suitable for the combination of the technique with the monomer consumption method, allowing the determination of complete kinetic profiles.

The utilizing of the gas-phase polymerizations in fixed bed reactor took advantage of direct comparison between slurry and gas-phase medium surrounding the proceeding polymerization. These characteristics include the method to the family of procedures suitable for the characterization of the initial stages of the polymer formation. Moreover, the fast changes in the gas phase content surrounding the polymerizing particles allow boundless possibility of sequential polymerizations at variable conditions.

2 ZIEGLER-NATTA CATALYTIC SYSTEM

2.1 $MgCl_2$-supported Catalysts for α-Olefin Polymerization

The application of $MgCl_2$ as a support for $TiCl_4$ molecules has a dual effect. The first and most obvious is as a more efficient dispersant of the active titanium atoms. With conventional $TiCl_3$-based catalysts, the interior titanium atoms are inaccessible to the cocatalyst and monomer. Hence, only a minor part of the amount of titanium is responsible for polymer production during polymerization, because the encapsulated titanium could not be transformed into the active propagative centers. For supported catalysts, all the titanium is on the surface and potentially active. The second effect is that the $MgCl_2$ significantly enhances the polymerization activity [4,5]. This phenomenon is discussed in detail in the section below. The important advantage of this high activity catalyst is the elimination of the need to remove titanium from the polymer.

Because of the inherent low stereospecificity for propylene polymerization, the use of $MgCl_2$-supported catalysts was initially limited only to polyethene synthesis. This disadvantage was overcome by the addition of an appropriate Lewis base. Therefore co-milling $MgCl_2$, $TiCl_4$ and a Lewis base, usually referred to as an “internal donor” (ID), produces highly active and stereospecific catalysts. The catalysts are further combined with triethylaluminium (TEA) as cocatalyst and a second Lewis base, usually called an “external donor” (ED) [4,5].

2.1.1 Polymerization Kinetics with $MgCl_2$-supported Catalysts

The heterogeneous nature of $MgCl_2$-supported catalysts and the presence of different types of active centers on its surface make it difficult to study the polymerization kinetics with these catalysts. Also the activity decay during the polymerization, influence of catalyst compounds and experimental conditions have an unfavorable impact on kinetic measurements. The typical kinetic profile of $MgCl_2$-supported catalyst exhibits a very fast activation period (active site formation) completed within 0.1 s [12-14]. A recent study performed by Mori et al. [15] indicated that the formation of active sites occurs within a very short period ~0.01 s by a reaction with cocatalyst.

Typically, after the fast activation, the $MgCl_2$-supported catalyst shows the characteristic high initial activities followed by a rapid deceleration in polymerization rate (Figure 1) [5,16].

Several contradictory theories were postulated to explain the high catalyst activity. One of them proposes that the high polymerization rate (activity) is caused by destabilizing the titanium-polymer bond by withdrawing an electron resulting in a higher propagation rate constant. On the other hand, some researchers assumed that the $MgCl_2$ electron donating effect on the more electronegative titanium stabilizes the coordination of the monomer, which results in an acceleration of the monomer insertion [3-5].

A wide range of plausible mechanisms have been proposed as a reason for the catalyst decay during polymerization. Some researchers assume that the rapid rate decrease could be caused by a physical phenomenon based on a monomer flux

diffusion limitation due to the encapsulation of the catalyst in the polymer layer [3,4,17,18].

On the contrary, Keii et al. [19] and Chien et al. [17,20] obtained results indicating that the monomer diffusion through the polymer is not responsible for the catalyst decay. They proposed the explanation based on the presumption that the deactivation occurs independently of the presence of a monomer, and is caused by the interaction of the catalyst with an alkylaluminium compound. This reduces Ti (III) to lower oxidation states, mainly Ti (II) [5,17,19]. The theory was promoted by Busico et al. [21], who reported that the Ti (II) and lower oxidation states were inactive in propene polymerization. The presented explanation of the activity deceleration is suitable for propene polymerization, but in the case of ethylene it was proven that the Ti (II) species were still active [19,21].

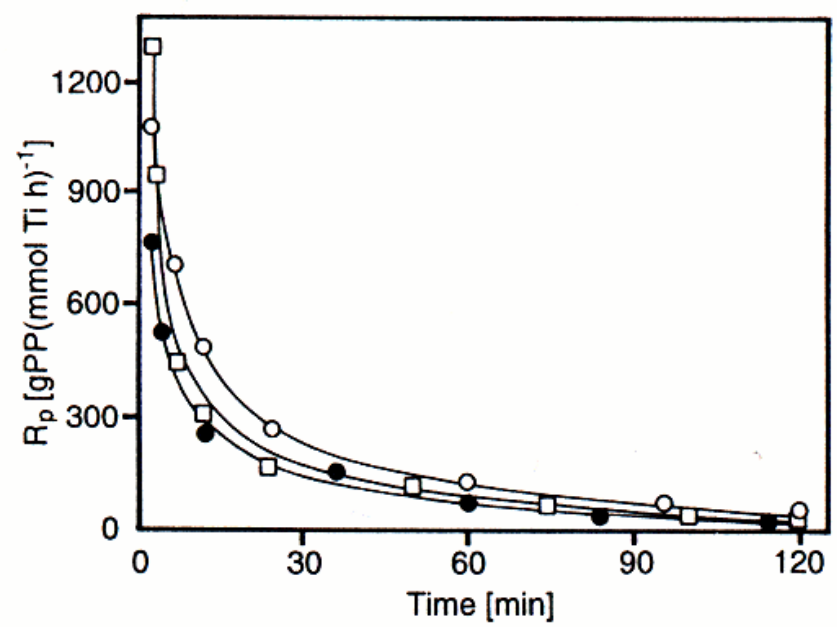

Figure 1: *Typical decelerating kinetic profiles of $MgCl_2$ (ball milled)/EB/$TiCl_4$-TEA catalytic system in propene polymerization expressed as a plot of polymerization rate R_p vs. time. Polym. conditions: temperature 60℃; pressure 1 atm; TEA/Ti molar ratio: ● = 176, ○ = 235 and □ = 588. Reproduced from* [16].

Some authors suggest that the main reason for the decrease of catalyst activity is the poisoning with ethylaluminium dichloride (EADC), which is the product of the interaction of catalyst with triethylaluminium (TEA) or diethylaluminium chloride (DEAC) [22,23]. Further Mori et al. [24] found that the catalyst activation and deactivation is related to the variation in the titanium species arising from various alkylaluminium compounds created during polymerization. The highly active cocatalyst leads to the high decay rate due to active site over-reduction at the beginning of polymerization. On the contrary, highly active cocatalyst showed a low decay rate at 30 min, suggesting that reductive active site precursors were almost absent.

A novel insight into the catalyst deactivation was presented by Lim and Choung [25]. They assumed that the catalyst deactivation was caused by a combination of chemical and physical phenomena, such as active sites reduction and monomer diffusion resistance.

Recently, Terano et al. [26,27] reported a plausible protective effect on the active sites by coordinating monomers and growing polymer chains. They suggest that the growing polymer chain, always present on the active center during the polymerization, prevents it from further reaction with TEA compound and thus protects it from deactivation. A similar guarding effect was observed with ethylaluminoxane cocatalyst by Wang et al. [28] indicating that the interaction between the bulkiness of the cocatalyst and the active site enhances its stability at high temperatures.

Kissin et al. [29-31] proposed a plausible explanation for the catalyst deactivation in the case of ethene polymerization. They assumed that the active Ti – C_2H_5 bond originated from the first monomer insertion after the β-elimination or transfer reaction with a monomer or hydrogen is in equilibrium with the stable form of the Ti – C_2H_5 species. The stability of the Ti – C_2H_5 bond is a result of a strong β-agostic interaction between the hydrogen atom of its methyl group and the Ti atom (Scheme 1). The propagation rate constant of this "dormant" site is very low.

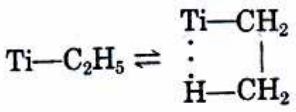

Scheme 1: *Schematic illustration of the equilibrium between active and dormant site stabilized by β-agostic interaction* [29-31].

The irregular (2,1)-monomer insertion into the growing chain is considered to be a main reason for the activity decay in propene polymerization [18]. It is generally accepted that (2,1)-inserted propene units slow down the chain propagation, due to the steric hindrance of the methyl group close to the Ti atom (Scheme 2) [32-34]. Busico et al. [33,34] determined that the $MgCl_2$-supported catalyst has ca. 10 – 30 % of all active sites at a given time in the "dormant" state. Then the dormant site can be reactivated by a transfer reaction with hydrogen [32-37]. The role of hydrogen will be further discussed in the section below.

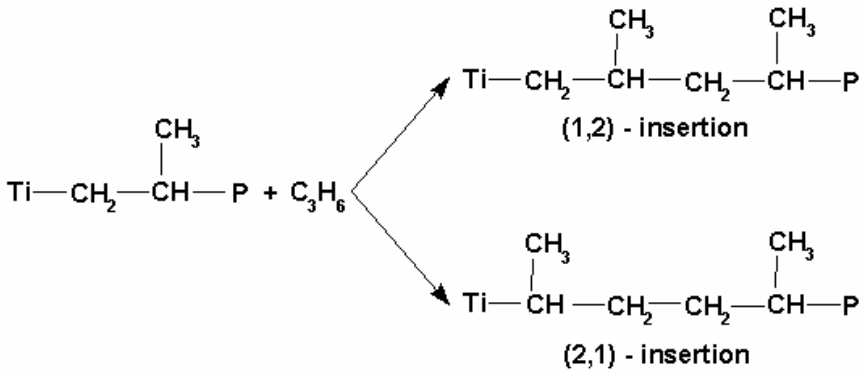

Scheme 2: *Regiorregular (1,2) and regioirregular (2,1) insertion of propene.*

Another explanation of a dormant site formation was proposed by Guyot et at. [38,39]. They found that the β-hydride elimination is very limited in a case of $MgCl_2$-supported $TiCl_4$ catalysts and suggest that the dormant site results from a monomer transfer reaction. This transfer reaction leads to a stable dormant π-allyl structure, and it is dominant mainly after a (2,1)-insertion.

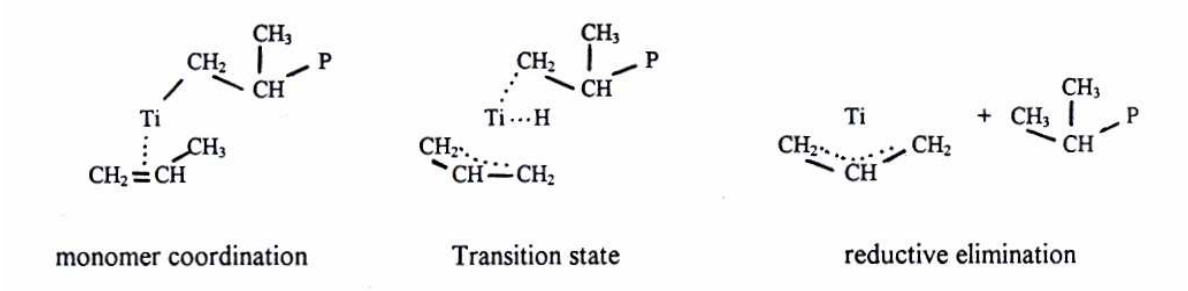

Scheme 3: *Proposed mechanism of dormant π-allyl site formation. Reproduced from* [39].

2.1.1.1 Kinetic Models

A wide range of studies were performed to evaluate the kinetic order and, consequently, the nature of polymerization activity deceleration [4,5,40]. For all that, the generally accepted kinetic model suitable for the ZN catalysts is still missing due to a wide complex of interconnected phenomena accompanying the polymerization process.

Several researchers conclude that the catalyst deactivation occurs as a second-order reaction [19,25,41]. Keii et al. [42] described the rate decay as a third-order at the beginning stage of the polymerization process, followed by a second-order deceleration and then approaches a first order.

Kissin [40] and some other authors [18,43-45] consider the first-order decay satisfactory for the characterization of kinetic curves. He proposed that the polymerization system contains two types of active sites: stable and highly unstable. Then the total amount of C* can be expressed [40]:

$$C^* = C_1^* + C_2^* \tag{1}$$

The concentration of the stable active sites C_2^* remains almost unchanged during the polymerization and corresponds to the stationary part of the kinetic curve. The unstable sites C_1^*, which undergo a quick deactivation, are responsible for the activity decay.

Assuming that the active sites deactivation rate depends only on the catalyst concentration, then the decrease in active sites C_i^* could be defined as a first-order reaction with a deactivation rate constant k_{di} [18,40,45]:

$$-\frac{dC_i^*}{dt} = k_{di} \cdot C_i^* \tag{2}$$

After integration, C_i^* at varying time t is given as:

$$C_i^*(t) = C_i^*(0) \cdot \exp(-k_{di} \cdot t) \tag{3}$$

where $C_i^*(0)$ is the initial concentration of the active sites.

Zakharov et al. [46] postulated that the overall polymerization rate R_p could be described by the following equation:

$$R_p = k_p \cdot [M] \cdot C^* \tag{4}$$

where [M] is monomer concentration and k_p propagation rate constant.

Then the combination of Eqs. (3) and (4) gives kinetic equation [18,40,45]:

$$R_p(t) = k_p \cdot [M] \cdot C_i^*(0) \cdot \exp(-k_{di} \cdot t) \quad (5)$$

The resulting equation can be also expressed:

$$R_p(t) = R_p(0) \cdot \exp(-k_{di} \cdot t) \quad (6)$$

where $R_p(t)$ and $R_p(0)$ are the polymerization rates at time t and $t = 0$, respectively.

Thus, the catalytic system with more types of active centers, deactivating with different rate constants, could be expressed as a sum of kinetic equations:

$$R_p(t) = \sum_{i=1}^{n} R_{pi}(0) \cdot \exp(-k_{di} \cdot t) \quad (7)$$

A wide range of experimental kinetic data can be described by the proposed equation. However, it shall also be assumed that such different active centers with different deactivation rates may also differ in propagation rate.

Some of the models use the Langmuir-Hinshelwood adsorption isotherms, assuming a competitive reversible adsorption reaction of monomer and alkylaluminium with the active sites [3-5]. The overall polymerization rate is given as:

$$R_p = k_p \cdot C^* \cdot \frac{K_M \cdot [M]}{1 + K_A \cdot [A] + K_M \cdot [M]} \quad (8)$$

where k_p represents the propagation rate constant, C* is the concentration of active sites, [M] and [A] are the equilibrium concentrations of monomer and alkylaluminium, K_M and K_A are the equilibrium adsorption constants for monomer and alkylaluminium.

Another kinetic model was proposed by Böhm [47]. He describes the polymerization process as a set of subsequent elementary reactions. The complexation reaction of the active site with monomer was considered as the determining step. Then R_p can be expressed:

$$R_p = \frac{k_{ads} \cdot k_p \cdot [M]}{k_p + k_{des}} \cdot \frac{C^*}{1 + (b/a) + (c/a)} \quad (9)$$

where k_{ads} and k_{des} are adsorption and desorption rate constants of the active center-monomer complex. The term 1/[1 + (b/c) + (c/a)] describes the various adsorption processes which may occur.

Al-Haj Ali [48,49] modeled the polymerization rate and the deactivation constant as a function of hydrogen concentration and polymerization temperature using the dormant site theory. His model is based on assumptions that all active sites have the same average rate constants, the chain transfer with cocatalyst is neglected and a quasi steady state is assumed for dormant sites. Thus the actual catalyst site concentration is the difference between the maximum concentration of active sites and the concentration of sites being in the dormant state.

2.1.2 The Role of Alkylaluminium

Summarized information about the role of alkylaluminium in α-olefin polymerization with ZN catalysts could be found in reviews [3-5].

A general feature of the Ti based ZN catalysts is their activation by alkylaluminium such as triethylaluminium (TEA) or tri-*i*-butylaluminium (TIBA). TEA is the most common. Terano et al. [6,50] have observed that the number of active sites decreased drastically with an increase in the bulkiness of the alkyl group of the aluminium compound. On the contrary, the k_p value of active sites produced by different trialkylaluminium were the same regardless of the alkyl group. Hence, they assumed that the basic composition of the active sites formed is essentially similar, only their amount varies with different alkylaluminiums.

It is generally accepted that the activation reaction proceeds in two steps. First, alkylaluminium reduces Ti (IV) to Ti (III). Then it alkylates the Ti (III) forming the first metal-polymer bond accessible for monomer insertion [4,5]. It was also proved that in the case of TEA, the reduction of titanium could proceed further to Ti (II) [4,5,17]. Keii et. at [19], Chien et al. [17,20] and Busico et at. [21] assumed that the reduction to the Ti (II) oxidation state by TEA is a main reason of the activity decay during propene polymerization.

Kohara et al. [51] performed an experimental study on the elimination and replacement of organometallic cocatalyst during propene polymerization. The results obtained suggested that the active centers in heterogeneous ZN catalyst are most likely bimetallic complexes composed of titanium ion and organometallic cocatalyst. Further Xu et al. [52] found stereoblock structures in low isotacticity PP fractions produced by the donor-free $TiCl_4/MgCl_2$/TEA catalyst system. They proposed the existence of an equilibrium between the monometallic and the bimetallic active sites in terms of reversible complexation with TEA.

A significant decrease in stereospecificity of the $MgCl_2$-supported catalyst containing standard internal donor (ethyl benzoate (EB), di-*i*-butyl phthalate (DIBP) etc.) was observed upon their reaction with TEA. This phenomenon was explained by extraction of a major part of the internal donor from the surface of catalyst by triethylaluminium [5,43,53-56,60,61]. Thus, the external donor, able to replace the extracted internal donor, must be added to the catalyst system to maintain the high stereospecificity [5,53,57,60]. A more detailed discussion about the role of internal and external donors in Ziegler-Natta catalysts appears in the following chapter.

The average molecular weight decreases with the increasing TEA concentration, so that triethylaluminium might be considered as an active transfer agent during polymerization [4]. Marques et al. [59] have proven that this presumption is valid only for the polymerizations carried out in the absence of hydrogen. In the presence of hydrogen no change in average molecular weight was observed for different TEA concentrations. Also the recent studies performed by Bukatov et al. [62] and Yaluma et al. [63] indicated that the rate of chain transfer to aluminum is at least an order of magnitude slower than the rate of chain transfer with monomer.

2.1.3 The Influence of Internal (ID) and External (ED) Donors

The role of Lewis bases (LB) in $MgCl_2$-supported catalysts for polypropene production has been revised in several articles [4,5,57,60]. The majority of experimental data supports the hypothesis that the influence of the internal donor on the catalyst stereospecificity is based mainly on the prevention of $TiCl_4$ coordination on the $MgCl_2$ crystal faces where mostly non-stereospecific active sites would be formed.

Experiments and calculations performed by Busico et al. [53,54] indicated that the (100) and (110) faces have different acidities (the latter is more acidic). So, the ID effect on stereospecificity of supported catalysts might be related to the ability of $TiCl_4$ to displace the internal base only from the more basic (100) face, where binuclear stereospecific sites can be formed (Scheme 4). Similar conclusions were reached by Bukatov and Zakharov [62] on the basis of the number of active sites and the propagation rate coefficient determination at the catalysts containing different electron donors. Further Wank et al. [64] found that the internal donor poisons the aspecific sites and also improves the propagation rate parameters of isospecific sites.

Another supposed ID influence on the catalyst stereospecificity is the ability to transform the low-isospecific sites into the isospecific ones by the formation of steric hindrances of the coordinated donor in the neighborhood of the active center [57,58]. However, this phenomenon may be suppressed by extraction reactions with cocatalyst. Experimental studies proved that the internal donor could be partly removed by alkylaluminium from the catalyst surface [5,43,53-56].

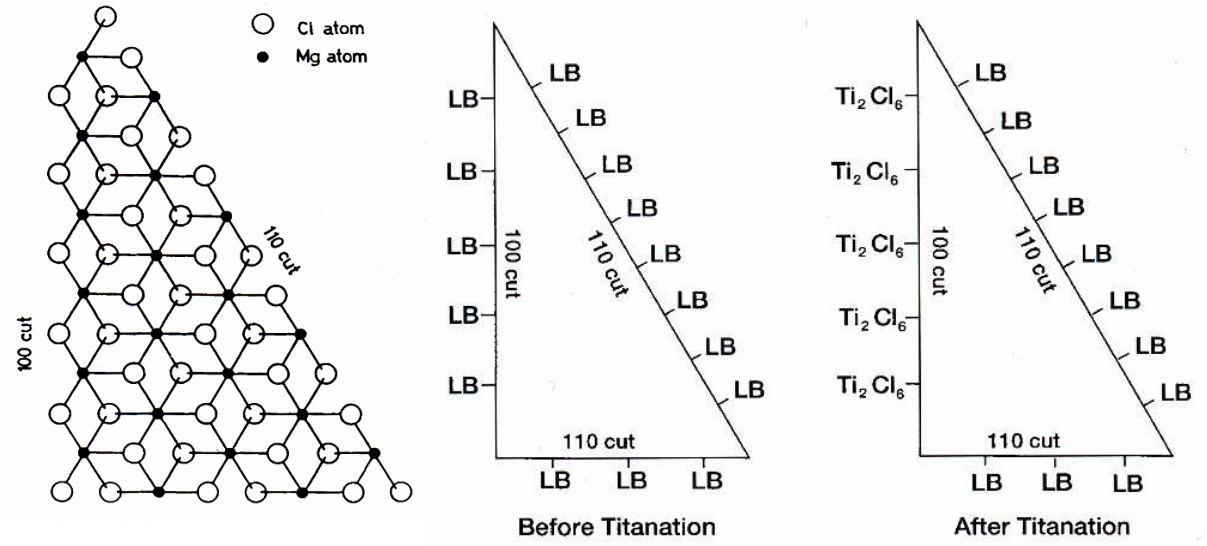

Scheme 4: *Model of $MgCl_2$ crystal layer and schematic drawing of the Lewis base (LB) and titanium distribution on the (100) and (110) crystal cuts. Reproduced from* [60].

As discussed above, the external donor must be added to the catalytic system as a part of cocatalyst to retain the stereospecificity of the active sites. Busico et al. [65] and Barbè et al. [66] suggested that ED acts through a combined poisoning of the non-stereospecific and promotion of the isospecific sites. Moreover Soga et al. [67] gave the experimental evidence that the aspecific sites could also be converted into the isospecific ones upon addition of the external donor. Consequently, other researchers [37,68] have also proven this finding.

Noristi et al. [61] performed the investigation of the interactions of $MgCl_2$-supported $TiCl_4$ catalyst with TEA for two different ID/ED systems (ethyl benzoate (EB)/methyl *p*-toluate (MPT) and di-*i*-butyl phthalate (DIBP)/triethoxy(phenyl)silane (TEPS)). They proposed the following reaction model based on acid-base interactions for the donor system EB/MPT:

$$\text{Cat-ID} + AlEt_3 \leftrightarrows AlEt_3\text{-ID} + \text{Cat-}\square$$

$$\text{Cat-}\square + AlEt_3 \leftrightarrows \text{Cat-}AlEt_3$$

$$AlEt_3 + \text{ED} \leftrightarrows AlEt_3\text{-ED}$$

$$\text{Cat-}\square + AlEt_3\text{-ED} \leftrightarrows \text{Cat-ED} + AlEt_3$$

In the case of the DIBP/TEPS donor system they suggest similar behavior, but with a peculiar feature concerning direct donor exchange:

$$\text{Cat-ID} + \text{ED} \leftrightarrows AlEt_3\text{-ED} + \text{ID}$$

They postulated that this feature is related to higher alkoxysilane basicity towards the $MgCl_2$ support than towards TEA. Xu et al. [52] suggest that the role of ED is believed to be twofold. The external donor should partially replace the extracted internal donor on the catalyst surface and/or complex with alkylaluminium to reduce its ability to remove the internal donor.

Further Terano et al. [6,69-71] presented that besides a decreased formation of aspecific active sites, the effect of adding an external donor is the occupation of one of the vacancies of some aspecific titanium species by coordination. Consequently, this sterically hindered aspecific site is transformed into an isospecific one with high, but not the highest isospecificity.

Bukatov et al. [62] indicated that the ID and ED absorbed on $MgCl_2$ near the active centers also affect the reactivity of these centers. They found that in the propene polymerization with stereospecific catalysts the value of k_p for stereospecific centers is higher than for non-stereospecific centers by one order of magnitude.

Recently, the 1,3-diethers were proposed as suitable electron donors for the heterogeneous $MgCl_2$-supported catalysts [57,60,72-74]. These donors have the main advantage that, when used as the internal donor, they are not extracted from the catalyst by alkylaluminium. So, there is no need to add the external donor. Diethers should also be applied as external donors in systems with internal donors extractable by alkylaluminium [57,60]. Furthermore Yaluma et al. [63] found that the high activity of diether-containing catalysts is due to an increased proportion of active centers rather than to a difference in propagation rate coefficients.

The internal donor structure determines the need for the specific external donor [5,18]. The suitable combinations of internal and external donors are shown in Table 1.

Table 1: *Suitable combinations of internal and external donors.*

Internal Donor	External Donor
Monoester (EB)	Monoester (EB, MPT)
Diester (DIBP)	Alkoxysilane (DIBDMS, CHMDMS)
1,3-Diether (DIPDMP, DCPDMP)	None

EB – ethyl benzoate; MPT – methyl *p*-toluate; DIBP – di-*i*-butyl phthalate;
DIBDMS – di-*i*-butyldimethoxysilane; CHMDMS – cyclohexylmethyldimethoxysilane;
DIPDMP – 2,2-*i*-propyl-1,3-dimethoxypropane;
DCPDMP – 2,2-dicyclopentyl-1,3-dimethoxypropane.

2.1.4 The Role of Hydrogen

Hydrogen is considered to be the most active transfer agent commonly used as a standard molecular weight modifier in commercial polyolefin production plants. Several researchers [37,75-77] demonstrated that the addition of hydrogen in propene polymerization caused a significant activity increase, but on the contrary, substantially reduces the activity in ethene polymerization.

It was proven that the hydrogen did not affect the propagation rate constant and did not lead to the formation of new active sites [77]. The experimental results indicate that the hydrogen activation effect in the propene polymerization corresponds to the regeneration of the dormant sites by the transfer reactions with hydrogen [32,35,37,77-81]. These inactive dormant sites originate from the irregular (2,1)-monomer insertions [32-34].

Kojoh et al. [82] applied ^{13}C-NMR for the detection of polymer chain ends in the PP produced with addition of H_2. It was demonstrated that the hydrogen addition leads not only to the conversion of the (2,1)-dormant sites into the active sites, but also to a decrease in the frequency of (2,1)-insertions.

Terano et al. [6,70,83], using the “stopped-flow” method, observed no effect of hydrogen in the initial stage of propene polymerization. Further studies showed that the chain transfer with H_2 occurs only with dissociated atomic hydrogen [6,84]. They applied $PdCl_2$ for enhancing the atomic hydrogen production by dissociation of H_2 molecules. Consequently, the atomic hydrogen induced a chain transfer in the initial stage of propene polymerization [6,85].

Kissin et al. [29-31] proposed a plausible explanation for the ethene polymerization activity decrease after the hydrogen introduction. He assumed that the Ti–C_2H_5 bond is unusually stable due to the strong β-agostic interaction between the hydrogen atom of the methyl group and the Ti atom. Such a formation is in equilibrium with Ti–C_2H_5 capable for ethene insertion (see Scheme 1). The introduction of hydrogen causes the more frequent generation of Ti–H bonds, leading to the formation of stabilized Ti–C_2H_5 bonds and, consequently, to a deceleration of polymerization.

Extensive investigation of the hydrogen effect on MWD was performed by Al-haj Ali [48,49] indicating that the dependence of average molecular weight on hydrogen could be described by the model based on dormant sites over the wide range of H_2 concentrations.

2.2 Active site models

It is generally known that the active site results from interaction of the solid catalyst with an organometallic (typically triethylaluminium) cocatalyst and that the forming of active center proceeds in two steps. Firstly, titanium is reduced to the lower oxidation state, followed by substitution of surface chloride by one of the cocatalyst alkyl groups [4,5].

In accordance with Cossee model of monometallic active center [86] (the octahedral complex Ti (III) located on a lateral face of $TiCl_3$ crystal) Kakugo et al. [87] proposed plausible model of isospecific and aspecific active sites. It is known that the β-$TiCl_3$ forms a linear structure, while the δ-$TiCl_3$ is coordinated in layers. The proposed model shows that the isospecific δ-$TiCl_3$ active site (model 1) consist of four firmly bound Cl atoms, an alkyl group and one vacancy. Model 2 with one loosely bonded Cl atom was attributed to the low isospecific center. And the active centers with two coordination vacancies represent the nonstereospecific sites (model 3). In the case of β-$TiCl_3$, the isospecific active site (model 4) consists of three firmly bonded Cl ions, a loosely bonded Cl, one vacancy and an alkyl group bound to a Ti atom.

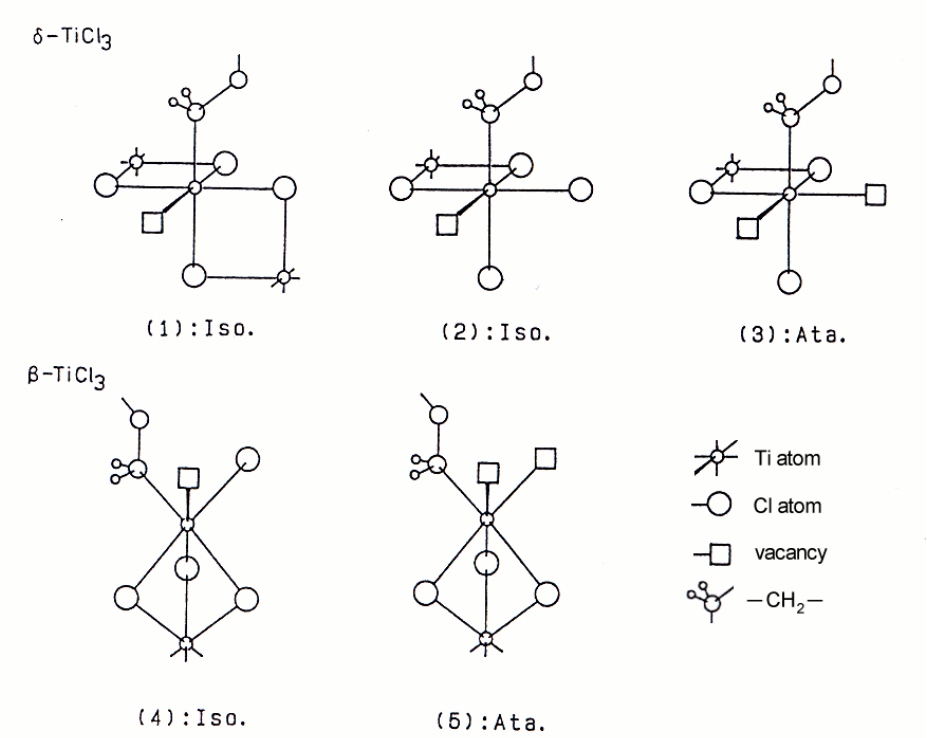

Scheme 5: *The active center models on $TiCl_3$ catalyst. Reproduced from* [87].

Busico et al. [88,89] and Härkönen et al. [90] fractionalized the polypropene samples with certain solvents for evaluating stereoregularity and analyzed them by high-resolution ^{13}C-NMR. The three-site model has been proposed, describing the heterogeneous Ziegler-Natta systems ($TiCl_3$-based or $MgCl_2$-supported) as a mixture of different classes of active centers producing polypropene structures with highly isotactic and poorly isotactic sequences.

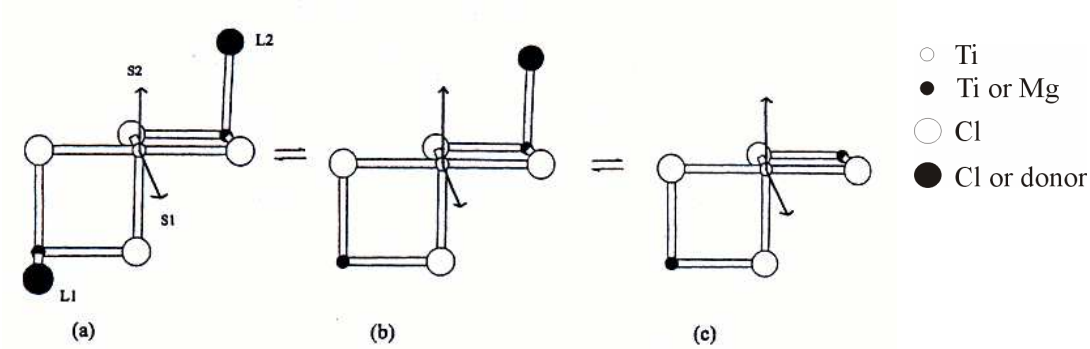

Scheme 6: *Possible models of active species for highly isotactic (a), poorly isotactic (b) and syndiotactic (c) propagation. Reproduced from* [88].

Busico et al. [88,89] postulated that the coordination position of two ligands (L1, L2) should be the most crucial in determining the stereospecificity of the active site. The ligand changing at the two coordination positions can result in reversible switches between the different types of stereocontrol. The resulting effects, such as an average content of stereoirregularities in polymer chains, can be related to the specific nature of ligands and in particular to the Lewis bases used as catalyst modifiers.

Recently, Terano et al. [58,91-93] applied the temperature rising elution fractionation (TREF) method to evaluate the distribution of the isotacticity of PP samples. Based on the results, they have concluded that there are four kinds of active sites with different stereospecificity, defined as aspecific sites (AS), poorly-isospecific sites (IS_1), the second highest isospecific sites (IS_2) and the highest isospecific sites (IS_3). They demonstrated that the introduction of a bulky alkyl group instead of chlorine atoms into the neighborhood of active sites is crucial for the generation of active sites with the highest isospecificity (IS_3). They also determined that the external donor could transform the aspecific site into an isospecific one with a high (IS_2), but not highest isospecifity [58,91-93]. According to the experimental results, Terano et al. [58,91,93,94] modified the three-site model, specifying the combined roles of catalytic titanium species, alkylaluminium cocatalyst, $MgCl_2$ support and external donor (Scheme 7).

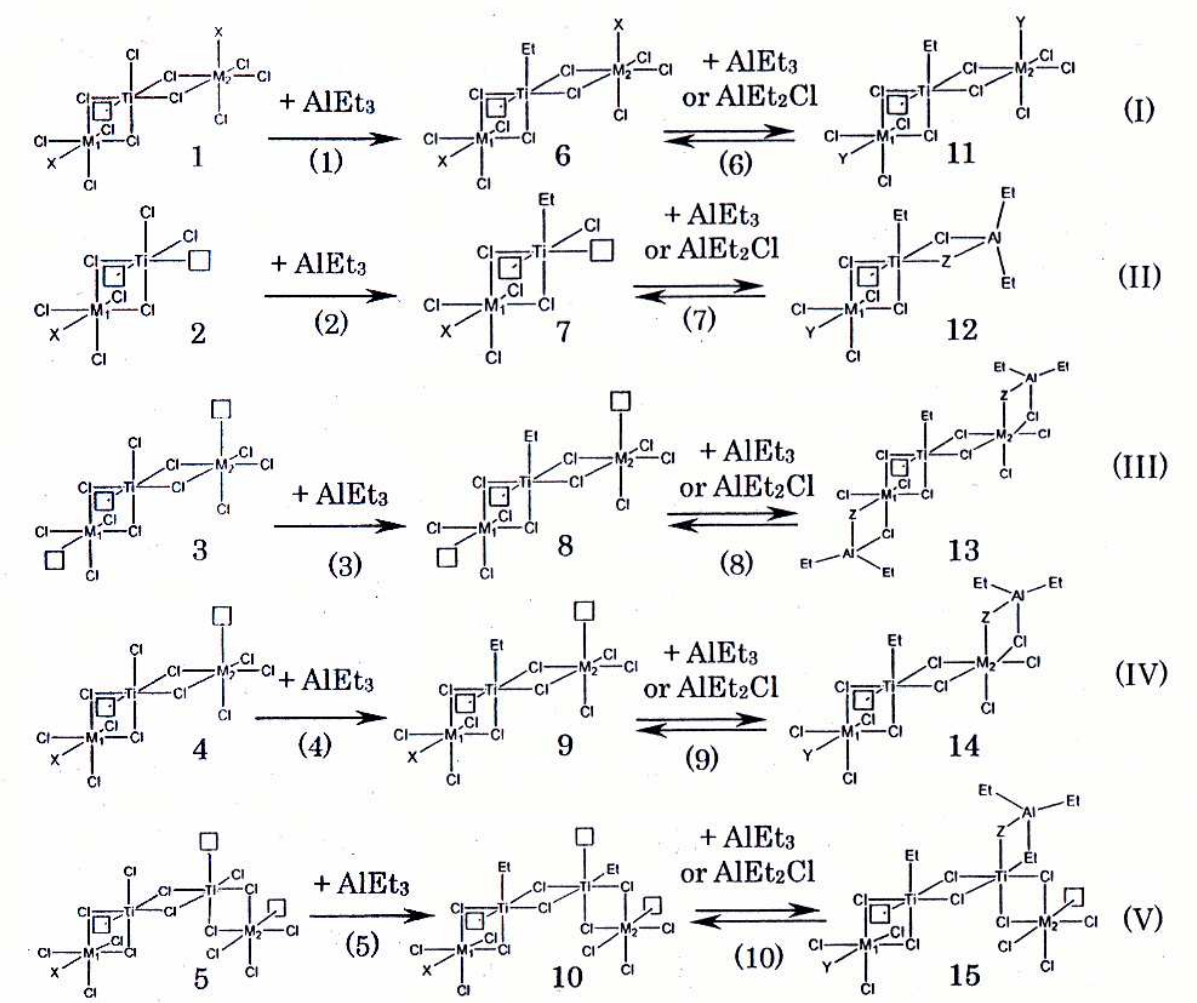

Scheme 7: *Modified three-sites model of the formation and transformation of stereospecific active sites. (M_1,M_2 = Ti or Mg bonded to the catalyst substrate through chlorine bridges; X = Cl or ED; Y = Cl, ethyl or ED; Z = Cl or ethyl; □ = coordination vacancy). Reproduced from* [93].

The typical active sites formation reactions are summarized as reactions (1) – (5) in Scheme 7. Before the contact with TEA cocatalyst, different kinds of Ti precursors exist (model 1 – 5) with different local steric environments. These Ti precursors could be transformed into the active sites after the contact with TEA (model 6 – 10). The isospecificity of these sites is determined by their local steric environments in terms of the number of coordination vacancies, pendant chlorine atoms and the external donor (ED). Interconversions between these active sites might be induced by a ligand migration on the surface of the catalyst substrate. Model 6 with the highest steric hindrance is the isospecific active site. It must be pointed out that model 6 with X = Cl in terms of its isospecificity is only IS_2, which can not produce PP with the highest isotacticity. This means that the bulkiness of the chlorine atoms in the X position in model 6 is still not enough to create IS_3. A further contact with TEA creates the highest isospecific site IS_3. When an external donor is present, then both 6 with X = ED and 11 with Y = ED are IS_3 sites. Model 7 with the lowest steric hindrance around is AS and can not act as an isospecific site even when X = ED due to the presence of two vacancies. A further contact with TEA can transfer model 7 (AS) into model 12 (IS_3) through a bimetallic complexation reaction. Model 8 is a syndiospecific site, after the complexation reaction with TEA, site 8 is transformed into site 13 (IS_3).

Models 9 and 10 (both IS_1), which can produce poorly isotactic PP, can be converted into active sites 14 and 15 (both IS_3), respectively, by bimetallic complexation reactions (9) and (10). Model 10 is actually a twin-site involving two (IS_1) centers. Then the bimetallic complexation reaction might deactivate one center and consequently the other transform into the center with the highest isospecificity 15 (IS_3) [93].

2.3 Mechanism of Polymerization

The basic assumption about the polymerization mechanism is that the monomer insertion proceeds in two steps: the coordination of the olefin to the catalytic site, followed by the insertion into the metal-carbon bond. In the catalytic complex thus formed, the double bond of the olefin is nearly parallel to the metal-growing chain bond (Scheme 8).

2.3.1 Monomer Coordination to Active Site

Considering that α-olefins are prochiral, containing one or more asymmetric carbons, the absolute configuration of the tertiary carbon atoms of the main chain is dictated by the enantioface undergoing the insertion, the insertion mode, and the stereochemistry (cis or trans) of the insertion [5]. Possible reciprocal coordinations of monomer and polymer chain on the active site are shown in Scheme 8. Models (a) and (b) in Scheme 8 represent monomer coordination in position “S” and models (c), (d) represent coordination in position “R”.

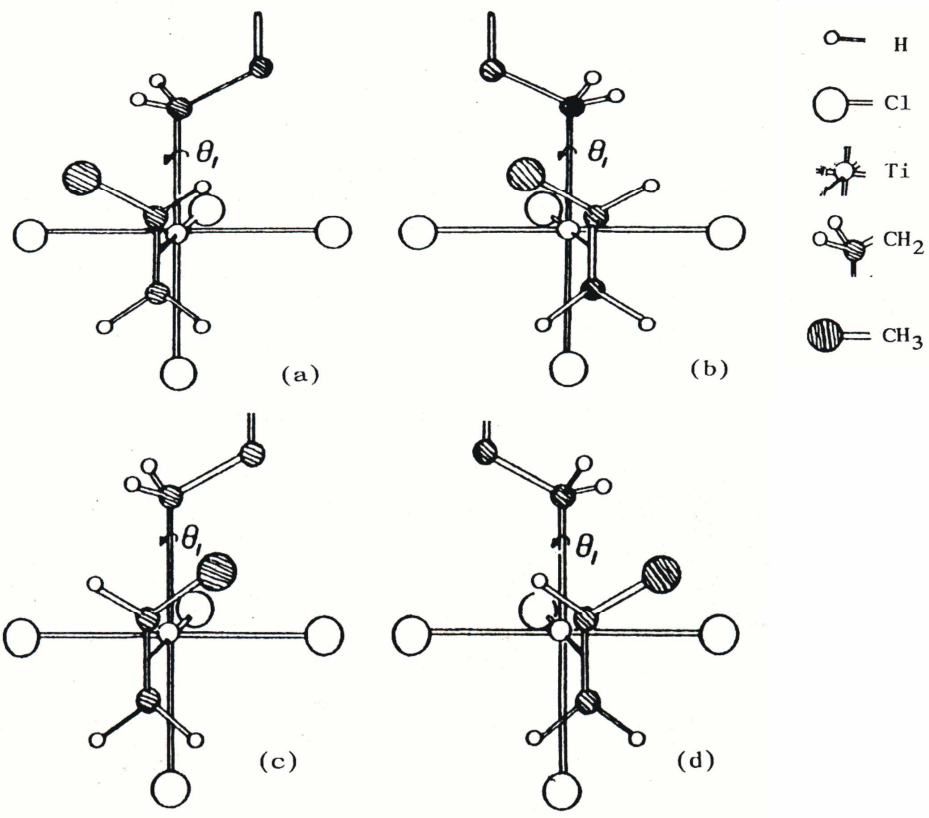

Scheme 8: *The possible propene coordinations to polymeric chain. Coordination position “S” is expressed by models (a), (b) and position “R” by models (c), (d). Reproduced from* [95].

If regioselectivity is high and insertion occurs only with cis stereochemistry, the multiple insertions of the same R or S coordinated monomers produce isotactic polymer. The syndiotactic polymer chains originate from multiple insertions of alternating R and S enantiofaces. The random enantioface insertion produces a polymer chain with no configurational regularity (atactic polymer).

The mechanism of stereoselection determined by chiral induction by the last monomer unit is referred to as “chain-end control”. Another possible element of chirality is the asymmetry of the potential active site. In this case, the stereoselection mechanism is referred as “enantiomorphic site control” [5,95].

Steric errors occurring during the chain growth lead to different chain microstructures, which could be considered like a fingerprint. Then the ^{13}C-NMR spectroscopy can be applied for distinguishing between chain-end and catalytic-site control mechanism [89]. This analysis showed that the most frequent steric defect in isotactic polymers obtained by heterogeneous catalysis consists of pairs of syndiotactic dyads (type A in Scheme 9) rather than isolated syndiotactic dyads (type B in Scheme 9). This finding implies that the formation of a configurational error in the growing chain is not determining for the configuration of the next monomeric unit. It indicates that the isospecific behavior of the relevant active site is not affected by the presence of configurational defects [95].

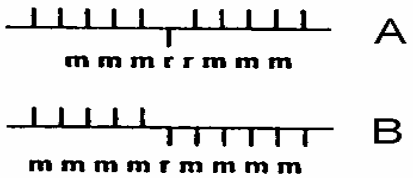

Scheme 9: *Schematic drawing of the configurational errors of isotactic polypropene chain. Type A represents pairs of syndiotactic dyads and B isolated syndiotactic dyads.*

Corradini et al. [95] investigated the impact of the bulkiness of the alkyl group bonded to the active site metal on the monomer coordination stereospecificity. It was found that, when during the first step of polymerization the alkyl group bonded to the metal is a methyl group, the insertion of the monomer is non-stereospecific. When the alkyl group is an ethyl the first insertion is partially stereospecific and, when the alkyl group is an isobutyl the first insertion is stereospecific (models A, B and C in Scheme 10).

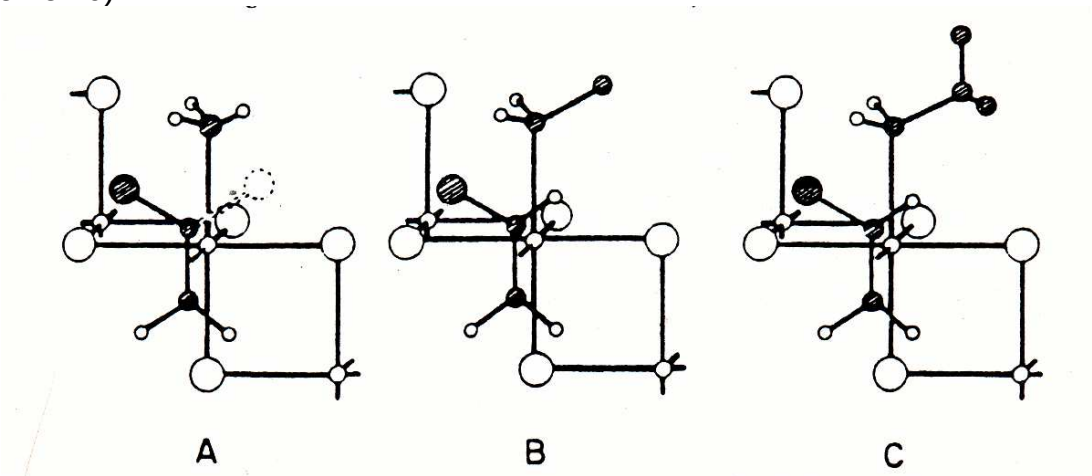

Scheme 10: *Catalyst complexes for the first steps of polymerization, when the alkyl group bonded to the metal atom is methyl (A), ethyl (B) and isobutyl (C). Reproduced from* [95].

2.3.2 Proposed Models of Polymerization

The early quantum-chemical calculations offered the first notion about the polymerization mechanism on the active center. The results lead to the conclusion that the monomer coordination to the active center is based on the interactions of the π-binding orbital of monomer molecules with free d-orbital of the active site transition metal at its vacant position [86]. According to this presumption Cossee [4,5,86] proposed a possible insertion mechanism, the so-called “monometallic Cossee mechanism”. The mechanism presented consists of two main steps: the coordination of the monomer at the vacant octahedral coordination site with the double bond parallel to the active metal-polymer bond, and the chain migratory insertion of coordinated monomer with migration of the growing chain to the position previously occupied by the coordinated monomer. The transition state is assumed to be a four-membered ring of Ti, the last carbon atom of the growing chain and the two carbon atoms forming the double bond of the monomer (see Scheme 11).

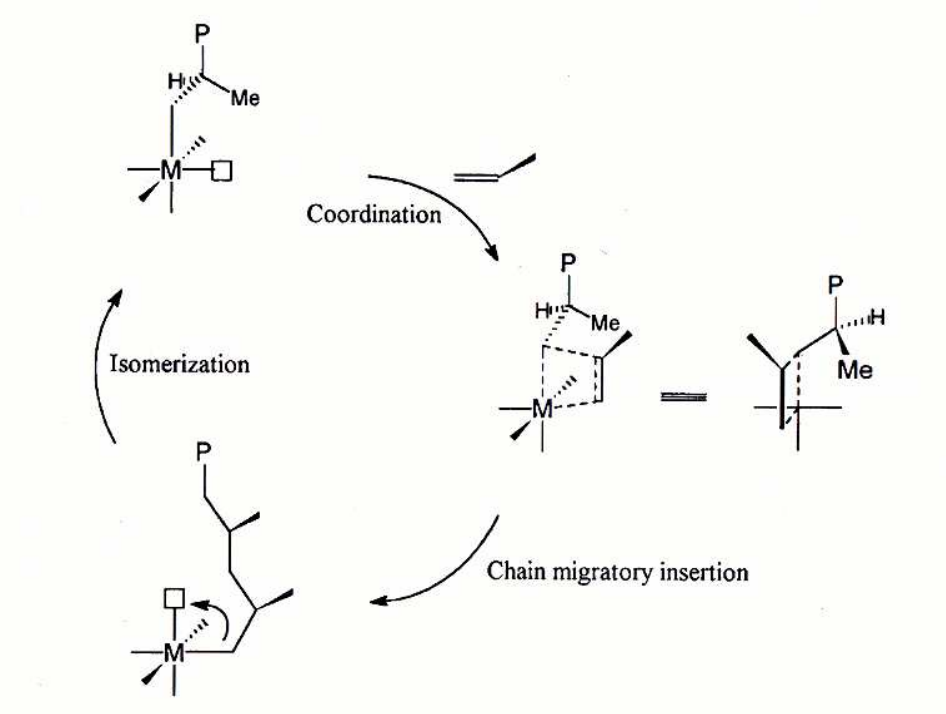

Scheme 11: *Monometallic Cossee mechanism of polymerization. Reproduced from* [5].

In the case of ethene polymerization the monometallic mechanism agreed well with the experimental results. For the stereospecific polymerization of α-olefins, the growing polymer chain must migrate back to its original position after each insertion in order to maintain sterically identical propagation steps [4,5]. This chain migration before further monomer insertion seems to be the most problematic part of the proposed mechanism.

Rodriguez and van Looy [96] proposed the “bimetallic mechanism” to solve the problematic chain skip in the Cossee monometallic model. They assume that the alkylaluminium cocatalyst is a part of an active catalytic complex, where a ligand (Cl or alkyl group) and the last carbon atom of the growing chain link Ti and Al through a double bridge (see Scheme 12). In the bimetallic mechanism, which is similar to the Cossee mechanism, the double bridge represents the driving force to shift back at its

initial position the bridged alkyl group (the growing chain) after the migratory insertion step. Lately Kohara et al. [51] gave experimental evidence about the existence of bimetallic complex.

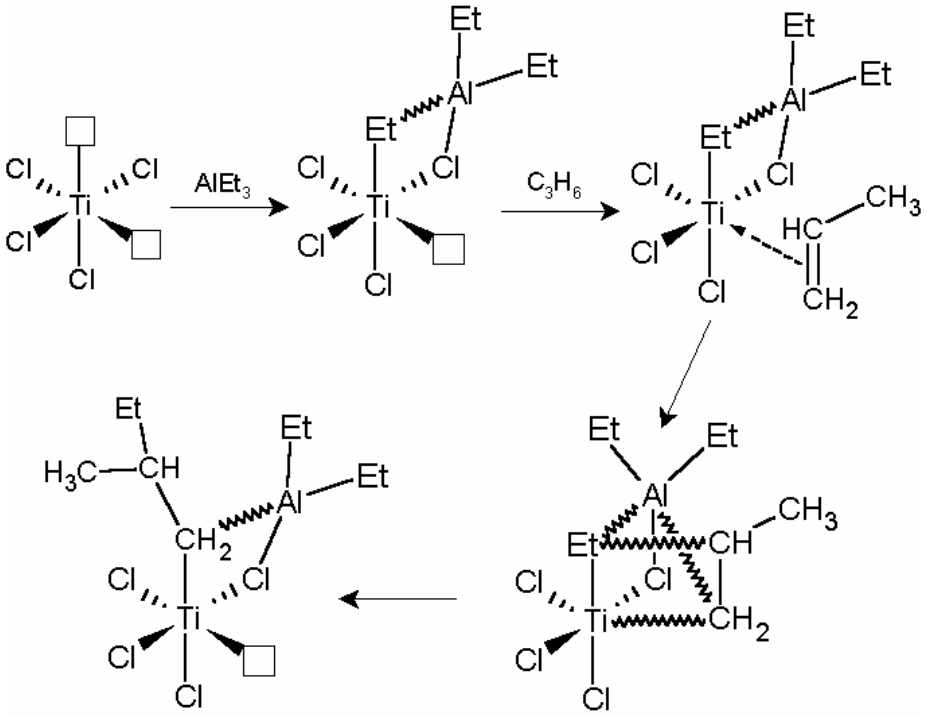

Scheme 12: *Mechanism of coordination polymerization on the bimetallic active center. Redraw from* [5].

Another theory [46] assumes that the olefin polymerization proceeds via carbene intermediates. It is based on presumption that the α-hydrogen atom from the bonded alkyl could be transferred to the transition metal vacant d-orbitals, forming an intermediate complex with the Ti-H bond. If the α-hydrogen migration between alkyl and titanium is fast and reversible, the coordination polymerization could proceed according to the mechanism presented in Scheme 13.

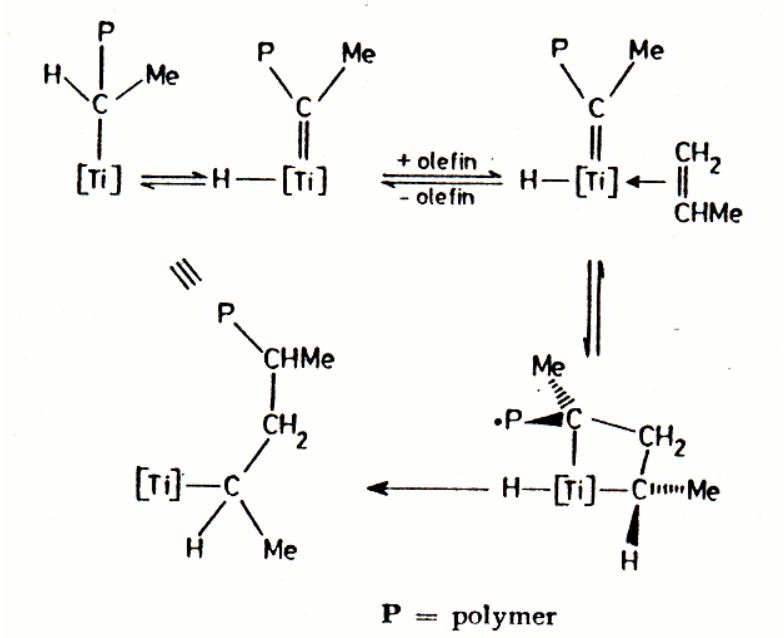

Scheme 13: *Olefin polymerization via carbene intermediates. Reproduced from* [46].

2.4 Active Sites Determination

The number of active sites responsible for polymer production is one of the most important characteristics of ZN catalysts. Various methods were proposed for the active sites determination [97-99]. However, due to the heterogeneity and different stability of active sites and diversity of reactions involved, there is no general acceptance as to which method gives the most accurate assessment of the number and types of active centers involved in the polymerization.

The most commonly used methods could be classified into several groups [98]:

I. Methods based on selective labeling of macromolecules.
   1. Labeling of macromolecules by radioactive organometals.
   2. Labeling of growing chains.
      a. The number of macromolecules.
      b. The number of metal-polymer bonds.
      c. Selective tagging of growing chains.
      d. Combination of quenching and tagging techniques.

II. Methods based on consumption of effective catalyst poison.

2.4.1 Selective Labeling of Macromolecules

2.4.1.1 Labeling of Macromolecules by Radioactive Organometals

This method was developed by Natta as early as the late 50's [100]. It is based on an alkylation of a transitional metal by an isotopically labeled organometallic compound. The radioactive tag is first incorporated on the central metal of the active site. Subsequently, after the first monomer insertion, the radioactive tag becomes a part of a growing chain [100]. However, a chain transfer reaction with another labeled organometal causes the main complication of this method, in other words, one active center could create more labeled macromolecules. So, only a part of the labeled macromolecules corresponds to the number of active sites [101-103]. Due to the above-described disadvantage the practical application of this method is low.

2.4.1.2 Labeling of Growing Chains

2.4.1.2.1 The Number of Macromolecules (N)

Determination of the number of macromolecules via M_n assessed by GPC/SEC analysis is one of the most widely used procedures for the active sites evaluation (for example [11,97,98,100,104-108]). This method has the main advantage in its universality, because it is independent of chemical assumptions like a quantitative reaction with a labeling agent without any side reactions.

In practice the method requires the determination of the average polymerization degree $\overline{P}_n$ as a function of time along with the corresponding polymerization rate R_p. From experimental plot of $1/\overline{P}_n$ versus $1/t$ the average lifetime of the growing polymer chain τ could be evaluated [97]:

$$\tau = \frac{d\left(1/\overline{P}_n\right)}{d\left(1/t\right)} \cdot \overline{P}_n \tag{10}$$

Then the relation between the average lifetime of the growing polymer chain τ and the number of active sites C* is expressed [97]:

$$C^* = \frac{\tau \cdot R_p}{\overline{P}_n} \tag{11}$$

The equation (10) validity is limited for an extremely short initial period, where the average molecular weight is still changing with time. It means, that for C* evaluation the experimental time must be comparable with the average lifetime of growing polymer [97]. Then τ and C* represent average values over the time of determination.

The “stopped-flow” method [6,13,14] has been developed to evaluate the kinetic parameters during very short polymerization times, including the average values of the coefficients of propagation k_p and chain transfer k_{tr}, as well as the concentration of polymerization centers C*. Using this technique the extremely short “quasi-living polymerization” could be realized (ca. 0.2 s). The polymerization conducted within this extremely short period is much less than the average lifetime of growing polymer chains, so it can be assumed that the state of the active sites are constant without time-dependent changes and occurrence of chain-transfer reactions.

The average value of the kinetic parameters k_p, k_{tr} and C* could be determined from the following relations [6,13,14]:

$$\frac{1}{\overline{P}_n} = \frac{M_0}{\overline{M}_n} = \frac{k_{tr}}{k_p \cdot [M]} + \frac{1}{k_p \cdot [M]} \cdot \frac{1}{t} \tag{12}$$

$$Y = k_p \cdot [M] \cdot C^* \cdot t \tag{13}$$

where $\overline{P}_n$, M_0, $\overline{M}_n$, t, Y and [M] are number-average degree of polymerization, molecular weight of monomer, number-average molecular weight of polymer, time of polymerization, yield of polymer and monomer concentration, respectively. The values of k_p and k_{tr} should be obtained from the slope and the intercept of the plot of $1/\overline{P}_n$ versus $1/t$. Then the value of C* should be calculated from equation (13).

For the active sites determination of the polymerization times longer than the average lifetime of growing polymer chains the dependence of the number of macromolecules N on polymerization time t could be applied [97,104]. Then the equation (14) extrapolated to the zero time allows evaluation of the number of active sites:

$$N = \frac{Y}{\overline{M}_n} = C_0^* + k_{tr} \cdot [X] \cdot C_0^* \cdot t \tag{14}$$

where [X] is a concentration of transfer agent such as alkylaluminium or monomer. Consequently, the k_p value could be determined from the equation [11,104,106-108]:

$$R_p = k_p \cdot [M] \cdot C^* \tag{15}$$

This procedure is applicable for the systems with a low variation of C* vs. time and with limited chain transfer reactions [97]. If only transfer processes are considered as

the chain-terminating reactions and polymerization rate R_p is time-independent [98], then the equation (14) could be modified [11,106-108]:

$$N = \frac{Y}{\overline{M}_n} = C_0^* + \left(\frac{k_{tr} \cdot [X]}{k_p \cdot [M]} \right) \cdot Y \qquad (16)$$

Then the k_p and C* values are determined similarly to the former case.

2.4.1.2.2 The Number of Metal-Polymer Bonds (MPB)

The basis of this method is the assumption that the growing polymer chain has a basic carbon atom bound to the metal of the active center [97,98]. This basic carbon is accessible for splitting or insertion reactions caused by a quenching agent with the labeling group [98].

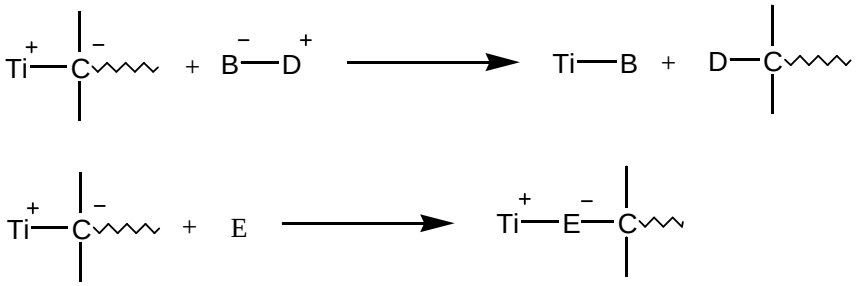

D and E are atoms or groups easily detectable in the polymer. A number of quenching agents has been reported recently in reviews [97,98]. Among commonly used quenchers are for example: radioactive iodine [109], hydroxy-tritiated alcohols [63,105,111,112], tritiated water [113], sulphur dioxide [105] and deuterated methanol and water [96].

The basic presumptions, which must be accomplished before the quench method is applied, are the following [97]:

I. The quenching agent should react with all propagating centers so that all growing chains are labeled.
II. The quenching agent should preferentially interact only with active-metal--polymer bonds (MPB).
III. There should be no contamination of the polymer from the quenching agent.
IV. Ideally kinetic isotope effects should be absent or directly measurable.

The second item is a real complication of this method, due to the chain transfer with alkylaluminium. Thus, non-propagative metal-polymer bonds can exist in addition to those corresponding to the active sites [97,98]. This particular transfer reaction could be interpreted as an exchange of the growing polymer chain [98].

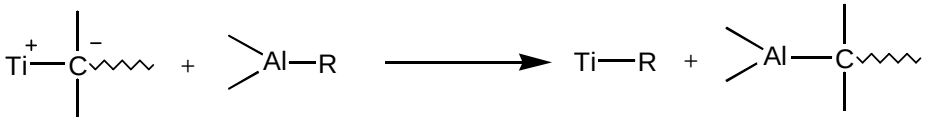

Both propagative and non-propagative metal-polymer bonds react with the quenching agent to yield labeled polymer chains. Hence, in systems where quenching is quantitative, the measured MPB will relate to all polymer molecules containing reactive metal-carbon bonds including non-propagative chains attached to

aluminium. Thus the total number of MPB will increase with time, being given by the equation [97]:

$$[MPB]_t = C_0^* + [N_{tr}]_t \quad (17)$$

where $[MPB]_t$ is the total concentration of metal-polymer bonds at time *t* and $[N_{tr}]_t$ is the concentration of transferred aluminum-polymer bonds. The C_0^* value could be obtained from a plot [MPB] versus time or conversion fitted by equation (17) and extrapolated to zero time or conversion, respectively [97].

Incorporation of a labeling atom or group into the polymer chain in positions that do not correspond to metal-polymer bonds could be another problem. The addition of I_2 to the terminal non-saturated polymer end, resulting from β-hydride elimination, is a major disadvantage of using iodine [97].

In the case of radioactive quenching agents, such as tritiated methanol, major problems may arise due to main chain isotopic substitution reactions [97,112]. Where the isotopic substitution is directly proportional to the polymer yield, the equation (17) could be modified in form [97]:

$$[MPB]_t = C_0^* + [N_{tr}]_t + [MPB]_{ex} \quad (18)$$

where $[MPB]_{ex}$ is the metal-polymer bond equivalent of the exchanged tritium. Then the equation could be employed for the active sites evaluation by extrapolation to the zero yield.

Furthermore, if the isotopic labeling agent is applied, then the kinetic isotope effect (KIE) could take place and be one of the major sources of uncertainty [97]. So, due to the above-mentioned disadvantages, only the systems where the KIE is absent and/or the non-isotopic quenchers are applied can be suitable for MPB determination.

2.4.1.2.3 Selective Tagging of Growing Chains

This method is based on the application of an effective catalytic poison, which can be inserted into the active transition-metal carbon bond. Subsequent termination by alcohol causes the catalytic poison molecule to become a part of a polymer chain. These inserted molecules are considered as labels, which could be analytically detected. The most commonly used tagging agents are carbon monoxide and carbon dioxide, which can be determined in the polymer as carbonyl groups [98,105,114] or CO and CO_2 isotopically labeled with ^{14}C detectable as radioactive tags [46,80,97,98,110-112,115,116]. The following steps represent the overall reaction sequence for CO as a tagging agent [46,97,98,117]:

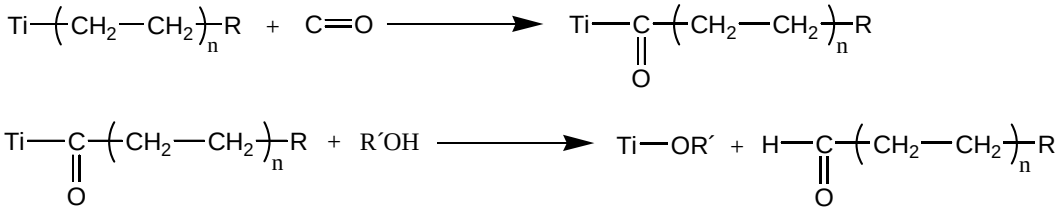

The CO_2 application has the main disadvantage with its insertion into the non-propagative metal-polymer bonds formed due to the transfer reactions with

alkylaluminium [98]. In the case of CO the insertion into the non-propagative metal-polymer bonds was not observed, but multiple insertion reactions [97] or copolymerization with monomer [46,110] could occur. Recently the direct evidence of multiple CO insertion in a case of metallocene catalyst was published by Busico et al. [118]. Furthermore the increase in the number of tags in the polymer could be caused by the regeneration of the active centers by alkylaluminium [46].

Recently, COS, CS_2 [112,119-122], acetyl chloride [121,122] and benzoyl chloride [123] have been proposed as suitable tagging agents. However, the above-mentioned catalytic poisons exhibit slow and reversible incorporation into the polymer chain. Furthermore, various side reactions with alkylaluminium also proceed. So, their applicability for the active sites determination is low.

The methods employing selective poisons do not allow a direct determination of the active centers reactivity distribution. However, the active center distribution can be obtained indirectly by correlating the length of macromolecules (after the polymer fractionation) with the content of the catalyst poison. The methods covered in this chapter allow the evaluation of the dependence of the k_p value on the stereospecificity of the centers, simply by fractionating the polymer according to its stereoregularity and determining the tag in the isolated fractions [98].

2.4.1.2.4 Combination of Quenching and Tagging Techniques

For a more detailed investigation of the catalyst behavior during polymerization, the procedure based on a combination of a selective tagging method and a method based on metal-polymer bonds determination, was proposed [124].

The active chains were first tagged with ^{14}C-labeled carbon monoxide and then quenched with tritium labeled methanol to provide labeled polymer chains containing both ^{14}C and T (^3H) isotopes. The radioactivity of the two isotopes may be assayed individually by liquid scintillation because of the differences in the β-energy spectrum [124].

It was found that the number of incorporated ^{14}C tags assessed via standard procedure compared with values obtained via the combined labeling technique was almost the same. On the contrary the amount of incorporated tritium labels was significantly lower. This discrepancy was explained by the inability of tritium to label the polymer chains with the incorporated carbon monoxide isotope. So, the determined tritium labels correspond to the metal-polymer bonds formed due to the transfer reactions with alkylaluminium [124].

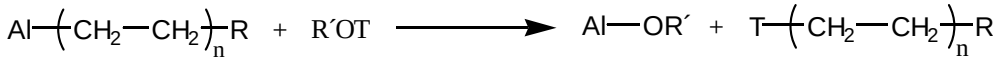

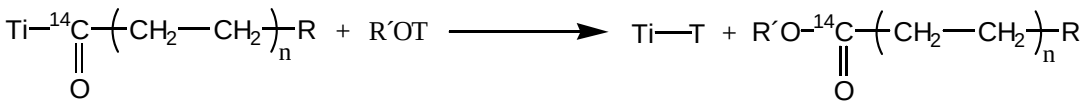

It could be assumed, that under the optimum conditions, ^{14}CO and CH_3OT dual labeling can lead to a mixture of single radioactive isotope labeled polymer chains, where ^{14}C tags the propagative metal-polymer bonds, while tritium labels only the non-propagative aluminium-polymer bonds. So the tritiated alcohol quench, after the

tagging reaction, could provide information on the extent of the transfer reaction [124]. All problems with quenching and tagging procedures were described in the preceding chapters.

2.4.2 Consumption of Effective Catalyst Poisons

A small known quantity of a suitable inhibitor is injected into the polymerization system. A simultaneous measurement of polymerization rate is carried out, determining the corresponding drop in the overall rate of polymerization. This procedure allows the evaluation of the number of active propagative centers. In principal, the decrease in the polymerization rate is correlated with the poison consumption. The amount of poison consumed is determined from a material balance and it is a measure of the number of active sites. Typical poisons potentially suitable for retardation of polymerization with ZN catalyst are CO, CO_2, CS_2, acetylene and allene [97,98].

The criteria, which must be fulfilled in such determination, are summarized in reviews [97,98] and are as follows:

I. The compound adsorbed must remain on the catalyst surface as long as necessary for its concentration determination.
II. All centers must be covered at the time of determination and the system must have reached equilibrium.
III. The compound adsorbed must be of a similar chemical nature and size to the monomer so that adsorption takes place only on the propagating centers.
IV. Only one molecule of adsorbate should be adsorbed per active center or else the stoichiometry must be known.

When polymerization is carried out in a solvent, and a solid catalyst is employed, the determination of the adsorbed inhibitor may be difficult, because the main part of the poison remains dissolved in the liquid phase. Only a minor part of the injected quantity is adsorbed [98]. Also its consumption by side processes makes the determination of the adsorbed amount of the poison less certain [125]. A more favorable case is the gas-phase polymerization, where a more suitable ratio of the poison amount in gaseous and solid phases can be achieved.

Allene and CO are commonly used as inhibitors for the active sites determination [97,98,125,126]. On the assumption that one molecule of inhibitor is adsorbed on each active center, the number of active centers may then be evaluated by the extrapolation of the plots of the proportional drop in the polymerization rate versus the amount of inhibitor adsorbed to a 100 % drop in rate [97].

The method is considered to be well applicable to catalyst systems, which show reasonably steady rates of polymerization with time. The disadvantage of this method lies in its inability to distinguish centers of different stereospecificity.

3 OUTLINE OF THESIS

The present thesis is focused on the investigation of the initial kinetics of propene polymerization with $MgCl_2$-supported Ziegler-Natta catalyst and the determination of active sites. A new procedure for the initial kinetics evaluation in *n*-heptane slurry was developed and has been applied to the investigation of the impact of the starting concentration of different alkylaluminium cocatalysts on catalyst behavior during the first seconds and minutes of polymerization.

The initial kinetics assessed in *n*-heptane slurry by the short polymerization runs is also complemented by kinetic evaluations of longer polymerization runs. For this purpose, more accurate measurements of propene/heptane phase equilibrium data were performed. The combination of kinetic data assessed by both techniques provides exhaustive kinetic information about the catalyst from the first seconds of slurry polymerization. Then the kinetics was utilized for a comprehensive description of the catalyst performance under the different initial alkylaluminium concentrations in the heptane slurry. For the explanation of observed kinetic profiles the theory based on the alkylaluminium monomer-dimer equilibrium was proposed.

Moreover, the polymer samples obtained from the short-time experiments were utilized for the determination of molecular weight distribution by GPC/SEC analysis. Then the number of active sites and propagation rate coefficients could be evaluated from the dependence of the number of macromolecules on polymer yield. Furthermore the microstructure of the selected samples was analyzed by ^{13}C-NMR measurement. On the basis of presented results the possible influence of TEA cocatalyst on active site behavior is discussed.

The short-time polymerization procedure for the initial kinetics evaluation was further utilized for studying the prepolymerization effect in *n*-heptane slurry. This study includes, in particular, the effects connected with the replenishment of the low TEA amount used for the prepolymerization by its high concentration, which is typical for the main polymerization period and under which the catalyst exhibits optimal polymerization performance also under industrial conditions.

In the last Chapter the short-time experiments carried out in *n*-heptane slurry are compared with the gas-phase experiments carried out in the fixed-bed reactor. Presented study was focused on the investigation of a possible comparability of the kinetics and polymer properties obtained with using completely different methods. Also the possible explanation of observed differences in the catalyst behavior during the gas-phase and slurry experiments is discussed.

4 EXPERIMENTAL PART

4.1 Slurry Polymerizations

4.1.1 Chemicals

All experiments in *n*-heptane were performed with commercial high-activity $MgCl_2$/phthalate/$TiCl_4$ catalyst slurried in mineral oil, supplied by BASF Catalysts LLC, TX USA. The catalyst concentration was 2.7 wt.-% (content of titanium in dry catalyst 1.6 wt.-%). The mineral oil density was $\rho(25℃) = (0.86 – 0.88)$ g/cm^3 and the viscosity $\eta(38℃) = (340 – 365).10^{-3}$ Pa.s. The catalyst slurry was stored in a glass vessel covered by a permanent flow of pure nitrogen.

Polymerization grade propene obtained from the PP plant (Chemopetrol Litvínov, Czech Republic) was used. The contents of critical impurities (CO, COS) were less than 10 ppb, water and oxygen levels were under 1 ppm.

Triethylaluminum (TEA) cocatalyst originating from Witco GmbH (Germany), were dissolved in heptane and kept in glass vessels similar to the catalyst.

n-Heptane used as the polymerization medium was purchased from Aldrich (99 % spectrophotometric grade). Prior to the polymerization, the removal of water and oxygen was conducted inside the reactor by stripping. About 10 % of the heptane was stripped-off by high-purity nitrogen (70℃, 40 min) to remove water and oxygen. The contents of O_2 and H_2O in the nitrogen were under 0.5 ppm.

4.1.2 Polymerization Apparatus

The low-pressure polymerization apparatus with the glass reactor was used for the propene polymerizations. The apparatus was equipped with a PC control and with an automatic injection system for the quenching agent. The whole apparatus and all the connecting tubing were made of stainless steel.

A mass flow meter (Bronkhorst High-Tech B.V., The Netherlands) was employed for the adjustment of the monomer flow blanket and for the measurement of monomer consumption. After the calibration, the mass flow meter allowed the measurement of propene flow in the range of 0 – 250 mg/min with accuracy ±0.5 % of reading. The apparatus was also equipped with a by-pass tubing increasing the range of mass flow meter (0 – 1500 mg/min). An external PLC based microprocessor unit DIG-S3 was applied for the integration of the monomer flow. The processor reading frequency was 5 Hz, the average integration of monomer consumption was sent every second to the computer, where the value from each third second was saved. It was proven that the deviation of the integrated monomer consumption was less than 40 mg in the range of 1 – 8 g.

The glass reactor was connected to the apparatus by a bellows connection with a Teflon seal. The bellows was attached to the special vacuum regulating valve suitable for a gradual evacuation of the apparatus and the reactor. Monomer and nitrogen incoming tubings led under the valve seat connected with a manometer for measuring of actual pressure in the reactor. Between the individual experiments, the connection bellows and the vacuum valve were protected against air contamination by the nitrogen flow.

A digital manometer PM4 (PMA GmbH, Germany) was used for measuring reactor pressure with 0.1 mbar accuracy. The two-stage reduction valve with metal membrane (Druva Sonderventile GmbH, Germany) was employed for the control of overall pressure during the polymerization.

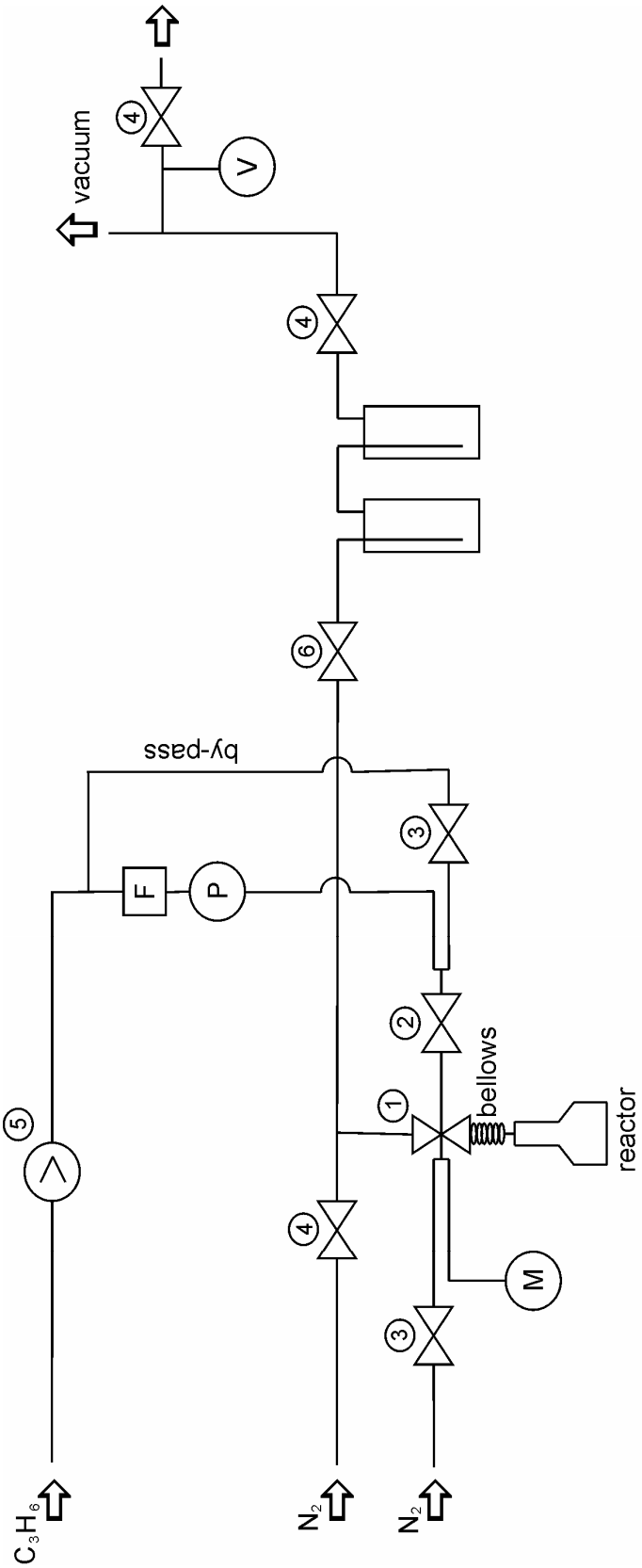

Scheme 14: Schematic illustration of polymerization apparatus:
M – digital manometer (900 – 1200 mbar),
P – mass flow meter (0 – 250 mg/min),
F – filter,
V – vacuometer.

Valves description:
1. regulating vacuum bellows valve (PIB),
2. regulating needle valve (Swagelok),
3. shut-off valve with minimalized inner volume (Supelco),
4. vacuum bellows valve (Balzers),
5. two-stage reduction valve with metal membrane (Druva),
6. glass valve.

4.1.2.1 Polymerization Reactor

The slurry polymerizations were carried out in a water-jacketed glass reactor (240 ml). The reactor was equipped with magnetic stirrer and thermostatic circuit (Julabo HP-4, Julabo Labortechnik GmbH, Germany) for temperature regulation, both under the control of a personal computer (PC). The reactor was connected to the PC--operated low-pressure polymerization apparatus and the neck of the reactor was closed by a special Teflon valve with a thermometer (Pt100). The temperature inside the reactor was measured with a 0.01℃ accuracy.

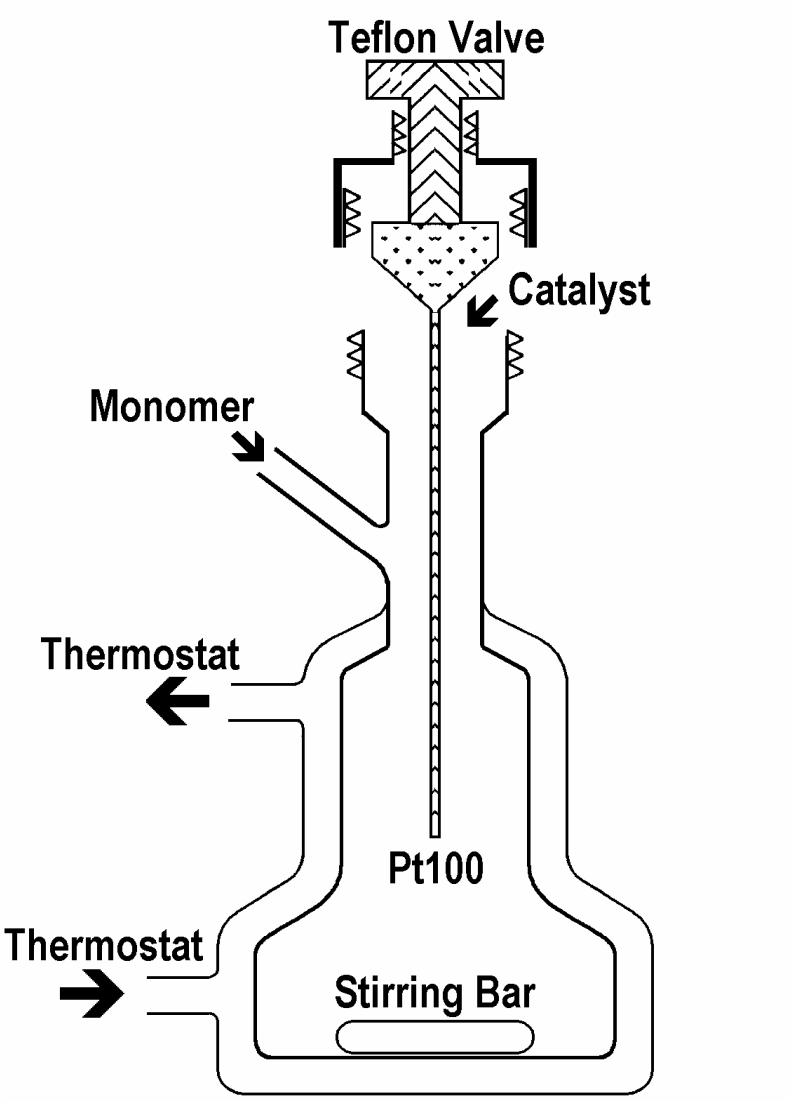

Scheme 15: *Schematic drawing of the glass polymerization reactor.*

4.1.3 Polymerization Procedure

All the slurry polymerizations were carried out in ca. 180 ml of previously stripped *n*-heptane saturated with propene to the atmospheric pressure. The polymerization temperature was typically 30℃ or 40℃ in the case of monomer concentration study. All the experiments were performed without external donor and hydrogen. The concentration of pure propene in *n*-heptane at 30℃ was 0.61 mol/L and 0.47 mol/L

at 40℃. Short experiments for the initial kinetics determination (1 – 600 s) were performed under propene flow blanked at atmospheric pressure. Longer kinetic polymerizations (typically 30 – 60 min) were carried out at the pressure of (1030 ± 20 mbar) in the closed reactor.

The clean and dry reactor was filled up by ca. 200 ml of *n*-heptane. Prior to the polymerization, heptane was stripped with high-purity nitrogen at 70℃ for ca. 40 min to remove dissolved water and oxygen. During this purification procedure about 10 % of the heptane was removed. Then the reactor was closed by a special Teflon valve with Pt-thermometer and cooled to the polymerization temperature. Using an oil-rotary vacuum pump, the remaining nitrogen was gradually evacuated until the pressure inside the reactor reached almost the saturated vapor pressure of heptane (ca. 90 mbar at 30℃).

After the nitrogen evacuation procedure, the saturation with propene followed. When the pressure inside the reactor reached the level close to the atmospheric pressure, the monomer inlet was closed. If the kinetic profile determination was based on a measurement of monomer consumption (long polymerizations), the amount of propene needed for the equilibrium saturation was used for computing the heptane amount presented in the reactor.

During the catalyst and cocatalyst dosing, the reactor inner volume was covered by a monomer flow through the opened by-pass. The cover flow was minimally 1000 mg/min. At first, the alkylaluminium cocatalyst was introduced via a syringe and the reactor content was homogenized by a short period of stirring. Next, the stirrer was turned off and an appropriate amount of the catalyst-oil slurry was slowly dosed into the reactor by means of a syringe with a long metal injector leading close to the bottom of the reactor. The application of viscous mineral oil prevents sedimentation of homogenized catalyst slurry during the charging procedure. Thanks to a near-zero mass transfer between the oil and the heptane phases, the catalyst remained separated from the cocatalyst dissolved in the heptane phase until the stirrer was turned on. The blank experiment has proven that no polymer was obtained during a non-stirring period of up to 30 s duration.

Scheme 16: *Schematic illustration and real picture of the oil (catalyst)/heptane (cocatalyst) diffusion interface before the start of stirring. TEA – triethylaluminium or different cocatalyst, D – external donor (if applied).*

Typically, 10 – 15 s after the catalyst was dosed the magnetic stirrer was turned on. The stirrer was operated at a minimum 600 rpm during polymerization. The stirring speed was high enough to homogenize the oil/heptane mixture within very

short period (ca. 0.3 s corresponding to 3 – 4 stirrer revolutions). It was proven that for the long polymerizations the stirring speed was sufficient to avoid the undesirable limitation of mass transfer through the gas-liquid interface. In the case of short polymerizations the conversion corresponded to a max. 10 % of the monomer dissolved in the polymerization slurry; therefore the effect of mass transfer limitation through the gas-liquid interface was negligible.

A PC-controlled automatic fluid drive injector was employed for the quenching of the short-time polymerizations performed for the initial kinetics determination. The main part of the injector was a syringe connected by tube to a solenoid-operated valve. The syringe was loaded with ca. 0.5 mL of a quenching agent (methanol, 2-propanol, and concentrated hydrochloric acid, volume ratio 4:4:1) and connected to the neck of the glass reactor. The moment of the stirrer being switching-on was considered as the start of polymerization. After the preset polymerization time had elapsed, the solenoid valve was automatically opened. Water pressure pushed down the syringe piston and injected the quenching agent into the reactor. This ensured a fast and complete termination of the polymerization reaction. It was proven, that the reproducibility of the repeated experiments, in the range of polymer yields 10 – 500 mg and polymerization times 1 – 600 s, was always within about 10 %. During the short-time experiments the thermostatic circuit with internal thermometer controlled the reactor temperature.

In the case of long kinetic measurements, before the stirrer was switched on, the reactor was closed by the Teflon valve with thermometer. At the end of polymerization, the quenching agent was injected into the reactor by a syringe.

4.1.4 Polymer extraction and purification

After termination of polymerization reaction, the heptane slurry with polymer and residues of catalytic components were transferred into the 500 mL distillation flask. The reactor was washed up with ca. 50 mL of 2-propanol and added, together with ca. 100 mL of distilled water, to the polymer slurry in the distillation flask. Water and heptane solutions created a two-phase system, where the polymer remains slurried in the upper part consisting of heptane, 2-propanol, methanol and mineral oil. The first three organic components were removed by a consequent azeotropic distillation and resulting water/polymer/mineral oil slurry was filtered through a sintered glass filter.

Polymer, which was slurried and partially dissolved in the remaining mineral oil, was extracted by boiling acetone for ca. 1 h to remove the mineral oil. Afterwards, the sample was dried in a nitrogen flow at room temperature to a constant mass.

4.1.5 *n*-Heptane/Propene Thermodynamic Equilibrium Determination

A detailed description of heptane/propene liquid phase composition changes caused by experimental scatter of pressure and temperature is crucial for the correct determination of polymerization kinetics assessed via monomer consumption. The thermodynamic equilibrium measurements were carried out in the same experimental set-up, which was then applied for the polymerizations. This arrangement also took

into consideration the temperature and composition inhomogeneity connected with the volume of the reactor inlet.

Before the thermodynamic equilibrium measurements, the reactor was filled with *n*-heptane and then slightly evacuated to remove the nitrogen remaining in the heptane after its purification. The exact *n*-heptane amount was determined by the weighing the evacuated reactor. Then the slow saturation with propene followed under intensive stirring (>600 rpm) to avoid mass transfer limitations through the gas/liquid interface. The dependence of the saturated propene amount on actual reactor pressure in the range of 900 – 1200 mbar was determined. Two series of phase equilibrium measurements were performed for the exact description of the thermodynamic range needed for the corrections subsequently applied on the monomer consumption data during polymerization experiments:

1. Isothermal measurements of total pressure under constant temperature 30℃ with variable propylene and *n*-heptane amount (110 – 135 g).
2. Measurements with constant *n*-heptane amount (~ 117 g) with variable propylene amount at different temperatures in the range 25 – 45℃.

The resulting total pressure profiles were described by suitable semiempirical functions. Their parameters were first optimized separately with the two data sets by the program TableCurve 3D. Then, a linear combination of the functions was used for the whole data set description. The resulting function expression is the following:

$$p = \exp\left[A + B \cdot \ln(m_P) + C \cdot \ln(m_H)\right] + \exp\left[D + E \cdot \ln(m_P) + F \cdot \ln(T)\right] \qquad (19)$$

,where p is actual pressure [mbar], m_P amount of saturated propene [g], m_H amount of *n*-heptane [g], T temperature [℃] and A, B, C, D, E, F are function parameters.

The final parameter optimization was performed with a simplex optimization procedure based on the least squares method. The procedure (programmed in Pascal) minimized the size of the standard deviation of the whole experimental set of total pressure data from the computed pressure according to the function (19). The resulting standard deviation of the whole data set was 0.8 mbar. Thus, the optimized function allows precise evaluation of the actual propene solubility in heptane in defined experimental range (pressure 900 – 1200 mbar, temperature 25 – 45℃ and *n*-heptane amount 110 – 135 g). The optimized parameters of the function (19) are presented in Table 2.

Table 2: *Optimized parameters of function (19).*

A	10.911
B	0.9051
C	-1.2143
D	-1.0321
E	0.7125
F	1.7248

4.1.6 Polymerization Kinetics Assessed via Monomer Consumption

For the kinetic profiles determination in experiments longer than 10 min, the method based on the monomer consumption during the polymerization was developed. The instant polymer amount formed in the system was determined as a difference of overall monomer amount introduced since the start of polymerization and actual monomer amount dissolved in *n*-heptane. The instant monomer solubility was calculated on the basis of experimentally evaluated propene/heptane equilibrium (see the Chapter 4.1.5) using the exact *n*-heptane amount determined prior to the start of the experiment from the monomer consumption necessary for heptane saturation to atmospheric pressure after the nitrogen evacuation. The determined amount of dissolved monomer was considered as initial monomer amount presented in the closed reactor after the catalyst introduction. Then, the resulting polymerization kinetics is determined as a function of the calculated polymer yield over time (Figure 2 and Figure 3).

It was proved that the deviation of the real polymer yield at the end of polymerization and yield calculated from monomer consumption was in good agreement. The deviation was always lower than 10 %.

Comparison with initial kinetics assessed via short-time experiments revealed that the described method allows the determination of the correct kinetic profile after ca. 30 – 60 s from the start of polymerization. The initial discrepancy was caused by non-equilibrated conditions within the starting period. However, as shown in comparative Figure 4, the combination of both methods is suitable for the precise investigation of overall catalyst kinetic behavior from the first seconds of polymerization.

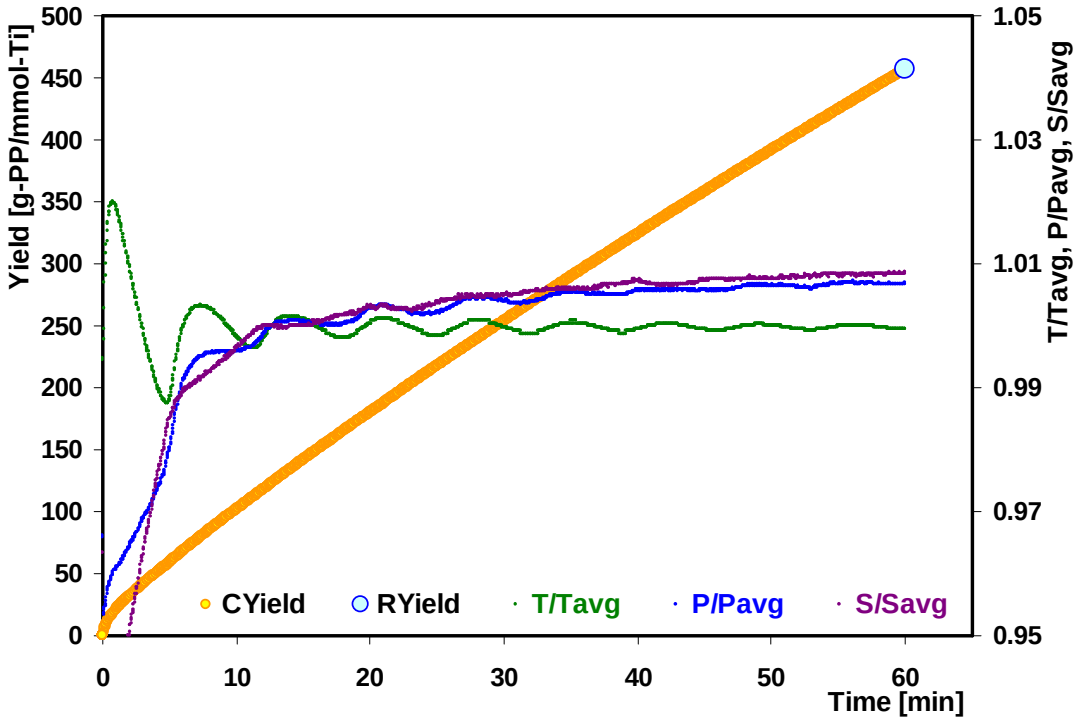

Figure 2: *Kinetic profile expressed as polymer yield vs. time dependence (integral form). CYield – calculated polymer yield; RYield – final polymer amount; T/Tavg – temperature profile; P/Pavg – pressure profile; S/Savg – propene solubility profile.*

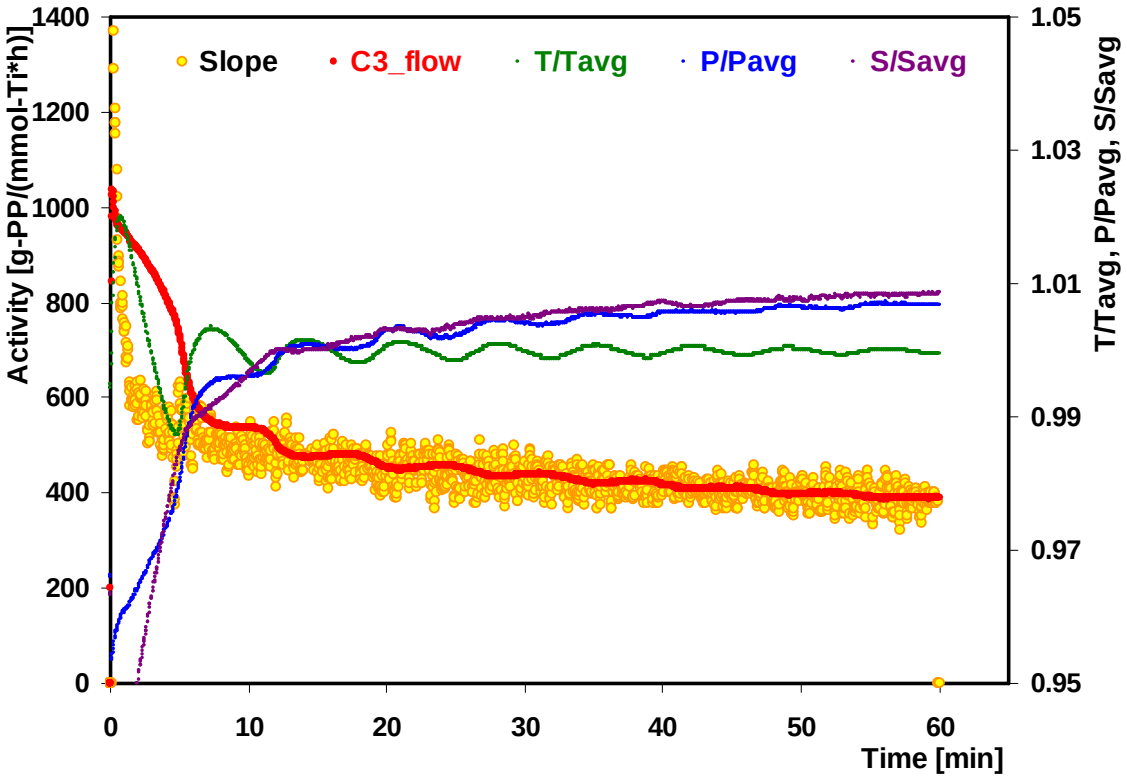

Figure 3: *Kinetic profile in derivative form as dependence of catalyst activity vs. time. Slope – numerical derivation of calculated polymer yield; C3_flow – monomer consumption during polymerization.*

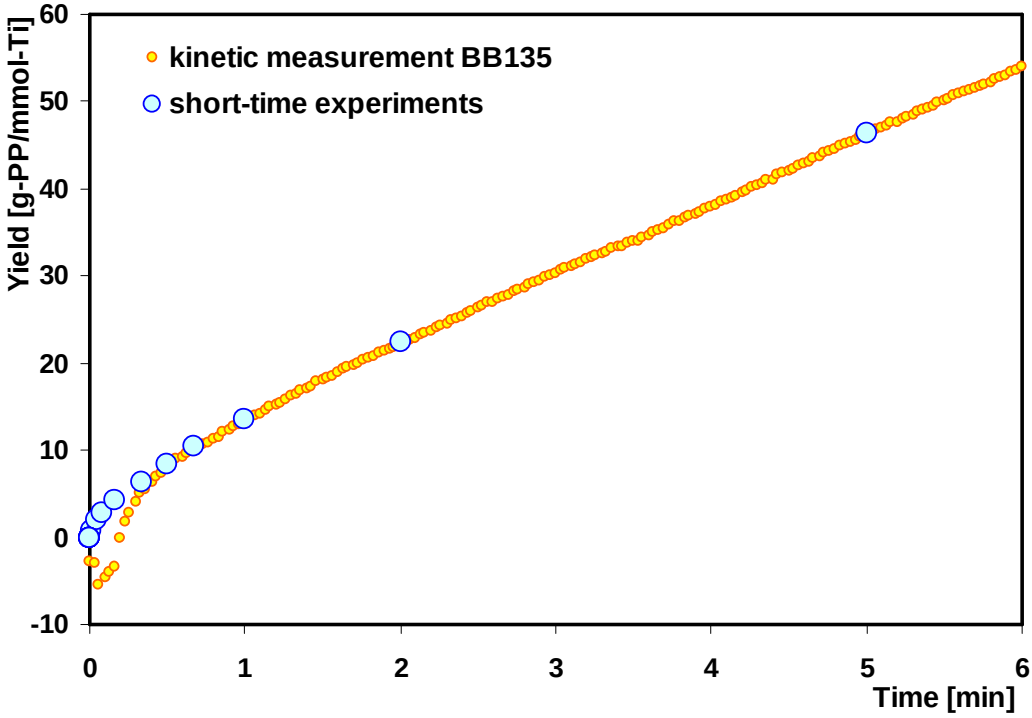

Figure 4: *Comparison of kinetic profile assessed via short-time experiments and kinetics determined from monomer consumption during polymerization. Polymerization conditions: temperature 30℃; atm. pressure; heptane 180 mL; propene 0.61 mol/L; initial TEA concentration 4.4 mmol/L; catalyst amount 11.2 µmol-Ti.*

4.1.7 Mathematical Function for Kinetic Profiles Description

A suitable function was evaluated with the presumption that the two basic types of active sites are presented in the system during the polymerization. These sites exhibit different kinetic behavior, where the unstable sites have very fast activation and high initial activities followed by fast deactivation. On the contrary, the stable sites exhibit relatively slow activation with a stable kinetic profile.

Because the activation of unstable sites occurs in a very short period (<0.1 s), only the deactivation profile could be determined by applied techniques. Then the mathematical function for the description of the kinetic profile of unstable sites was constructed on the basis of a commonly used kinetic model expressed in equation (20) combined with *n*-order kinetic equation of deactivation:

$$R_p = k_p \cdot [M] \cdot C^* \tag{20}$$

$$-\frac{dC_i^*}{dt} = k_{di}\left(C_i^*\right)^n \tag{21}$$

However, the presented equation (21) has only an empirical meaning. Then the combination of expressed equations gives the general function for the description of fast deactivation of unstable sites according to the *n*-order reaction kinetics:

$$R_p(t) = \left[R_p(0)^{1-n} + (n-1)\cdot K_D \cdot [M]^{1-n} \cdot t\right]^{\frac{1}{1-n}};\ K_D = k_p^{1-n} \cdot k_{df} \tag{22}$$

The integration form is expressed as dependence of yield on polymerization time:

$$Y(t) = \frac{R_p(0)^{2-n} - \left[R_p(0)^{1-n} + (n-1)\cdot K_D \cdot [M]^{1-n} \cdot t\right]^{\frac{2-n}{1-n}}}{(2-n)\cdot K_D \cdot [M]^{1-n}};\ n \neq 1,2 \tag{23}$$

For the description of stable active sites the kinetic function with the first order activation followed by first order deactivation (subsequent reactions) was applied. Then the derivative and integral form could be expressed:

$$R_p(t) = (1 - \exp(-k_a \cdot t)) \cdot \left(R_p(0) \cdot \exp(-k_{ds} \cdot t)\right) \tag{24}$$

$$Y(t) = \frac{R_p(0)}{(-k_{ds})} \cdot (\exp(-k_{ds} \cdot t) - 1) - \frac{R_p(0)}{(-k_a - k_{ds})} \cdot (\exp((-k_a - k_{ds}) \cdot t) - 1) \tag{25}$$

,where k_a is a activation rate constant of stable sites.

Finally, the linear combination of integral functions (23) and (25) was applied for the overall characterization of polymerization kinetics with high-activity $MgCl_2$--supported $TiCl_4$ catalyst. The simplex optimization procedure complemented with the least square method for the minimization of standard deviation was used for the fit of described 6-parameters mathematical kinetic function on the determined experimental data (Figure 5 and Figure 6).

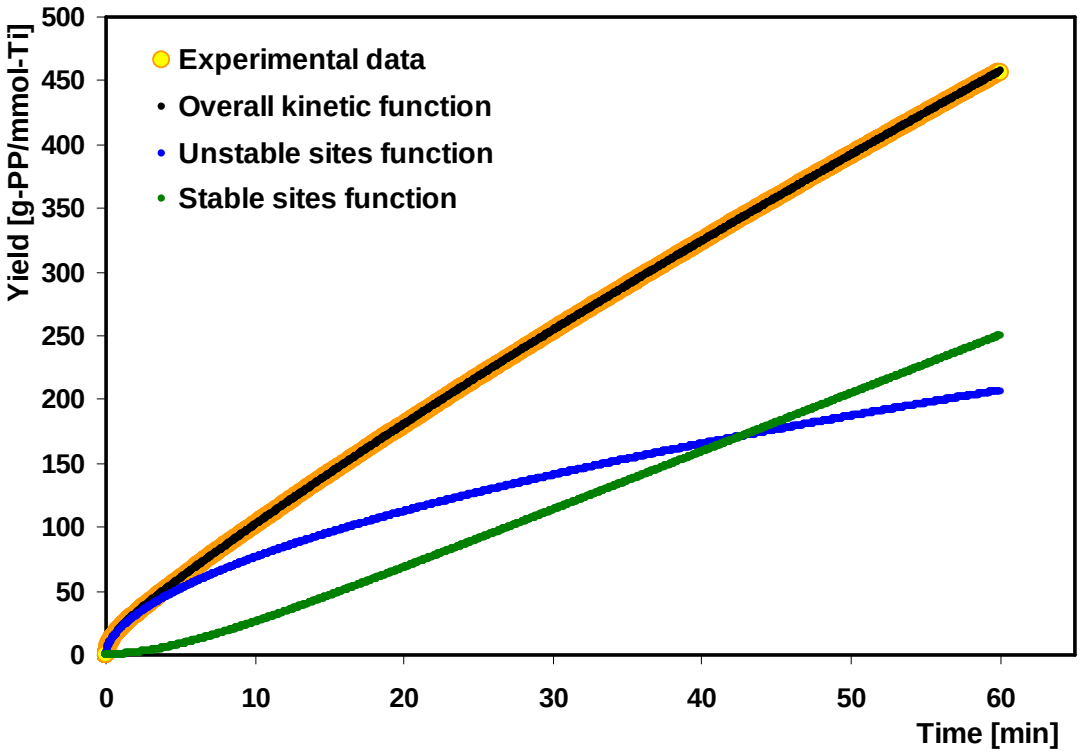

Figure 5: *Example of fit of overall kinetic function in integral form on determined experimental data and illustration of profiles corresponding to unstable and stable active sites, equation (23) and (25) respectively.*

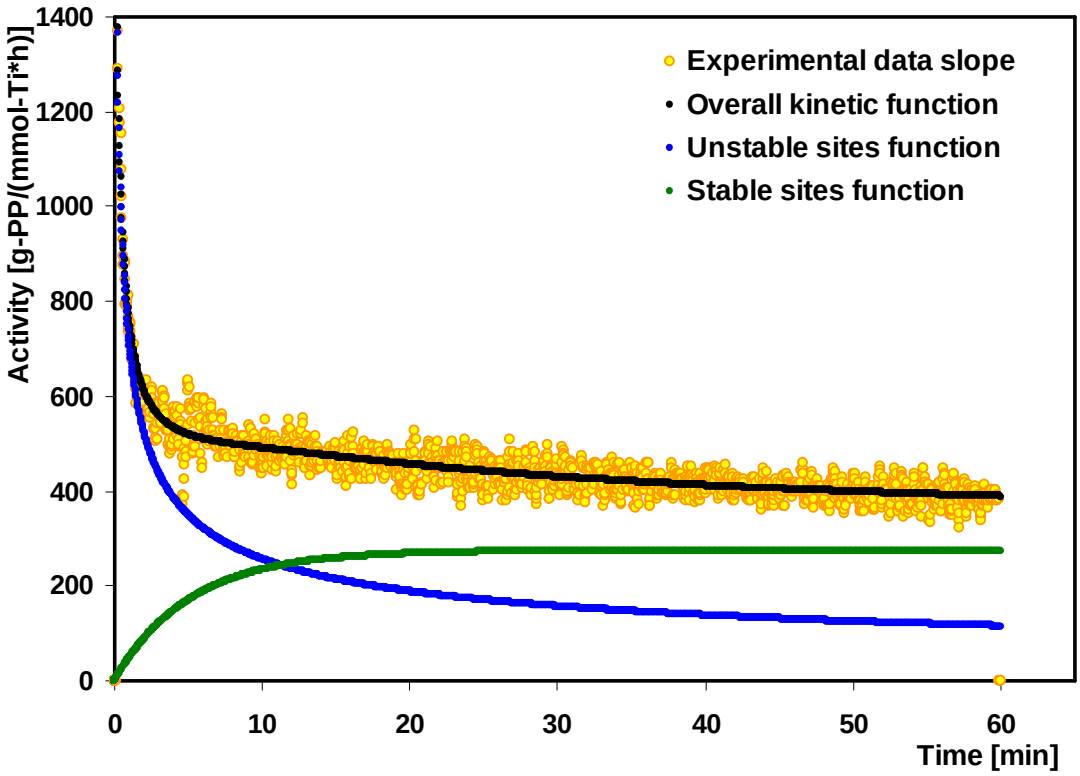

Figure 6: *Illustration of overall kinetic function in derivative expression with separated profiles pertaining to unstable and stable sites, equations (22) and (24), respectively.*

4.2 Gas-phase Polymerizations

4.2.1 Chemicals

For the gas-phase experiments the same high-activity $MgCl_2$/phthalate/$TiCl_4$ catalyst supplied from BASF Catalysts LLC, TX USA as mineral oil slurry was used (catalyst concentration 23 wt.-%, titanium content in dry catalyst 1.6 wt.-%). The catalyst was stored in a glass vessel under a nitrogen atmosphere in the glove box (oxygen content <1 ppm).

The polymerization grade propene originated from Westfalen AG (Germany) was applied without further purification (content of water and oxygen under 1 ppm).

The nitrogen purchased also from Westfalen AG (Germany) was further purified over molecular sieve 13X and Cu catalyst. The resulting content of water and oxygen was under 1 ppm.

The triethylaluminum (TEA) cocatalyst originating from Witco GmbH (Germany), were dissolved in hexane and kept in glass vessels in a glove box similarly as the catalyst.

The high-purity NaCl, purchased from Merck, was used as a fixed bed for catalyst and cocatalyst during the polymerization. NaCl was also stored in the glove box.

4.2.2 Gas-phase Polymerization Apparatus

Polymerizations in gaseous propene were performed in a special glass reactor connected to the low-pressure metallic apparatus equipped with automatic mass flow controllers (Brooks Instrument B.V., The Netherlands) for nitrogen and propene (flow range 0 – 1000 mL/min). The whole apparatus and all the connecting tubing were made from stainless steel. Pressure in the apparatus was monitored by a pressure sensor (Omni Instruments, UK).

The apparatus was under PC control, connected to mass flow controllers operating unit Model 5878 (Brooks Instrument B.V., The Netherlands). The Hewlett--Packard 3852A Data Acquisition Unit was applied for the temperature and flow rate data acquisition.

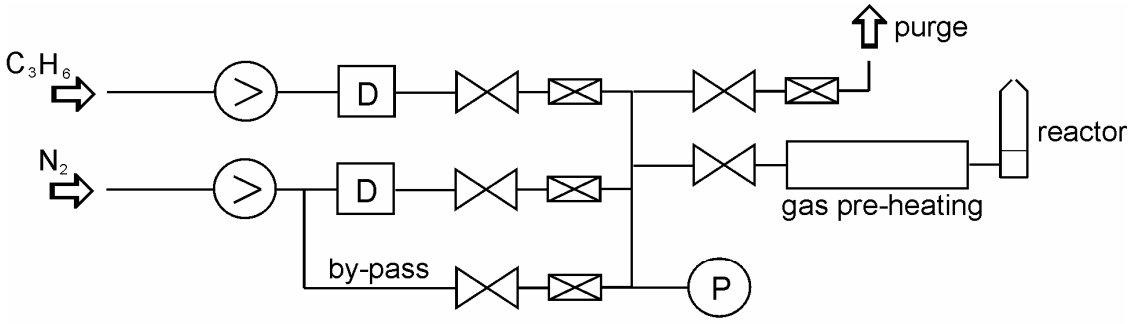

D - automatic mass-flow controller (Brooks Instruments),
P - pressure sensor (Omni Instruments),
⊳ - reduction valve (Druva),
⋈ - ball valve (Hoke),
⊠ - backflow preventer (Hoke).

Scheme 17: *Schematic illustration of apparatus for gas-phase polymerizations.*

4.2.2.1 Fixed-bed Reactor for Gas-phase Polymerizations

The gas-phase experiments were performed with catalyst dispersed in salt inside the water-jacketed glass reactor with porous glass frit bottom. Then the applied gas was introduced under the glass frit bottom and flew through the frit and the salt bed containing catalyst and cocatalyst.

Two thermocouples (type K; diameter 0.5 mm) with fast response to temperature change were applied for the accurate temperature determination. During the experiment, one thermocouple placed under the reactor glass frit bottom, measured the temperature of the gas coming into the salt bed. The second one was placed close to the salt bed surface, measuring the temperature of the outgoing gas.

For the transformation of the analog thermocouple voltage to the digital temperature data MyPClab (Novus Electronics, Brazil) data acquisition unit with automatic cold junction compensation was used. The resulting temperature was collected with 0.1℃ accuracy.

The two separate thermostatic circuits (Julabo M-5, Julabo Labortechnik GmbH, Germany) were applied for accurate control of the reactor and gas temperature during the experiment. The separate gas pre-heating system was necessary for avoiding the gas temperature change during its flow through the salt bed.

4.2.3 Polymerization Procedure

Gaseous propene polymerizations were performed in ca. 20 mL of pure NaCl at 40℃ and atmospheric pressure.

The dried and cleaned reactor was connected to the apparatus and purged by a nitrogen flow (1000 mL/min) for 20 minutes. During the purging procedure the reactor was heated to the polymerization temperature.

After the reactor purge, the TEA pre-activated catalyst/salt mixture was prepared in the glove box. The defined amount of catalyst/mineral oil slurry was dosed inside the transport glass vessel by a PE syringe with thin metal injector and the exact catalyst weight was determined by analytical balances. Then, the appropriate TEA/hexane solution was introduced. The hexane amount was sufficient for the complete dissolving of mineral oil, necessary for good dispersion of the catalyst in the salt support. After the salt introduction, the mixture was homogenized by gentle shaking, immediately removed from the glove box, and transferred to the reactor.

The gas-phase polymerization procedure with catalyst fixed on surface of salt grains can be divided into tree main steps:

1. The catalyst/TEA/salt mixture in the reactor is heated up to polymerization temperature under the nitrogen flow (1000 mL/min). The nitrogen flow is also important for removing hexane residues from TEA/hexane solution. Typically, 600 s is enough to reach the steady-state conditions.
2. When the first period elapsed, the gas flow is automatically switched from nitrogen to propene (1000 mL/min). It was proven that the gas change occurred during period shorter than 2 s. So, the monomer introduction is considered as the start of polymerization. During the whole experiment, the temperature change caused by the polymerization reaction was lower than 3℃.

3. After the pre-set polymerization time, the monomer flow is switched back to nitrogen, which removes remaining monomer from salt and stops the polymerization.

Then the salt was dissolved by hot water and mineral oil residues were extracted by boiling acetone similarly as in the slurry experiments (see Chapter 4.1.4). The reproducibility of gaseous propene experiments within the polymerization time 30 – 1800 s and polymer yields 10 – 300 mg was determined to be about 10 %.

4.3 GPC/SEC – Molecular Mass Distribution Determination

Molecular mass distribution was assessed in the following manner via Size Exclusion Chromatography (SEC). The SEC used in this study consisted of a Polymer Laboratories PL-GPC 220 equipped with PL-220DRI (differential refractive index detector) and Viscotek model 220R differential bridge VD (viscometer detector). All the detectors were installed in the column oven compartment together with a set of columns. The set of applied columns consists of three PL gel 10 μm MIXED-B, 300 x 7.5 mm.

All sample solutions were prepared in filtered 1,2,4-trichlorobenzene containing 0.05 wt.-% of an antioxidant Santonox R ($C_{22}H_{30}O_2S$, M = 358) to prevent oxidative degradation of the polymer. Typically 10 mg of the polymer was used for the sample preparation. The same solvent was used as the SEC eluant. The sample concentration of 0.5 mg/mL and the injection volume of 200 μL were employed throughout. The experiments were undertaken with a flow rate 1.0 mL/min at 165℃.

The columns were calibrated using 14 polystyrene standards supplied by Waters with molecular weights M_w ranging from 2350 to 3700000. Data handling was accomplished using the Viscotek TriSEC software - Universal Calibration Modul was used for calculation.

4.4 ^{13}C-NMR – Isotactic Pentad Distribution Determination

For the determination of the isotactic pentad distribution in polypropene samples 210 mg of PP powder was dissolved in a mixture of 1,2,4-trichlorobenzene (1.7 mL) and deuterated benzene (0.4 mL) and homogenized for 6 – 8 h at 125 – 130℃ under a nitrogen atmosphere.

Prepared samples were analyzed with a 500 MHz Bruker DRX NMR instrument at 120 – 125℃. Pulses were applied at a 77° angle wit h 5 s time delays. The ^{1}H interaction was eliminated by Waltz decoupling. The total number of scans was ca. 2500. The resulting FID signals were transformed by Fourier transformation and the molar percentage of each pentad was evaluated on the basis of signal integral intensity.

5 RESULTS AND DISCUSSION

5.1 Influence of Catalyst Amount, Al/Ti Molar Ratio and Initial TEA Concentration on Polymerization Activity in Slurry

Three experiments compared in Table 3 were performed in order to evaluate which of the parameters (Al/Ti molar ratio or initial TEA concentration) is important for ZN catalyst activation in slurry polymerizations. The polymerization runs performed at constant Al/Ti molar ratio and constant catalyst amount but with different starting TEA concentrations (constant TEA dose and different *n*-heptane amounts) exhibited significant changes in polymer yields (see Table 3). On the contrary no remarkable changes in polymer yields were observed in experiments with constant initial TEA concentration in the reactor (ca. 4.4 mmol/L) and different Al/Ti molar ratio (amount of dosed TEA was changed to obtain the same starting TEA concentration in different heptane amounts). These experiments indicate that the influence of initial TEA concentration is dominant, while the changes in Al/Ti ratio do not have a significant effect on the catalyst activity in the first seconds of polymerization. The importance of the initial TEA concentration to the catalyst activation was also pointed out by Shimizu et. al [18] and formerly by Spitz et al. [127].

Table 3: *Influence of Al/Ti molar ratio and initial TEA concentration on polymer yield at 30℃ and atm. pressure; propene 0.61 mol/L; catalyst amount 11.1 µmol-Ti; polymerization time 20 s.*

Exp. No.	V (heptane) [mL]	n (TEA) [mmol]	Al/Ti [mol/mol]	[TEA] [mmol/L]	Yield [mg]
AC50	180	0.8	70	4.4	71.9
AC53	30	0.1	10	4.3	63.2
AC52	180	0.1	10	0.7	29.9

The influence of the catalyst amount on polymerization yield was investigated at constant initial TEA concentration in *n*-heptane (0.8 mmol/L). The series of short-time experiments (20 s) presented in Table 4 and Figure 7 show that the dependence of polymer yield on catalyst amount has a linearly increasing character. This observation indicates that the polymerization activity does not depend on the catalyst amount applied in the polymerization in the range of 5 – 50 µmol-Ti. Also it could be presumed that the non-isothermal deviation during polymerization is not significant and the experiments can be considered as quasi-isothermal. Moreover, the application of a low amount of TEA was a proof of the system purity and experiment procedure reproducibility. The extrapolation to zero yield in Figure 7 shows that the content of impurities capable to poison the catalyst was remarkably below the critical level of applied TEA (act as a poison scavenger in addition to catalyst activation), even at very low TEA amounts applied in this study (0.14 mmol). Further, the set of four identical experiments (Table 4) with catalyst amount typically used in polymerizations (ca. 10 – 13 µmol-Ti) indicated that the experiment procedure reproducibility is within 10 %.

Table 4: *Influence of catalyst amount on polymer yield. Experimental conditions: polymerization time 20 s; temperature 30℃; atm. pressure; heptane 180 mL; propene 0.61 mol/L; initial TEA concentration in the reactor 0.8 mmol/L.*

Exp. No.	Cat. Amount [µmol-Ti]	Yield [mg]
AC59	4.7	13.1
AC54	13.1	38.6
AC56	13.1	35.6
AC57	13.1	36.0
AC58	13.1	38.1
AC60	28.1	74.3
AC61	49.8	140.3

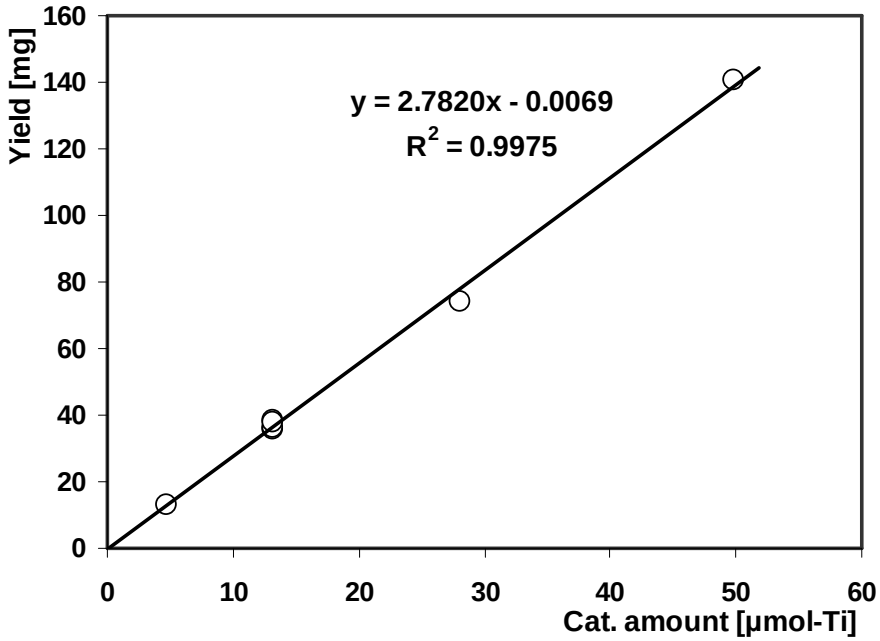

Figure 7: *Influence of catalyst amount on polymer yield. Experimental conditions: polymerization time 20 s; temperature 30℃; atm. pressure; heptane 180 mL; propene 0.61 mol/L; initial TEA concentration in the reactor 0.8 mmol/L.*

5.2 Alkylaluminium Cocatalyst Influence on $MgCl_2$-supported $TiCl_4$ Catalyst

5.2.1 Impact of Initial TEA Concentration in Slurry on Net Polymerization Rate

The influence of initial TEA concentration on catalyst performance was formerly investigated by many authors [19,25,128,129]. These were indicating that the dependence of polymerization rate on TEA concentration can be described by the Langmuir-Hinshelwood equation (26) exhibiting the sharp increase of the polymerization rate with increasing TEA concentration to a certain maximum depending on the type of catalyst and applied experimental conditions. Further, increasing the amount of TEA leads to the decrease of the polymerization rate due to the active sites over-reduction by the excess TEA [5,17,19,21].

$$R_p = k_p \cdot \frac{K_A \cdot [A]_0}{(1 + K_A \cdot [A]_0)^2} \quad (26)$$

Where $[A]_0$ is initial TEA concentration, K_A TEA adsorption equilibrium constant and k_p propagation rate coefficient.

However, the experimental data assessed at slurry polymerization (Table 5) performed at relatively low temperature and pressure do not fit well to such theory. As exhibited in the left part of the Figure 8, the dependence of the linearized form of the equation (26) on the overall TEA concentration $[TEA]_0$ exhibits a non-linear profile. It indicates that the presented Langmuir-Hinshelwood equation is not suitable for the description of the determined data. The reason of the discrepancy between the Langmuir-Hinshelwood model and the experimental data could be found in the difference of the applied experimental conditions.

It is well known that the trialkylaluminum compounds as trimethylaluminium (TMA), triethylaluminium (TEA), tri-*i*-butylaluminium (TIBA) etc. create associated dimer structures in solution [130]. The dimer stability decreases with an increasing bulkiness of alkyl substituents, depending also on the temperature and its concentration. The extensive calorimetric study of TEA monomer-dimer equilibria in *n*-hexadecane, formerly performed by Smith [131], revealed that the TEA is strongly associated in hydrocarbon solutions forming dimeric structures. On the contrary, in the gas phase and at high temperatures almost all TEA molecules are present in dissociated monomeric form.

Smith [131] determined that only ca. 6 – 17 % of the TEA molecules are present in the monomeric form in the *n*-hexadecane solution at 30℃, depending also on the concentration. More recent study of the TEA monomer-dimer equilibria in *n*-heptane was performed by Černý et al. [132] on the basis of ^{27}Al-NMR measurements. He determined the empirical equation for the evaluation of the TEA dissociation constant in *n*-heptane at various temperatures. Then the concentration of monomeric TEA could be calculated using the simple dissociation equation:

$$Al_2(C_2H_5)_6 \leftrightarrows 2\ Al(C_2H_5)_3$$

$$K_{Diss} = \frac{[A]_M^2}{[A]_D} = \frac{2 \cdot [A]_M^2}{[A]_0 - [A]_M} \quad (27)$$

,where K_{Diss} is dissociation constant (K_{Diss}(30℃) = 1.1E-4 mol/L) of TEA dimer determined from an empirical equation published by Černý et al. [132], $[A]_0$ is concentration of TEA with the presumption that the all TEA molecules are in monomeric form, $[A]_M$ and $[A]_D$ are the actual concentrations of monomer and dimer TEA, respectively.

Referring to the high tendency of TEA towards formation of dimers, only the monomeric TEA concentration computed according to equation (27) was used for the investigation of the TEA influence on the catalyst polymerization rate in linearized coordinates $([TEA]_M/R_p net)^{1/2}$ presented in the right part of Figure 8. The obtained linear dependence indicates that the catalyst polymerization rate could be related to the adsorption of monomeric TEA on the catalyst surface. Then the dependence of $R_p$net on initial concentration of monomeric TEA fitted by Langmuir-Hinshelwood (26) equation is presented in Figure 9.

Table 5: *Influence of initial TEA concentration on polymer yield and catalyst net activity* ($R_p$net). *$[TEA]_0$ – all introduced TEA is considered being in monomeric form; $[TEA]_M$ – calculated real concentration of monomeric TEA. Experimental conditions: polymerization time 60 min; temperature 30℃; atm. pressure; heptane 180 mL; propene 0.61 m ol/L; catalyst amount 11.2 µmol-Ti.*

Exp. No.	$[TEA]_0$ [mmol/L]	$[TEA]_M$ [mmol/L]	Yield [g]	$R_p$net [g-PP/(mmol-Ti*h)]
BB142	0.2	0.07	1.663	148
BB138	0.7	0.12	3.068	273
BB141	1.9	0.22	4.197	373
BB135	4.4	0.33	4.719	420
BB131	9.4	0.49	4.995	444
BB140	18.5	0.69	5.136	457

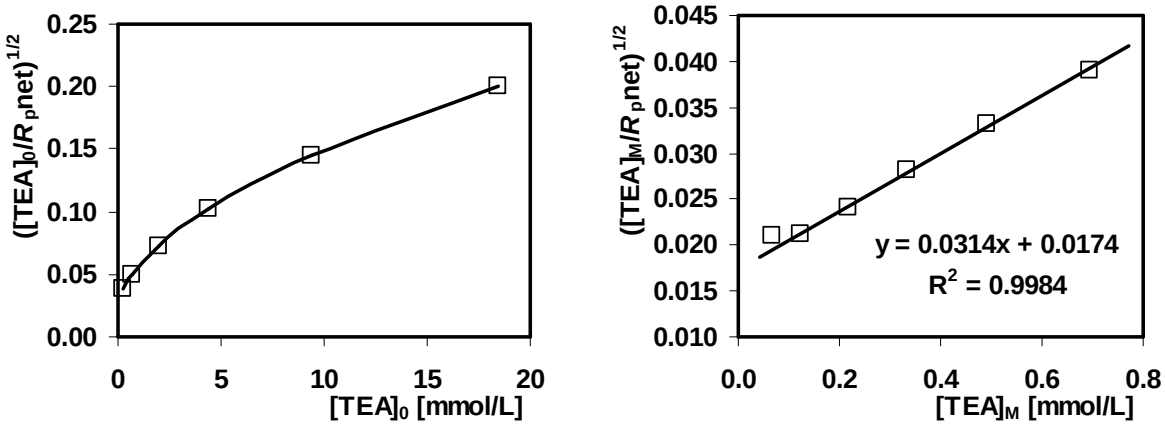

Figure 8: *Dependence of Langmuir-Hinshelwood equation in linear coordinates on initial TEA concentration. $[TEA]_0$ – all introduced TEA is considered being in monomer form; $[TEA]_M$ – calculated concentration of monomer TEA.*

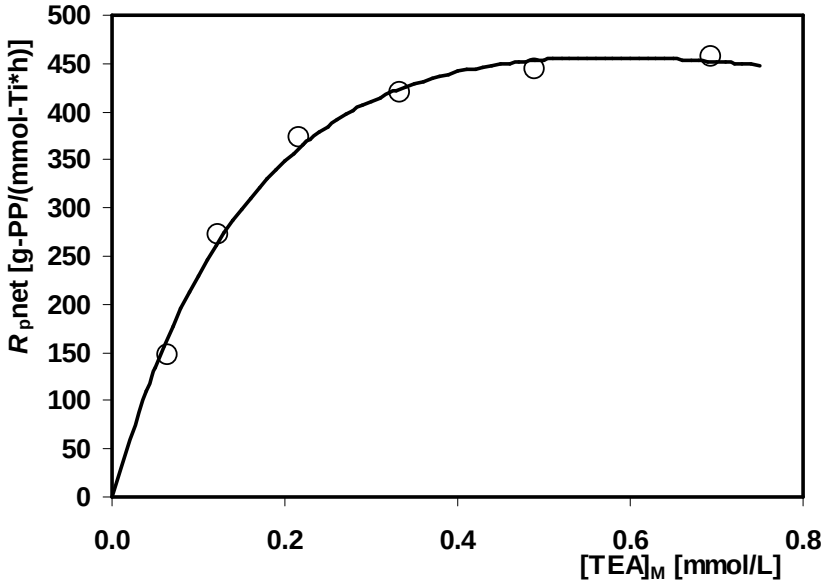

Figure 9: *Dependence of net polymerization rate on initial concentration of monomeric TEA fitted by Langmuir-Hinshelwood equation.*

It is obvious from Figure 9 that the concentration of monomeric TEA ca. 0.4 mmol/L (total TEA amount ca. 5 mmol/L) is the limiting concentration. Further TEA concentration enhancement to ca. 0.7 mmol/L (total TEA amount ca. 20 mmol/L) does not cause a significant change in overall polymerization rate. Nevertheless, the decrease in polymerization rate with further increasing of TEA could be predicted on the basis of the Langmuir-Hinshelwood model.

The distribution of the stereosequences, shown in Table 6, originated from the ^{13}C-NMR analyses of polymer prepared at different initial TEA concentrations (without presence of external donor) reveal only a slight decrease in the portion of isotactic pentad (*mmmm*) with the increased TEA concentration (Figure 10). The difference of the *mmmm* pentad amount between the two limiting concentrations is less than 2 %, exhibiting relatively high values around 92 mol.-%. This indicates that the extraction of internal donor by the cocatalyst is very limited for the studied di-ester type catalyst at 30℃. Also other researchers [43,5 3,93] have proven that the extraction of di-ester internal donor as DIBP (di-*i*-butyl phthalate) is much more difficult and slower than in the case of mono-ester EB (ethyl benzoate) internal donor.

Table 6: *Stereosequence distribution in polymer samples prepared at different initial TEA concentrations.*

Exp. No.	AC142	AC138	AC141	AC135	AC131	AC140
$[TEA]_0$	0.2	0.7	1.9	4.4	9.4	18.5
$[TEA]_M$	0.07	0.12	0.22	0.33	0.49	0.69
mmmm	92.7	92.1	92.0	91.8	91.1	91.2
mmmr	1.7	2.2	2.3	1.9	1.9	2.0
rmmr	0.2	0.2	0.2	0.2	0.3	0.2
mmrr	1.5	1.5	1.6	1.9	1.9	1.9
mrmm+ rmrr	0.7	0.7	0.6	0.9	0.8	0.9
rmrm	0.1	0.1	0.0	0.1	0.1	0.1
rrrr	1.4	1.5	1.7	1.5	1.7	1.7
rrrm	0.9	1.0	0.8	0.9	1.0	1.0
mrrm	0.9	0.8	0.7	0.9	1.1	0.9

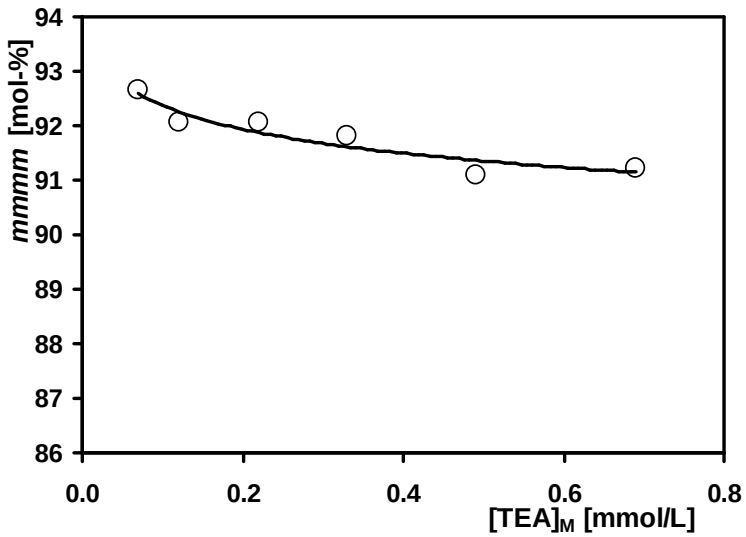

Figure 10: *Dependence of portion of isotactic pentad (mmmm) on initial concentration of monomeric TEA. Experimental conditions are same as those in Table 5.*

5.2.2 Impact of Initial TEA Concentration on Polymerization Kinetics

Presented study was focused on the investigation of TEA cocatalyst influence on the kinetics of $MgCl_2$-supported $TiCl_4$ catalyst under low temperature (30℃) and atmospheric pressure. A set of 60 min polymerization runs with different initial TEA concentrations was performed for this purpose. The polymerization kinetic profile was determined on the basis of monomer consumption and calculation of its solubility in *n*-heptane (see Chapter 4.1.6) within the first 30 min of polymerization. Consequently, the determined kinetic data were described by the mathematical kinetic function presented in Chapter 4.1.7.

The resulting optimized function parameters (n, $R_p(0)f$, K_D, k_a, $R_p(0)s$) are summarized in Table 7 and Figure 11. During the optimization the order of deactivation of unstable sites (parameter n in function (23) was restricted to the range between one and three. The parameter k_{ds} was excluded from the optimization and set up close to zero, because no deactivation of the stable active sites described by the function (25) occurred during the first 30 min of polymerization.

Consequently, the set of short-time experiments at three selected TEA concentrations with precisely measured polymerization time were employed for the determination of the initial kinetic profiles during the first 2 min of polymerization. The advantage of the method is that the resulting initial kinetic profiles are not dependent on material balance calculations. Therefore, they are not affected by non-stationary conditions in initial stages of polymerization such as the kinetic profiles determined from monomer consumption and material balance calculations. So, the exact information about the catalyst behavior in the first seconds of polymerization could be observed. More information about the procedure could be found in Chapters 4.1.3 and 4.1.6.

Then the complementation of initial kinetics from short-time experiments with kinetics assessed via monomer consumption allows determining of the overall kinetic profile from the first seconds to 30 min of polymerization (Figure 12 and Figure 13). The comparison of both methods is depicted in Figure 11, where it is apparent that the catalytic system exhibits a significant influence of TEA concentration on initial polymerization rate ($R_p(0)max$). As it is shown in Table 7 the increasing initial concentration of monomer TEA influences mainly the parameters describing the unstable sites (n, $R_p(0)f$, K_D). This exhibits namely Figure 14 showing also the difference between the initial polymerization kinetics evaluated from basic monomer consumption data (BB) and from the data complemented with determined initial kinetics (BB+AC). The catalyst exhibits very high initial activities, followed by a rapid deceleration during the first 30 s of polymerization. From Figure 14 it is obvious that these high initial activities would not be possible to determine by using conventional monomer consumption method, because of the unsteady conditions during the first minute of polymerization, where the correct calculation of actual monomer solubility in *n*-heptane is not possible.

The reasons of the catalyst deactivation and the order of the deactivation constant are not still fully understood and were investigated by many authors (see Chapters 2.1.1 and 2.1.2). Barbè et al. [128] postulated that the effect that the cocatalyst has on polymerization kinetics is impossible to generalize, because of the many factors

influencing it (catalyst and cocatalyst type, experimental conditions etc.). Formerly Keii et al. [19] performed a study under similar conditions (41℃, low pressure) with $MgCl_2$-supported $TiCl_4$/EB/TEA, proposing that the third order decay is suitable for the description of initial stages of polymerization, followed by the second and first order at the later stages of polymerization, respectively. Further, the experiments in liquid propene performed by Samson et al. [133] for the investigation of the influence of temperature on the order of deactivation were published. They found that the order of deactivation linearly decreases from the third to first order with the increasing polymerization temperature in the range of 27 – 67°C. They proposed the explanation that the deactivation could occur by different ways depending on polymerization temperature. Unfortunately the isothermal calorimetry applied by Samson et al. [133] does not purvey the information about the early stage of polymerization.

Results presented in Table 7 and Figure 11 show that the order of deactivation of unstable sites (parameter *n*) is dependent on the initial TEA concentration, increasing from the second order at low TEA concentration and reaching the third order at the concentration of monomeric TEA ca. 0.5 mmol/L (total 10 mmol/L). This finding is in basic agreement with observations published by Keii et al. [19] and Samson et al. [133]. The determined changing order of deactivation indicates that besides the catalyst deactivation resulting from the interaction with TEA (Ti reduction to inactive form [5,17,19,21]), also other mechanisms occur at the same time (mainly formation of dormant sites in the system without hydrogen [18,32-34]). So, in accordance with Barbè et al. [128], the complex order of deactivation in heterogeneous Ziegler-Natta catalysts could not be described by the simple first or second order model.

Table 7: *Comparison of optimized parameters of mathematical function applied for the kinetic profile description at various initial TEA concentrations (parameter k_{ds} is excluded from optimization). The kinetics was determined from the first 30 min of polymerization. SD is the value of resulting standard deviation. Polymerization conditions: temperature 30℃; atm. p ressure; heptane 180 mL; propene 0.61 mol/L; catalyst amount 11.2 µmol-Ti.*

Exp. No.	$[TEA]_0$ [mmol/L]	$[TEA]_M$ [mmol/L]	$R_p(0)max^+$ [g-PP/(mmol-Ti*h)]	n-order	$R_p(0)f$ [g-PP/(mmol-Ti*h)]	K_D [mmol-Ti/m^3]	k_a [1/h]	$R_p(0)s$ [g-PP/(mmol-Ti*h)]	k_{ds} [1/h]	SD [g]
BB142	0.2	0.07	1162	1.9	958	38.3	3.0	204	1.0E-11	0.002
BB138	0.7	0.12	1110	2.0	837	23.2	13.3	273	1.0E-11	0.003
BB141	1.9	0.22	1218	2.3	878	4.9	34.6	341	1.0E-11	0.003
BB135	4.4	0.33	1726	2.3	1364	2.1	23.3	362	1.0E-11	0.002
BB131	9.4	0.49	2219	2.5	1869	0.9	17.7	350	1.0E-11	0.001
BB140	18.5	0.69	3877	2.5	3512	1.0	21.2	365	1.0E-11	0.002
AC3+BB138^{++}	0.7	0.12	1126	2.0	854	23.1	13.4	273	1.0E-11	0.003
AC2+BB135^{++}	4.4	0.33	3537	2.7	3189	1.1	28.5	348	1.0E-11	0.002
AC1+BB131^{++}	9.2	0.49	8103	2.9	7771	0.4	21.3	332	1.0E-11	0.002

$^+R_p(0)max = R_p(0)f + R_p(0)s$

$^{++}$Combination of short-time experiments (AC) with real-time kinetic data assessed via monomer consumption (BB).

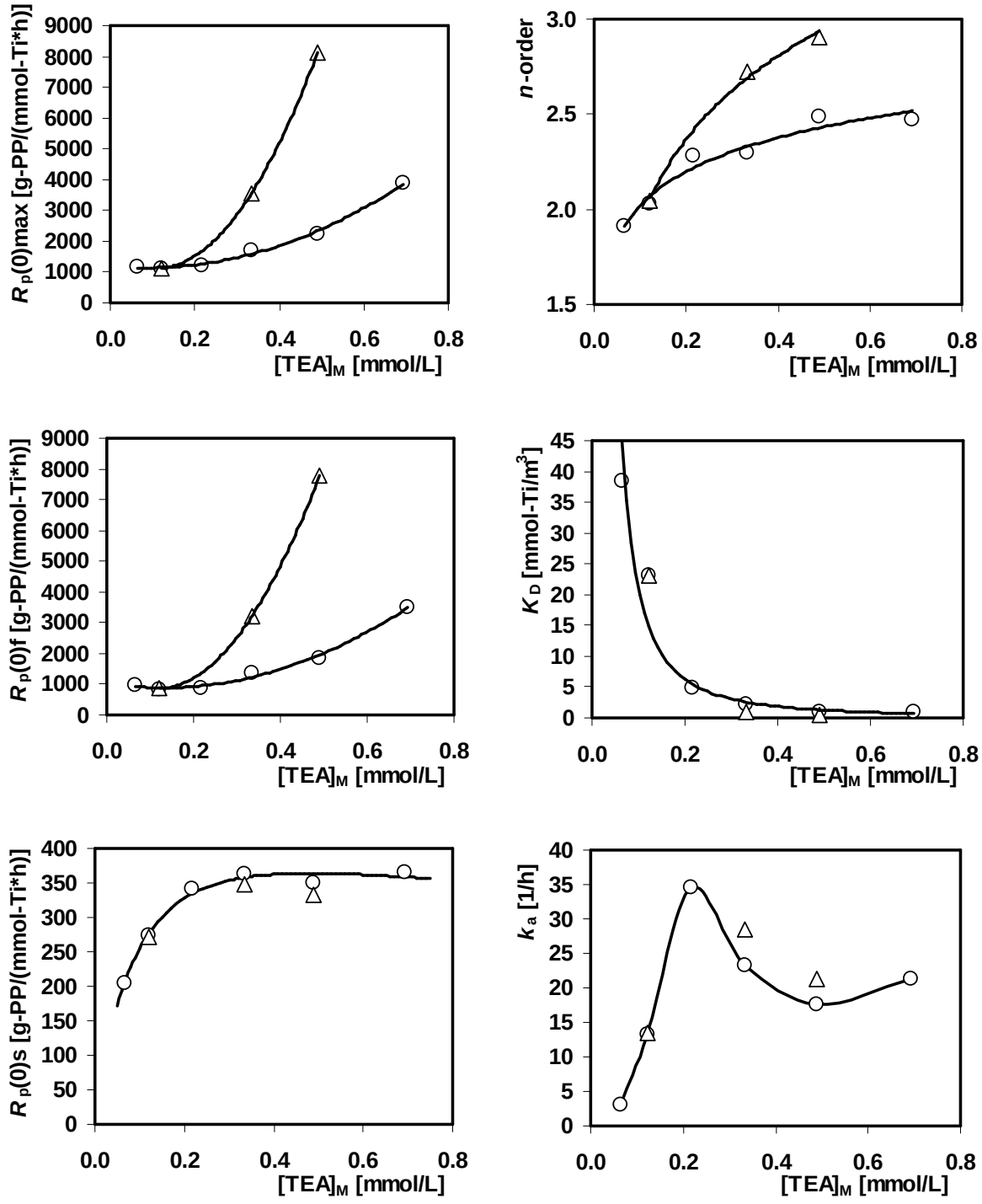

Figure 11: *Relation between the optimized values of mathematical function parameters (n, $R_p(0)f$, K_D, $R_p(0)s$, k_a) and initial concentration of monomeric TEA.* (○) *correspond to the parameter values determined only from the fitting of basic monomer consumption kinetic data;* (△) *parameter values were determined from the monomer consumption kinetics complemented with short-time experiments describing the initial kinetics.*

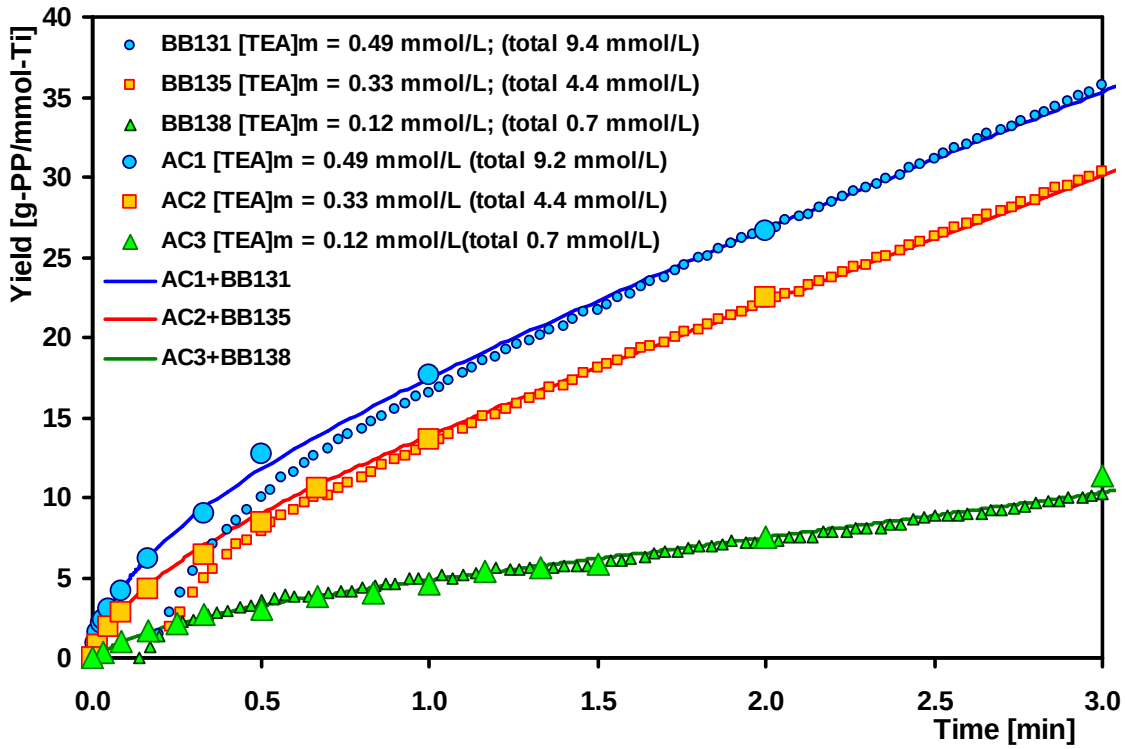

Figure 12: *Combination of initial kinetic profiles assessed via short-time experiments (AC) with kinetic data determined on the basis of monomer consumption (BB) fitted by kinetic mathematical function in integral form. Experimental conditions are same as those in Table 7.*

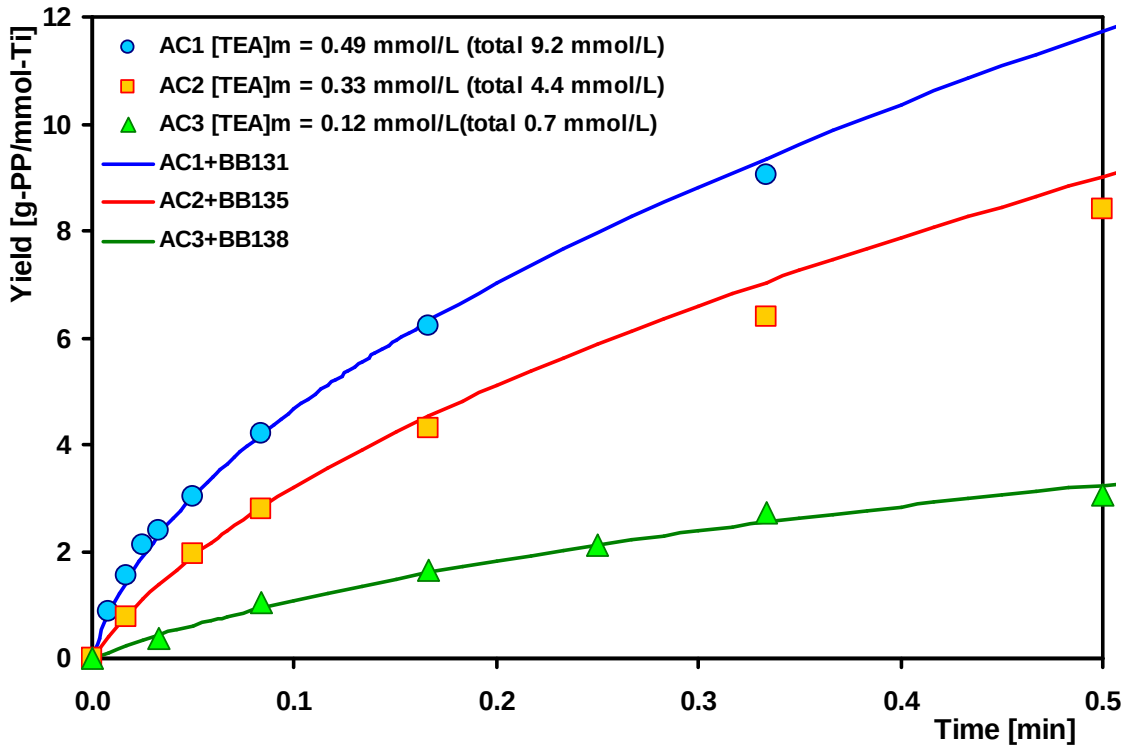

Figure 13: *More detailed insight on initial kinetic profiles determined by short-time experiments.*

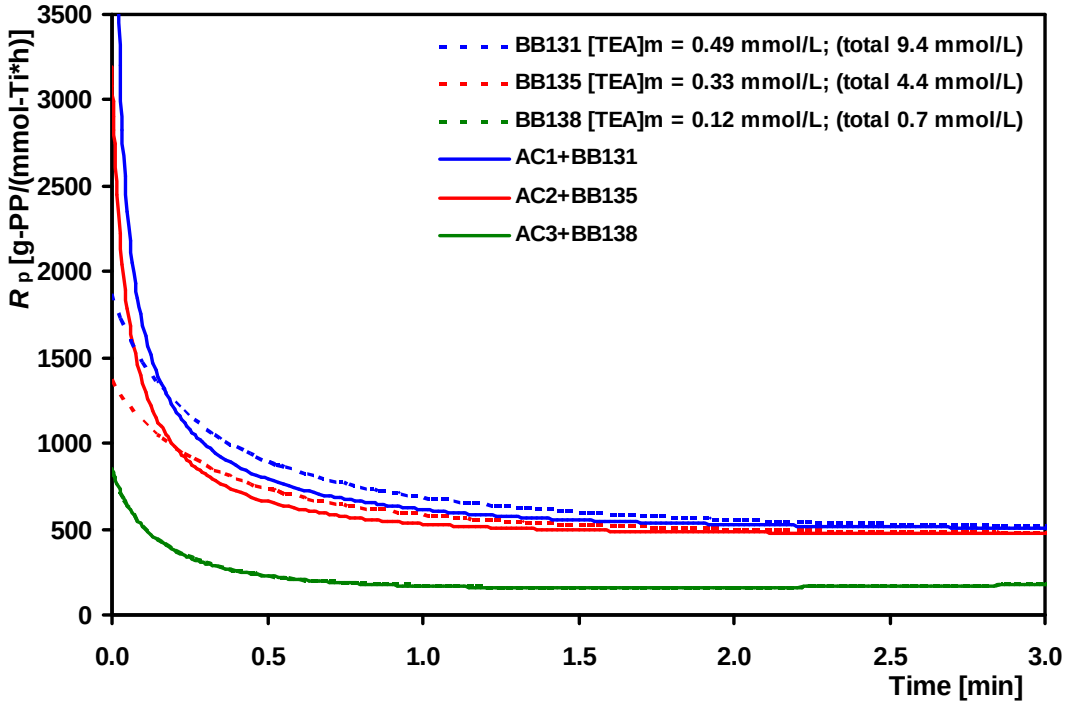

Figure 14: *Initial kinetic profiles determined from the monomer consumption kinetics (dashed lines) compared with kinetics evaluated with complemented short-time experiments (solid lines).*

The influence of the initial concentration of monomeric TEA on the kinetic profiles with $TiCl_4$/phthalate/$MgCl_2$ catalyst at 30℃ and low pressure is presented in Figure 15 (integral form) and Figure 16 (derived form) and the corresponding function parameters in Table 7 and Figure 11. It is obvious that the investigated catalyst exhibits the decay-type kinetics, which is typical for the $MgCl_2$-supported $TiCl_4$ catalysts activated by TEA [5,16,19,128,133]. Furthermore, the kinetics of the first 30 seconds of polymerization determined by short-time experiments presented in Figure 13, indicate very fast catalyst activation by the interaction with TEA cocatalyst, because the determined profiles do not reveal any activation period in the first seconds of polymerization. This corresponds to the results observed by Keii et al. [12,13] and recently by Terano et al. [14,15], showing that the formation of active sites at high-activity $MgCl_2$-supported $TiCl_4$ catalyst occurs within ~0.01 s.

The optimized function parameters $R_p(0)f$ and $R_p(0)s$ related to the initial concentration of dissociated TEA in Figure 11 show that the increase of cocatalyst concentration has the main impact on the value of polymerization rate of unstable sites $R_p(0)f$ exhibiting high initial polymerization rate followed by a fast deactivation during the first minute of polymerization. In the case of $R_p(0)s$, representing the active sites in the stable period of polymerization, the influence of TEA concentration could be found only at low concentrations, further enhancing beyond the ca. 0.4 mmol/L of monomer TEA (total amount ca. 5 mmol/L) does not lead to the noticeable change in $R_p(0)s$ value. As it was shown in previous Chapter 5.2.1, the monomer TEA concentration ca. 0.4 mmol/L (total TEA amount ca. 5 mmol/L) is the limiting concentration, after which the overall polymerization rate ($R_p$net) does not increase. So, it could be concluded that the increase of TEA concentration, beyond the ca. 0.4 mmol/L of monomer TEA, enhances only the initial polymerization rate. Then,

the accurate adjustment of initial TEA concentration could be applicable for the exact control of the catalyst behavior in the initial stage of polymerization.

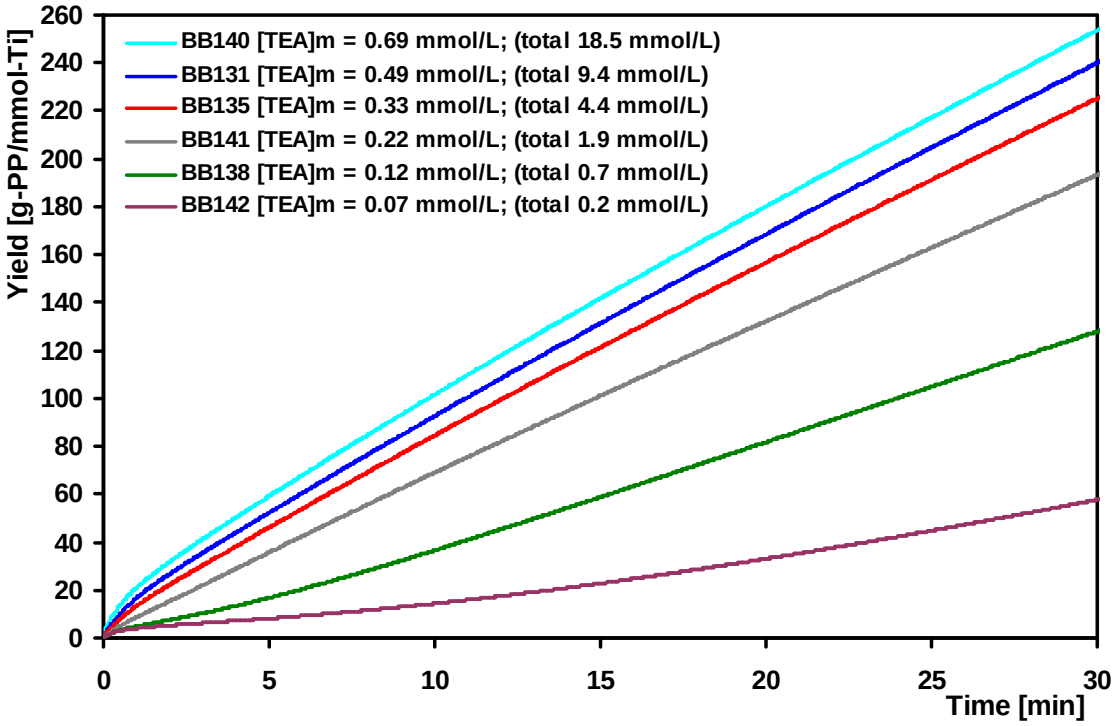

Figure 15: *Integral form of kinetic profiles with various initial TEA concentrations expressed as dependence of polymer yield on polymerization time. Polymerization conditions are the same as those in Table 7.*

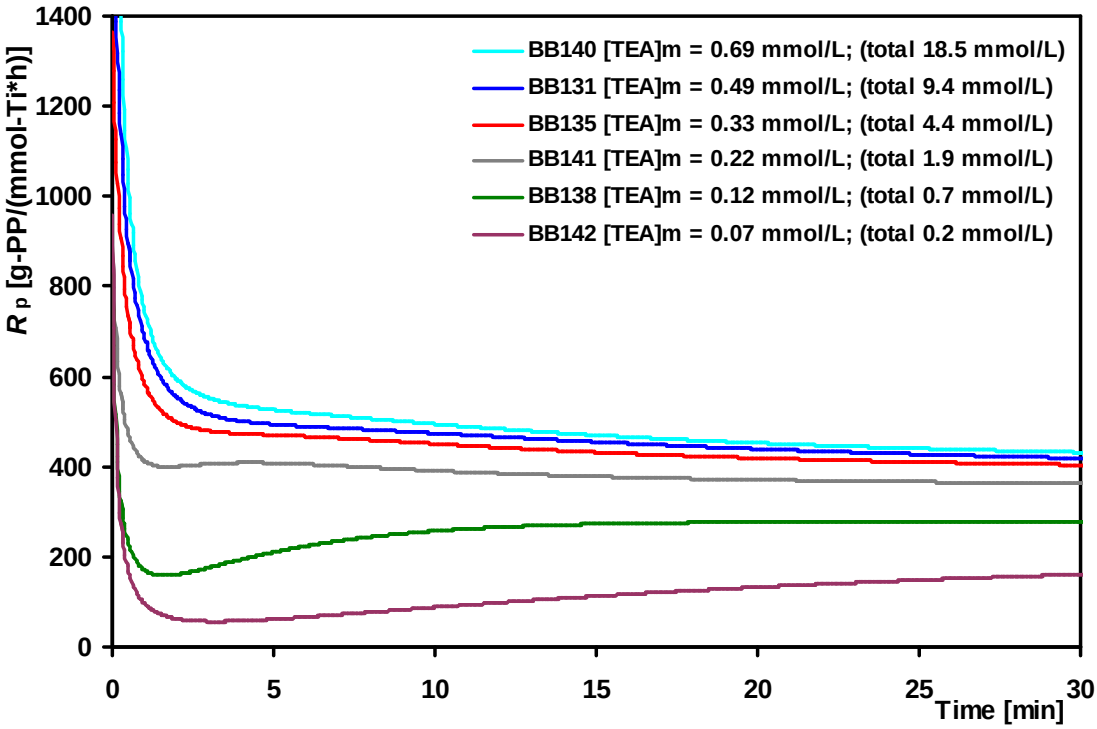

Figure 16: *Kinetic profiles expressed in derivative form as dependence of polymerization rate R_p on time.*

Kinetic profiles in the experiments performed at an initial TEA concentration lower than 0.4 mmol/L (total TEA amount 5 mmol/L), presented in Figure 15 and Figure 16, reveal a secondary increase in the polymerization rate. The observed phenomenon could be explained on the basis of the above-discussed existence of relatively stable TEA dimer under the applied experimental conditions (30℃, atm. pressure, slurry polymerizations in *n*-heptane), which is in equilibrium with the reactive monomeric form. So, it could be assumed that the amount of monomeric TEA at the low initial concentration is not sufficient for the interaction with all the available titanium tetrachloride molecules, which could be transformed into the propagative active sites. It means that all available monomeric TEA is quickly consumed for the initial catalyst activation, which leads to the disruption of TEA monomer-dimer equilibrium in the solution. Then the consumed monomeric TEA is replenished by the dissociation of dimeric TEA molecules. Consequently, the newly created monomer TEA cocatalyst could interact with the catalyst causing the secondary increase in polymerization rate. Whether or not the creation of new active sites or the transformation of the existing ones to the sites with higher activity is behind the secondary increase will be discussed in the following chapters.

To support the theory of an influence on the polymerization rate by TEA dissociation, several experiments at higher temperature were carried out, because it is presumed that the creation of new monomer TEA is controlled by temperature dependent dissociation [131,132]. The experiments were carried out at 40℃ with the monomer TEA concentration 0.12 mmol/L (total 0.7 mmol/L) under which the most obvious secondary increase was observed (Figure 16). Further diethylaluminium chloride (DEAC) was also applied as cocatalyst in the similar experiments. It is known that the DEAC forms very stable dimer molecules, bridged by its chlorine atoms, so almost all DEAC is present in dimer form in the solution and only traces are monomeric [130,134]. So if almost all DEAC molecules are supposed to be in dimeric form then it could be assumed that the catalyst activation with DEAC and the consequent kinetics are controlled by the dissociation rate of dimer DEAC molecules.

The high tendency of DEAC molecules to form the stable dimeric structures is supported by the *ab initio* calculations performed by Grůza [135] using the molecular modeling program, Spartan 02. He determined the most preferable conformations of the free and dimeric molecules and calculated the corresponding energies. The resulting difference between the energy of particular monomeric molecules and these molecules associated in the dimeric form is presented in Table 8. The negative energy indicates that the dimeric form has lower energy than free molecules, so the dimer-monomer equilibrium is more shifted to the dimeric form, mainly in the case of DEAC.

Table 8: *Difference between energies of monomer and dimer structures for TEA and DEAC molecules evaluated on the basis of ab initio calculations* [135].

Dimer structure	Interaction energy [kcal/mol]
TEA-TEA	-1.0
TEA-DEAC	-24.4
DEAC-DEAC	-58.9

Unfortunately any direct determination of the DEAC monomer-dimer equlibria and corresponding dissociation rate constants has not been found in the literature.

Table 9 summarizes the resulting net polymerization rates assessed from the final polymer yield obtained in the experiments performed at two different temperatures with TEA and DEAC as cocatalysts. It could be seen that, in the experiments with the DEAC as cocatalyst, very low catalyst activity was exhibited. The net polymerization rate is ca. 30 times lower than in the experiment with TEA at similar initial concentration (experiment BB131 in Table 5). This indicates that the DEAC has very limited ability to activate the catalyst. The application of higher polymerization temperature (40℃) causes the 50% increase in the p olymerization rate, however the value reached is still deeply below the activities observed in the case of the experiments with TEA.

Table 9: *Results from polymerization experiments performed at two different temperatures with TEA and DEAC as cocatalysts. Polymerization conditions: time 60 min; atm. pressure; heptane 180 mL; propene 0.61 mol/L; catalyst amount 12.1 μmol-Ti. $[Cocat.]_0$ – concentration of all introduced cocatalyst (formation of dimer structures is not considered); $[Cocat.]_M$ – calculated concentration of dissociated cocatalyst.*

Exp. No.	Cocatalyst type	T [℃]	K_{Diss} [+] [mol/L]	$[Cocat.]_0$ [mmol/L]	$[Cocat.]_M$ [mmol/L]	Yield [g]	$R_p$net [g-PP/(mmol-Ti*h)]
BB223	TEA	30	1.1E-04	0.7	0.12	3.358	281
BB224	TEA	40	1.9E-04	0.7	0.16	5.082	425
BB217	DEAC	30	---	9.6	---	0.167	14
BB218	DEAC	40	---	9.6	---	0.341	28

[+] Dissociation constants were calculated from empirical equation published by Černý et al. [132].

The kinetics from the polymerizations with TEA and DEAC as cocatalysts were described by the same mathematical equation, which was applied on the all previous kinetic data (see Chapter 4.1.7). Then the parameters k_a (rate constant of catalyst activation) and $R_p(0)$s (polymerization rate of stable sites at zero time) mediate to us the information about the intensity of the catalyst secondary activation after the initial deceleration period. Because no decrease in polymerization rate after the secondary activation was observed, the parameter k_{ds} (deactivation rate constant of stable sites) was excluded from the optimization and set up on the value close to zero. Then, the function describing the slow increase in polymerization rate (equation (24) in Chapter 4.1.7) is simplified, representing the basic first order reaction mechanism:

$$R_p(t) = R_p(0)\mathrm{s} \cdot (1 - \exp(-k_a \cdot t)) \tag{28}$$

$$Y(t) = \frac{R_p(0)\mathrm{s}}{(-k_a)} \cdot (\exp(-k_a \cdot t) - 1) \tag{29}$$

It was found that the slow secondary increase in polymerization rate observed in polymerizations with low TEA concentration could be described by the first order kinetic function with a good accuracy. Then, if we assume that the interaction of the monomeric TEA with catalyst occurs very fast, the dissociation rate of TEA dimer molecules could be considered as a rate determining step of the secondary activation, which corresponds to the first order reaction mechanism in accordance with the following chemical equation:

$$Al_2(C_2H_5)_6 \leftrightarrows 2\ Al(C_2H_5)_3$$

The resulting values of the parameter k_a and $R_p(0)$s for the experiments performed with TEA and DEAC as cocatalysts at two different temperatures are summarized in Table 10. Furthermore, the kinetic data indicate a possibility of the higher initial polymerization rate at higher temperature, however in the case of the experiment performed at 40℃ (BB 224) the values were not verified by short-time polymerizations. The comparison of the kinetic profiles determined at the polymerization temperature 30℃ and 40℃ using TEA as cocatalyst can be found in and Figure 18. It is assumed that the increase in the initial polymerization rate could be related mainly to the higher polymerization temperature, than to the increase in the initial concentration of monomeric TEA, because the change in the initial concentration of monomeric TEA is not very significant, as it is obvious from Table 9.

The kinetic profiles presented in and Figure 18 reveal that the increased temperature significantly increases the rate of secondary activation. The k_a value presented in Table 10 was enhanced by the factor 1.7 at temperature increase by 10℃. It is assumed that the faster secondary activation can be attributed to the enhanced rate of the TEA dimer dissociation.

Table 10: *Optimized kinetic parameters, describing determined polymerization profiles. Polymerization conditions are the same as those in Table 9.*

Exp. No.	Cocatalyst type	T [℃]	$R_p(0)$max [g-PP/(mmol-Ti*h)]	*n* -order	$R_p(0)$f [g-PP/(mmol-Ti*h)]	K_D [mmol-Ti/m^3]	**k_a [1/h]**	**$R_p(0)$s** [g-PP/(mmol-Ti*h)]	SD [g]
BB223	TEA	30	*877*	*2.0*	*587*	*22*	**16.8**	**290**	0.003
BB224	TEA	40	*1787*	*1.3*	*1371*	*185*	**28.4**	**416**	0.004
BB217	DEAC	30	---	---	---	---	**3.0**	**20**	0.002
BB218	DEAC	40	---	---	---	---	**5.5**	**34**	0.001

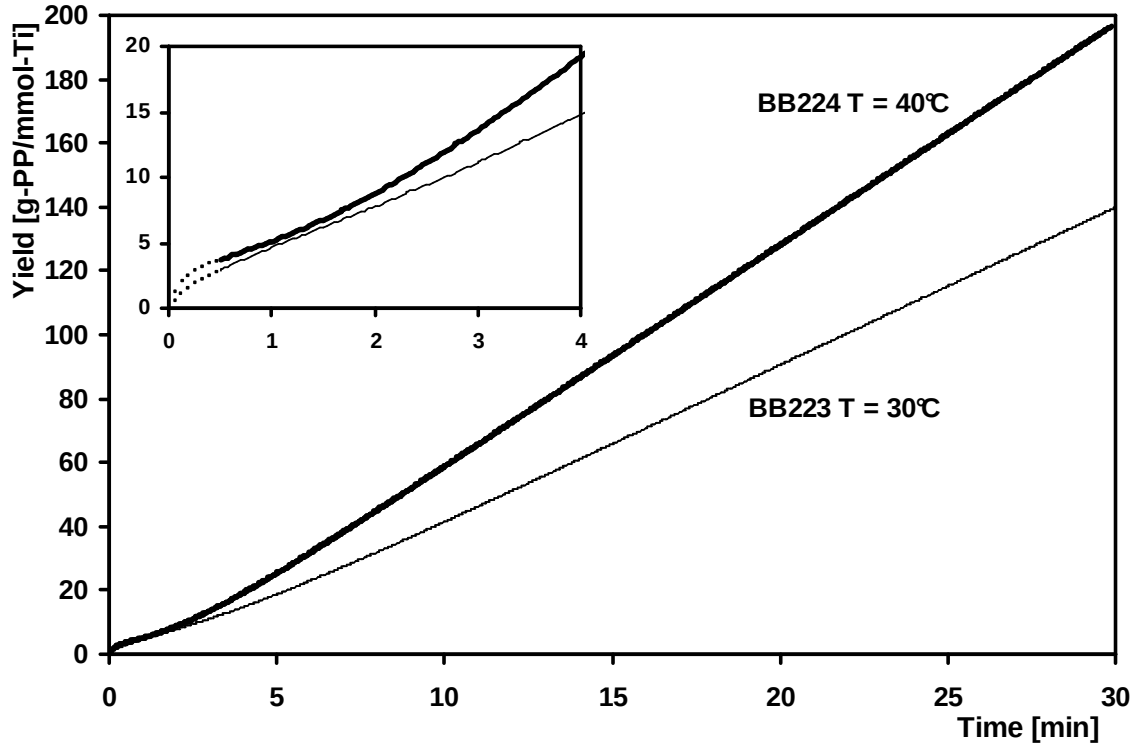

Figure 17: *Kinetic profiles of polymerizations performed with TEA as cocatalyst ($[TEA]_M$ = 0.12 mmol/L; $[TEA]_0$ = 0.7 mmol/L) at two different temperatures (integral expression). Polymerization conditions are the same as those in Table 9.*

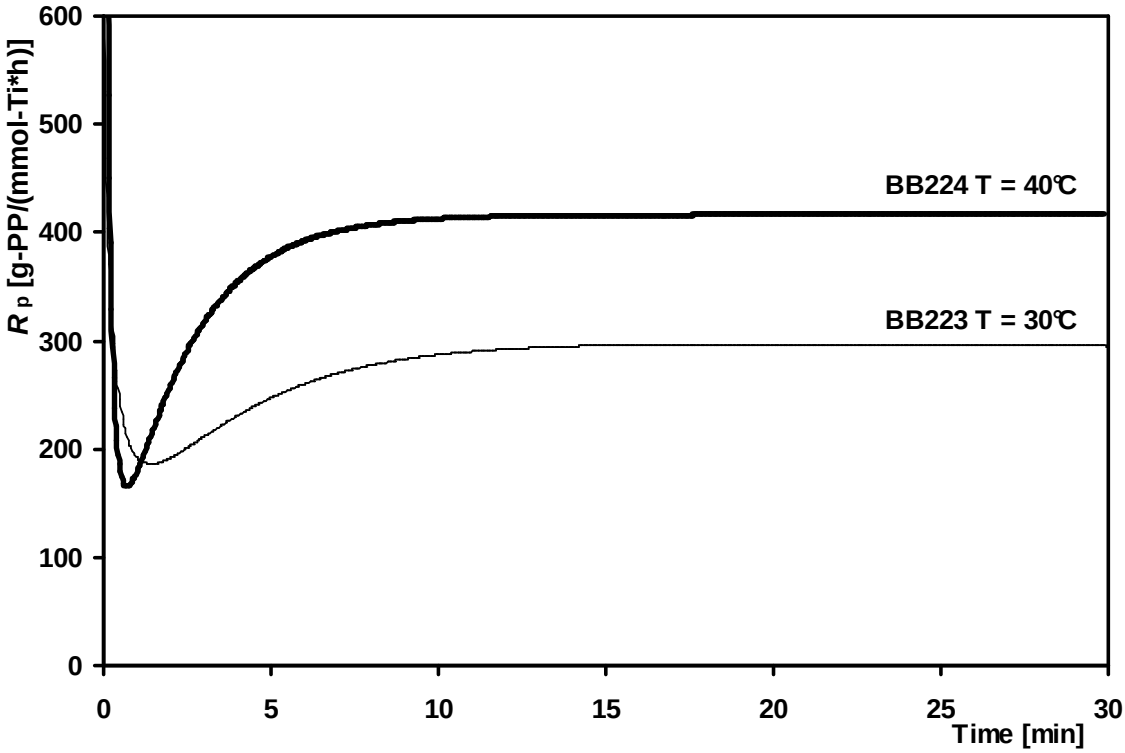

Figure 18: *Kinetic profiles of polymerizations performed with TEA as cocatalyst at two different temperatures expressed as dependence of polymerization rate on time (derivative form).*

The polymerizations with the DEAC as cocatalyst presented in Figure 19 and Figure 20 exhibit kinetics with a very slow activation profile. The acceleration period lasts ca. 30 min until it reaches the maximum of the polymerization rate. Because of the low polymerization rate and very slow catalyst activation, a longer time (60 min) was used for the determination of the kinetic profiles. The reason for the limited ability of the DEAC to activate the catalyst could be explained on the basis of the presumption that the DEAC molecules form a very stable dimeric complex and only a minor part is present in the monomeric form, which is able to create the active sites. Therefore, the observed activation-type kinetic profile is controlled by the rate of the DEAC dimer dissociation. This theory also supports the finding that the determined activation kinetics fits the first order equation (28). Further, the experiment performed at higher temperature (40℃) shows that the change in the temperature increases the rate of the catalyst activation k_a by the factor of 1.8, similar to the value determined in the case of TEA.

The similar kinetic behavior of the $MgCl_2$-supported $TiCl_4$ catalyst activated by DEAC was published by Mori et al. [24]. They assume that the low polymerization rates and activation-type kinetic profile are caused by the decreased ability of DEAC to create the active site precursors by reducing the titanium Ti (IV) to the lower oxidation state.

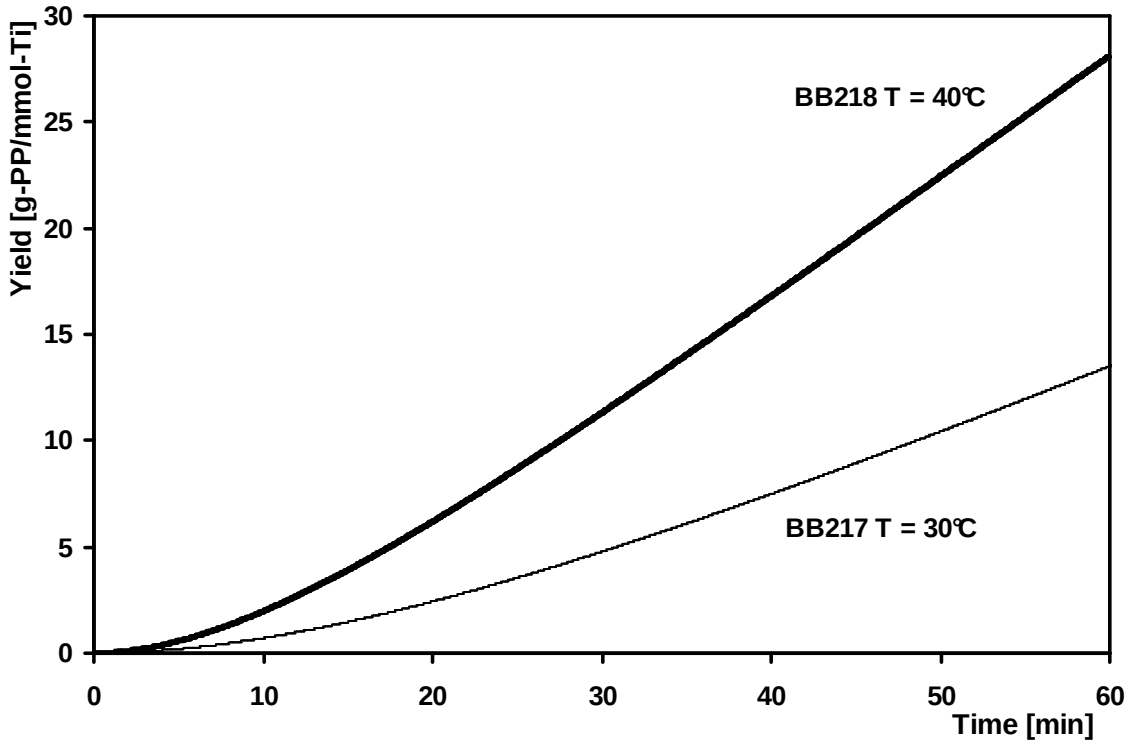

Figure 19: *Kinetic profiles of polymerizations performed with DEAC as cocatalyst ($[DEAC]_0$ = 9.6 mmol/L) at two different temperatures (integral expression). Polymerization conditions are the same as those in Table 9.*

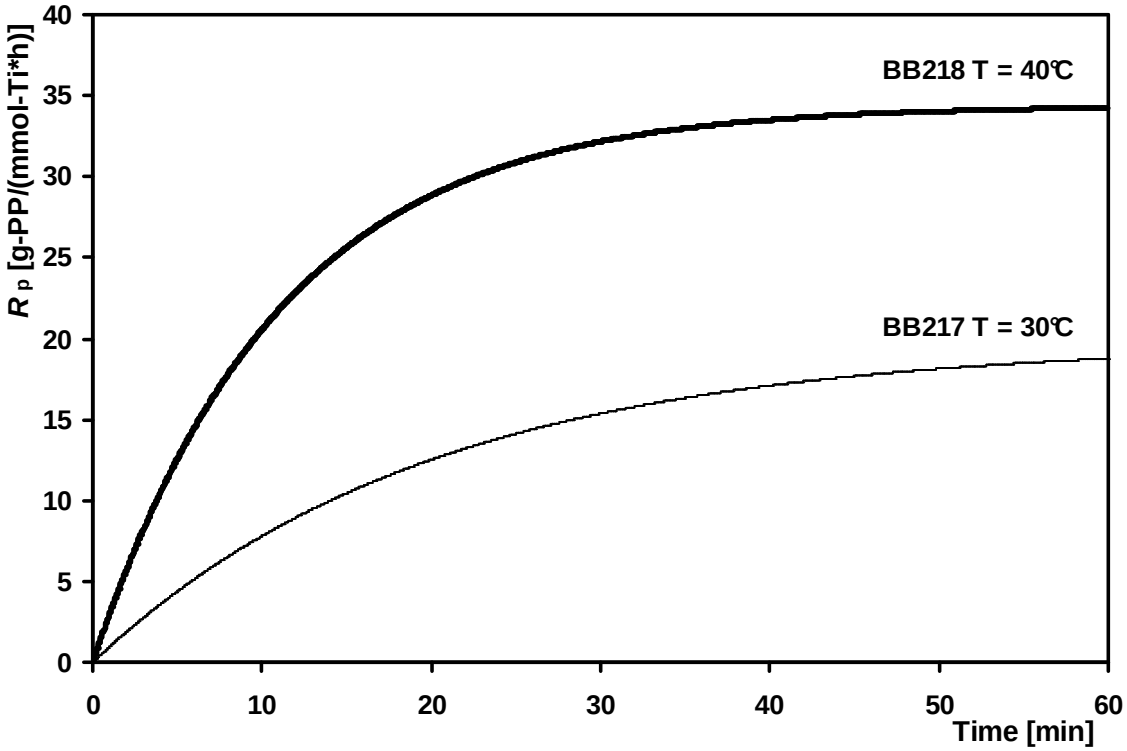

Figure 20: *Kinetic profiles of polymerizations performed with DEAC as cocatalyst at two different temperatures expressed as dependence of polymerization rate on time (derivative form).*

5.2.3 Impact of Initial TEA Concentration in Slurry on Catalyst and Polymer Properties

The investigation of the effect of applied conditions on the molecular weight distribution (MWD) of PP samples prepared on $MgCl_2$-supported $TiCl_4$ catalyst was published for example by Kashiwa et al. [106,107], Keii et. al [136], Chien et. al [137] and recently by Mori et. al [15]. A similar study was also performed by Marques et. al [59] in the ethene polymerization.

Keii et. al [136] presented that the number-average molar mass M_n of prepared PP samples remained unchanged during polymerization from 5 s to 3 h with $MgCl_2$/EB/$TiCl_4$ catalyst. Further they postulated that the Langmuir-Hinshelwood mechanism is suitable for the description of the M_n dependence on the TEA concentration:

$$\frac{1}{M_n} = k \cdot \left(\frac{K \cdot [A]_0}{1 + K \cdot [A]_0} \right) \tag{30}$$

where k and K are constants and $[A]_0$ initial concentration of TEA. However, they have also noted that the equation (30) is valid mainly for the experiments carried out at the higher TEA concentrations. Contrary to the time-independent M_n described by Keii et al. [136], Kashiwa et al. [106,107] presented results showing that the M_n and M_w values increase during the first 30 s of polymerization, then reach a constant value. The increase in M_n was also observed by Mori et. al [15] using the stopped-

-flow method. They found that the increase of M_n with the polymerization time occurs during a very short initial period ca. 0.4 s with the diester-type catalyst.

The polypropene samples from the first 120 s of polymerization assessed via the short-time experiments were utilized for the determination of number-average and weight-average molar mass by the GPC/SEC analysis. Resulting data for three different levels of initial TEA concentration are summarized in Table 11 accompanied by the calculations of the polymer sample polydispersity index (M_w/M_n) and number of macromolecules (*N*).

The dependence of M_n on polymerization time in Figure 21 reveals that the value of M_n increases intensively during the first ca. 30 s of polymerization. Then, the reached level of the constant molar mass could be related to the TEA amount present in the system at the beginning of polymerization. Also the dependence of M_w on time exhibits similar initial fast increase of molecular weight, but in the comparison with M_n, the slow gradual increase of M_w for the whole investigated period (Figure 22) was observed. This slow gradual M_w increase during the time period corresponding to the stable part of polymerization kinetics may be attributed to the change of the propagation and transfer rate coefficients with different length of polymer chains [5,136].

The comparison of the above described dependencies with the determined initial kinetic profiles presented in the previous Chapter 5.2.2 (Figure 14) shows that the end of the fast initial deceleration period, followed by the period of stable kinetics, corresponds to the moment when the polymer molar mass M_n becomes time-independent. So, on the basis of the presented observations, the theory proposed by Mori et al. [15] could be accepted for the explanation. It is assumed that the two basic types of active sites are formed on the $MgCl_2$-supported $TiCl_4$ catalyst, each producing polymer with different MWD:

I. Unstable sites exhibiting high polymerization rate and fast deactivation, which occur during the first seconds of polymerization. These sites are responsible for the producing of low-molecular weight polymer.
II. Sites with slower activation and stable polymerization kinetics, producing polymer with higher molecular weight.

Therefor the initial increase of molecular weight corresponds to the decrease of the amount of unstable sites, which are replaced by the stable sites with lower polymerization rate, but a higher molecular weight of resulting polymer.

Further, Figure 21 and Figure 22 show that the higher initial TEA concentration causes the increase in the final value of polymer molecular weight reached after the initial increase period. This observation is opposite to the data published by other authors [136,137] showing the decrease of molecular weight with increasing TEA concentration, which is explained by the enhanced transfer reactions with the cocatalyst. The reason for the different catalyst behavior could be found in the differences between the studied types of catalysts and conditions under which the polymerizations were carried out. The presented observation will be further discussed in the subsequent text.

The polydispersity index (M_w/M_n) exhibits similar time dependence as was presented in the case of M_n and M_w, showing the fast increase during the first 30 s up to the constant value around 6. Furthermore, from the Figure 23 it is also obvious

that the polydispersity index of samples prepared does not exhibit any significant influence of the initial TEA concentration on the MWD.

The determined relatively broad MWD (M_w/M_n increases from 2 to 6) is typical for $MgCl_2$-supported catalysts [5]. Formerly, three theories have been proposed as an explanation for the MWD broadening over time [5,136]:

I. Change in the rate constants for the propagation and transfer reactions at different polymer chain length;
II. non-uniform surface sites;
III. limitation of the monomer diffusion through the polymer layer covering the catalyst surface.

The latter one was formerly discounted by Keii et al. [19]. So, only the first two theories could be considered as reasons for the MWD broadening in the presented polymerizations. Further Keii et at. [136] found that the hydrogen does not influence the M_w/M_n values, which indicates that the theory based on non-uniformity of active sites is the most plausible cause for the explanation of MWD broadening. Also the recent studies performed by Terano et al. [6], using stopped-flow technique, implies that the MWD broadening at early stages of polymerization (<1 s) is caused by the existence of the non-uniform active sites in the system. However the direct distinguishing, which mechanism is responsible for the MWD broadening in the case of presented experiments would not be well founded, but it seems that the initial intensive M_w/M_n increase could be related to the decrease of the amount of unstable sites producing the polymer with different MWD.

Table 11: *Values of number-average M_n and weight-average M_w molar mass from GPC/SEC analysis of polymer samples from short-time experiments, accompanied by calculations of polydispersity index M_w/M_n and number of macromolecules N. Polymerization conditions: temperature 30℃; atm. pressure; heptane 180 mL; propene 0.61 mol/L; catalyst amount 11.2 µmol-Ti.*

Initial TEA concentration AC1: $[TEA]_M$ = 0.49 mmol/L; $[TEA]_0$ = 9.2 mmol/L

Exp. No.	Time [s]	Yield [g-PP/mmol-Ti]	M_n*10^{-3} [g/mol]	M_w*10^{-3} [g/mol]	M_w/M_n	*N* [mol/mol-Ti]
AC 79	1	1.5	75	208	2.9	0.021
AC 74	2	2.4	70	155	2.2	0.034
AC 71	5	4.2	94	255	2.7	0.044
AC 64	10	6.3	100	349	3.5	0.064
AC 73	20	9.0	101	450	4.2	0.089
AC 69	30	12.7	105	513	5.0	0.120
AC 67	60	18.0	118	646	5.5	0.152
AC 94	120	27.3	108	678	6.4	0.252

Initial TEA concentration AC2: $[TEA]_M$ = 0.33 mmol/L; $[TEA]_0$ = 4.4 mmol/L

Exp. No.	Time [s]	Yield [g-PP/mmol-Ti]	M_n*10^{-3} [g/mol]	M_w*10^{-3} [g/mol]	M_w/M_n	*N* [mol/mol-Ti]
AC 87	3	1.9	61	245	4.0	0.032
AC 81	5	2.8	78	291	3.7	0.036
AC 83	10	4.3	81	362	4.4	0.053
AC 80	20	6.4	91	435	4.8	0.071
AC 86	30	8.4	85	519	5.5	0.100
AC 88	40	10.5	96	477	5.0	0.114
AC 82	60	13.6	88	601	6.9	0.155
AC 84	120	22.5	106	711	6.7	0.212

Initial TEA concentration AC3: $[TEA]_M$ = 0.12 mmol/L; $[TEA]_0$ = 0.7 mmol/L

Exp. No.	Time [s]	Yield [g-PP/mmol-Ti]	M_n*10^{-3} [g/mol]	M_w*10^{-3} [g/mol]	M_w/M_n	*N* [mol/mol-Ti]
AC96	5	1.0	68	259	3.8	0.014
AC111	10	1.6	87	321	3.7	0.019
AC98	15	2.1	79	371	4.7	0.027
AC99	30	3.1	82	427	5.2	0.037
AC101	40	3.7	89	434	4.9	0.041
AC108	80	5.6	90	486	5.4	0.062
AC103	120	7.6	94	566	6.0	0.081
AC 139	300	17.9	101	660	6.5	0.177

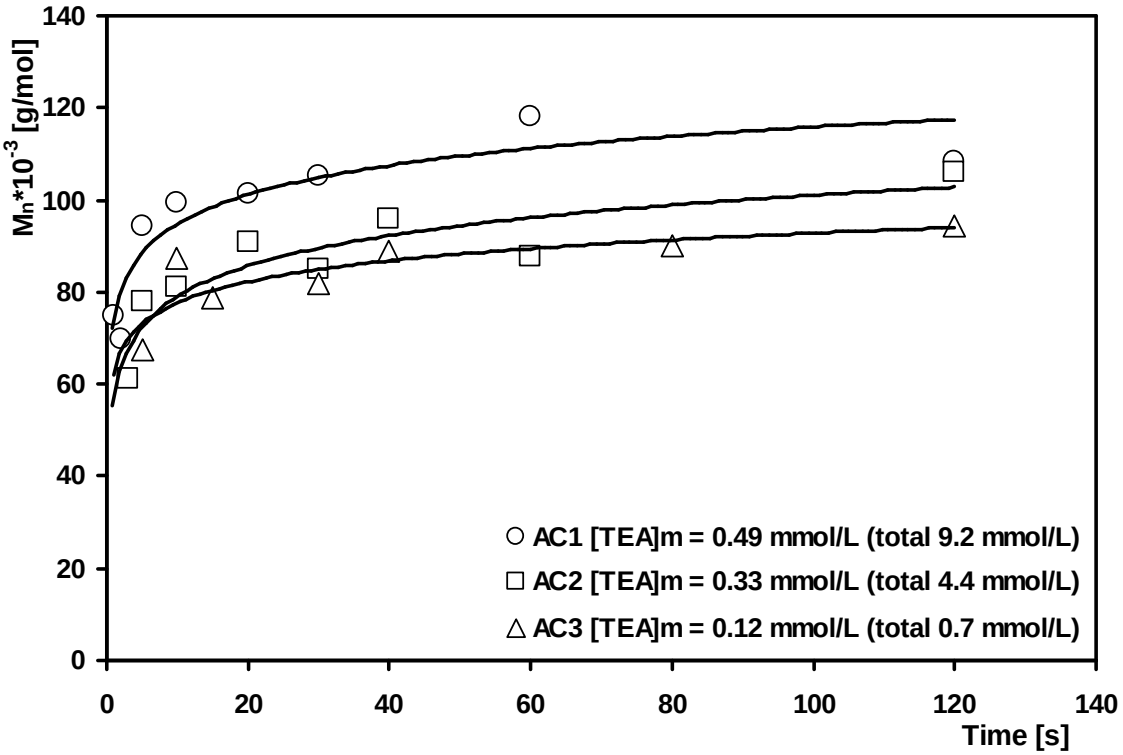

Figure 21: *Dependence of number-average molar mass M_n on polymerization time for three levels of initial TEA concentration.*

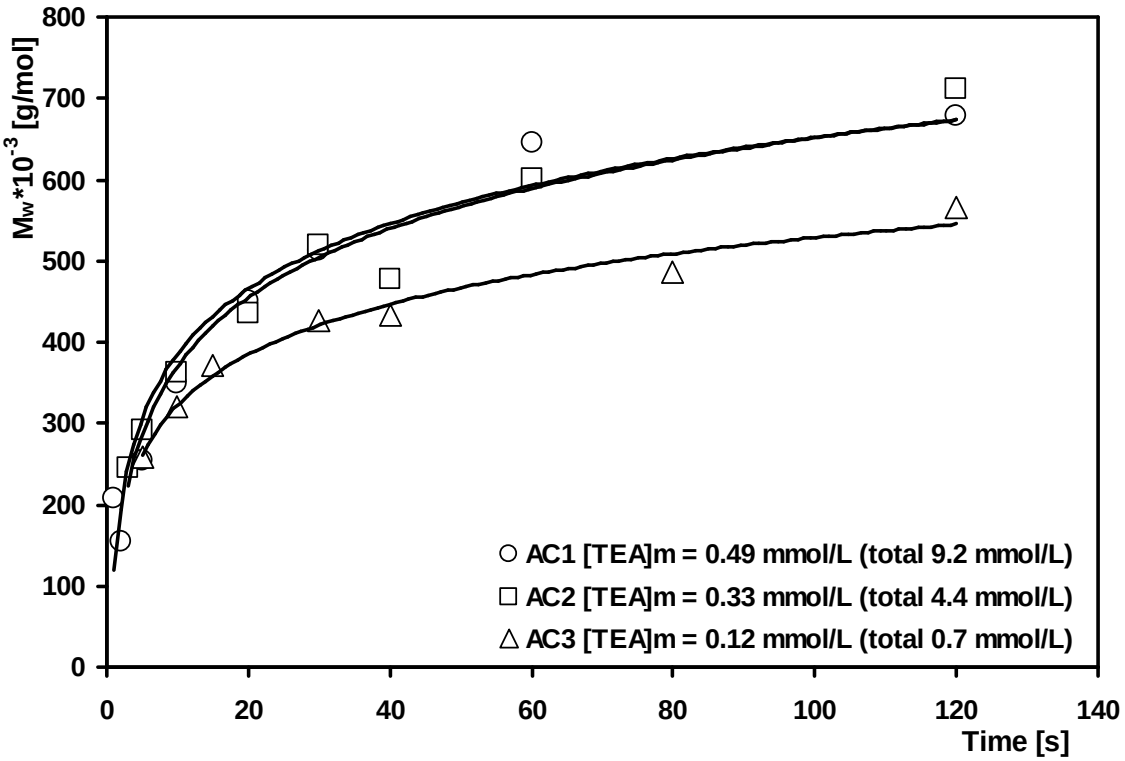

Figure 22: *Dependence of weight-average molar mass M_w on polymerization time for three levels of initial TEA concentration.*

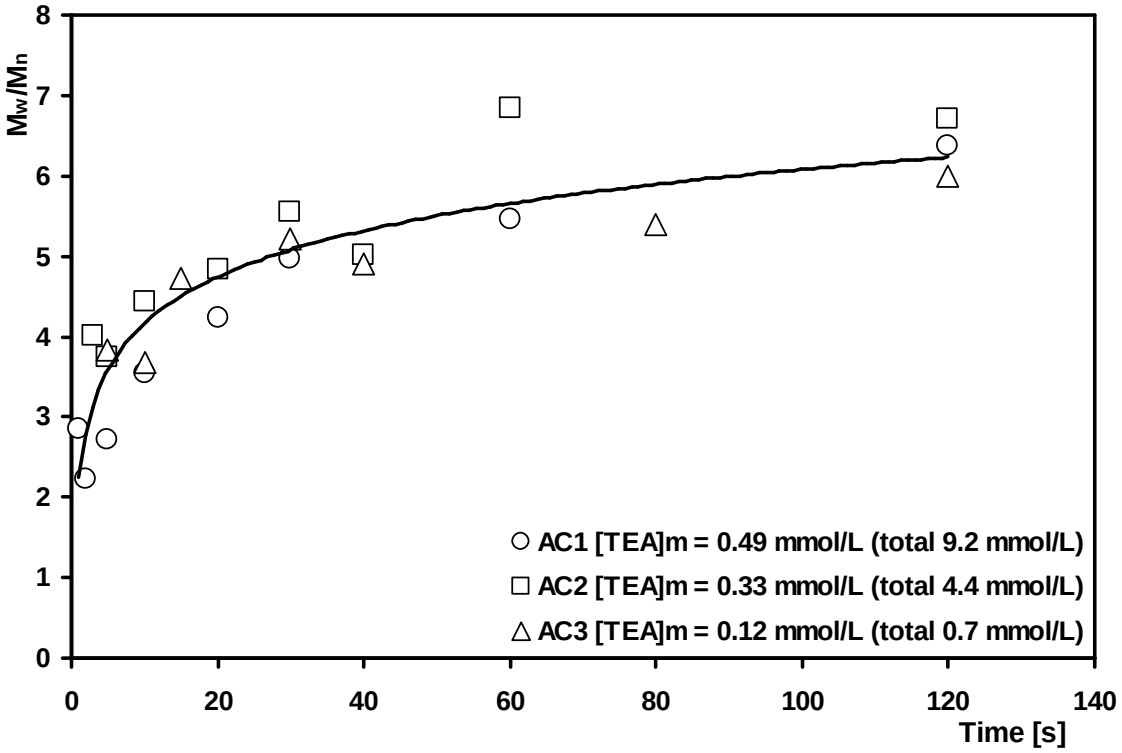

Figure 23: *Dependence of polydispersity index M_w/M_n on polymerization time for three levels of initial TEA concentration.*

From the determined number-average molar mass M_n divided by the corresponding polymer yield and catalyst amount, the average number of macromolecules was evaluated (equation (16) in Chapter 2.4.1.2.1). Then the dependence of the number of macromolecules versus polymer yield is suitable for the determination of the average number of active sites present in the system at the beginning of polymerization. The described procedure for the evaluation of the number of active sites was formerly applied by many authors and has been a subject of several reviews (for example Tait [97] and Mejzlík et al. [98]). More detailed description of the applied technique could be found in Chapter 2.4.1.2.1.

The average number of active sites is determined from the dependence of the number of macromolecules (*N*) on polymer yield, where the intercept of the linear extrapolation to zero yield corresponds to the average number of propagative centers formed at the beginning of polymerization and the slope of the linear dependence could be related to the intensity of transfer reactions. This procedure applied on the results obtained with varying TEA concentration presented in Figure 25 shows that only 1.1 % of all the introduced titanium tetrachloride was transformed into the active sites by the interaction with TEA cocatalyst.

The reason why only a minor part of all titanium atoms could create the propagative active sites could be explained on the basis of the “Island Model” proposed by Terano et al. [27,71]. It is assumed that the titanium tetrachloride molecules form surface monolayers, so-called “islands”, on the $MgCl_2$-support, where only the bordering Ti atoms have enough vacant positions for the growing polymer chain and coordination of monomer. In other words, only the bordering titanium species could be transformed into the active sites, the inner titanium atoms surrounded by other $TiCl_4$ molecules remain inactive. However, it must be pointed out that this is only a very simplified model, the catalyst particle morphology is in reality much more complicated.

In order to evaluate the number of active sites on ZN type catalysts, the wide range of experimental studies were performed using different techniques, as for example: stopped-flow technique [6], ^{14}CO inhibition [62,68] or tritiated methanol quenching [111]. Unfortunately, as it was formerly pointed out by Tait [97] and Mejzlík et al. [98,105], the direct comparison of the values of the number of active sites is not easy using different methods. The reason lies in the non-uniformity of active sites with different stability and reactivity to the labeling and quenching agents. Also the different catalyst preparation procedures and applied experimental conditions complicate the possible comparison of published results.

The data presented in Figure 25 indicate that the initial TEA concentration does not influence the number of active sites created. So, even the lowest TEA concentration is still sufficient for an activation of all active site precursors. However, as it was discussed above in Chapter 5.2.2, the initial TEA concentration has a direct impact on initial and overall polymerization rate. So, if all the generable active sites are created, even at very low TEA concentrations at which the catalyst exhibits significantly lower polymerization rate, only the existence of at least two different forms of one type of active site is suitable for the explanation of the observed catalyst behavior. The presented results show that the increase of TEA concentration enhances significantly the polymerization rate of the active sites. So, this implies that

the excess of TEA could form the bimetallic complexes with the active sites exhibiting higher rate of monomer insertion (rate of propagation). At low TEA concentrations, the amount of free monomeric TEA is still sufficient for the activation of all active site precursors, but it is not sufficient to create the bimetallic complexes with higher polymerization rate. The computed molar ratios between monomeric TEA and titanium could be found in Table 12. Therefor, the observed secondary increase in the polymerization rate in the case of the low TEA concentrations presented in Chapter 5.2.2 (Figure 15, Figure 16) could be explained by the interaction of newly dissociated monomeric TEA molecules with the initially created monometallic active sites, causing the consequent increase in polymerization rate.

The existence of the active sites with coordinated alkylaluminium molecule was firstly proposed by Rodriguez and van Looy [96]. Then Kohara et al. [51] gave the first experimental evidence about the existence of bimetallic complexes of titanium ion and organometallic cocatalyst by the replacing of organometallic compounds ($AlEt_3 \rightarrow ZnEt_2$) during the polymerization. Further Xu et al. [52] postulated that there is equilibrium between the monometallic and bimetallic active sites responsible for formation of stereoblock polymer structures.

From the presented results it could be also assumed that the ratio between the monometallic and bimetallic active sites is controlled by the cocatalyst concentration, increasing the amount of bimetallic active sites at higher TEA concentrations.

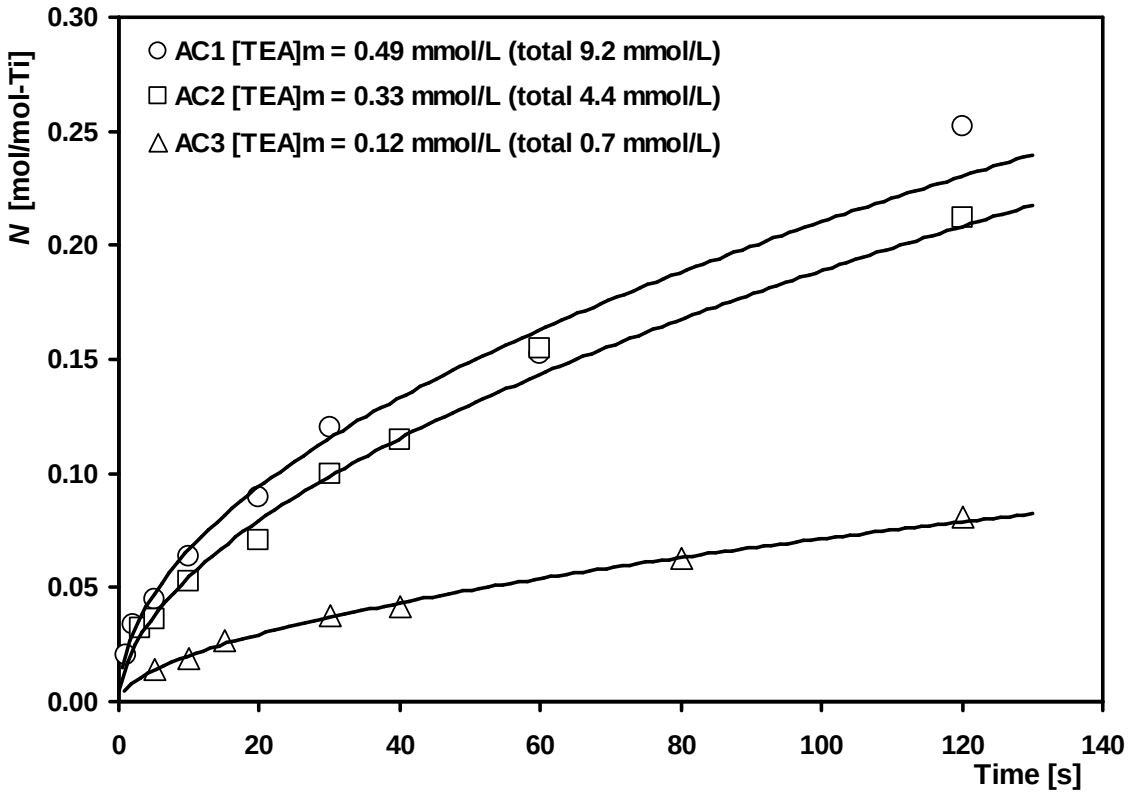

Figure 24: *Dependence of number of macromolecules N on polymerization time for three levels of initial TEA concentration.*

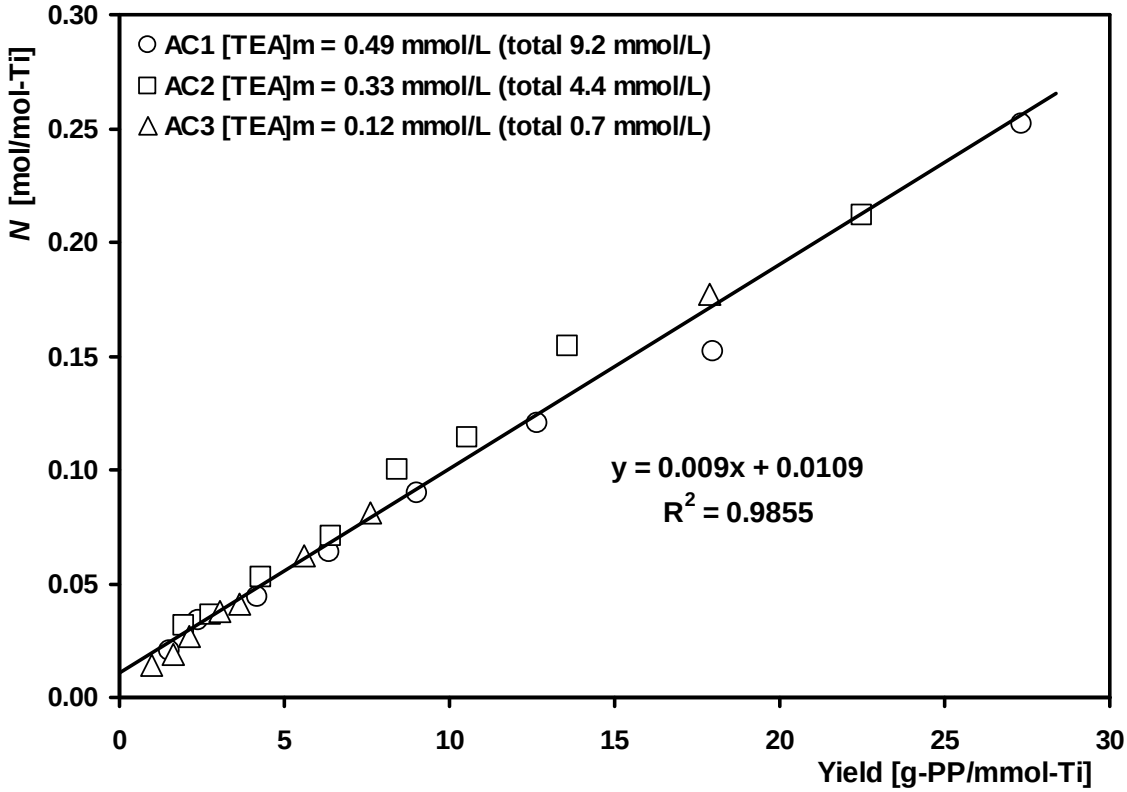

Figure 25: *Dependence of number of macromolecules N on polymer yield for three levels of initial TEA concentration with the determination of number of active sites by the extrapolation to zero yield.*

The dependence of the number of macromolecules on time shown in Figure 24 exhibits a similar profile corresponding to the polymerization kinetics presented in previous Chapter 5.2.2 (Figure 12 and Figure 13). This indicates that the increased amount of monomeric TEA causes the increase in the number of macromolecules created during the polymerization. However as it was shown in Figure 25, the enhanced TEA concentration did not lead to the creation of new active sites, so the increase in the number of macromolecules must be related to the increase of transfer reactions caused by the increased monomeric TEA concentration.

This presumption is supported in Figure 26, which shows the dependence of the number of macromolecules, created after 120 s of polymerization, on the concentration of monomeric TEA, where it is obvious that the increase of the number of macromolecules linearly depends on the concentration of monomeric TEA. This supports the theory that the TEA in monomeric form is required for the chain transfer. The similar presumption was proposed by several authors [5] investigating transfer reactions in the systems where the $AlEt_3$ and $ZnEt_2$ were applied as cocatalyst. They found that the chain transfer with $ZnEt_2$ is significantly higher probably due to the lower tendency of $ZnEt_2$ to form dimeric structures.

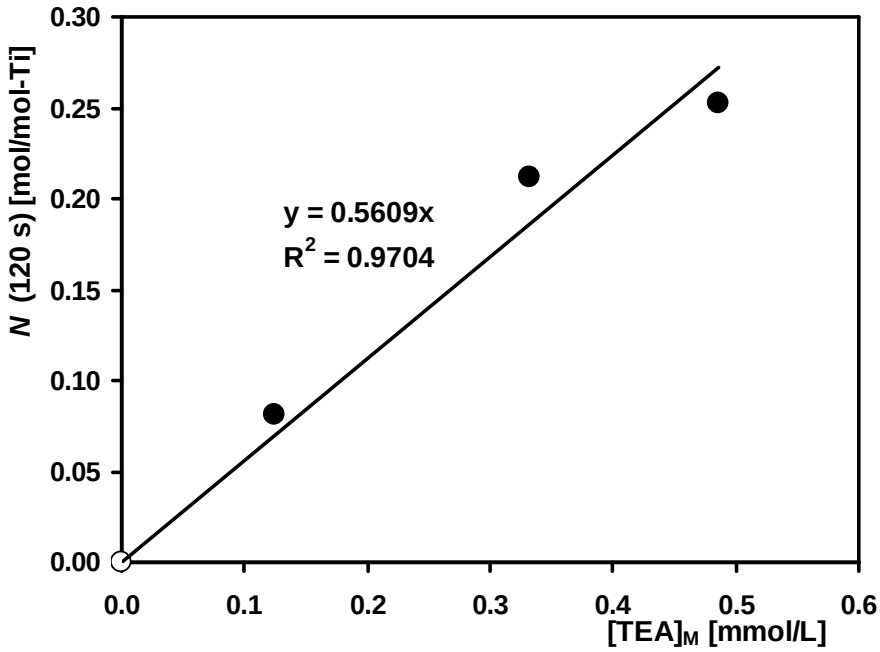

Figure 26: *Influence of the concentration of monomeric TEA on the number of macromolecules after the 120 s of polymerization.*

Apparently contradictious to the above conclusion could be considering the fact that the increasing TEA concentration does not lead to the noticeable change in the slope of the presented linear dependence of the number of macromolecules on polymerization yield (Figure 25). The dependence also corresponds to the intensity of transfer reactions occurring in the system as demonstrated by equation (16) in Chapter 2.4.1.2.1. However, the reasoning behind the alleged non-existing transfer with TEA could be explained in terms of the presumption that the change of the cocatalyst concentration influences in the same manner the transfer (k_{tr}) and the propagation rate (k_p) coefficients. Then the k_{tr}/k_p ratio in equation (16) remains constant, which in fact results in the constant slope of the dependence described in Figure 25.

Finally, the determined number of active sites combined with the value of the initial polymerization rate $R_p(0)max$ originated from the kinetics measurements allows calculation of the average propagation rate coefficient k_p using equation (15). The resulting values of k_p could be seen in Table 12, where it is apparent that the propagation rate coefficient increases significantly with the increasing TEA concentration. It could be assumed that the k_p value determined from the experiments performed with high TEA concentration corresponds to the propagation rate of sites being mainly in bimetallic form and on contrary the k_p determined from the experiments with low TEA concentration corresponds to the monometallic active sites. Then from the Table 12 it is apparent that the propagation rate coefficient for the bimetallic sites is ca. 8 times higher than the k_p coefficient belonging to the monometallic ones.

Table 12: *Calculated values of average propagation rate coefficients k_p for the three different initial TEA concentrations.*

Exp. No.	$[TEA]_0$	$[TEA]_M$	$[TEA]_M$/Ti	C*	$R_p(0)$max		k_p*10^{-3}
	[mmol/L]	[mmol/L]		[mol.-%]	[kg-PP/(mmol-Ti*h)]	[mol-C_3H_6/(mol-Ti*s)]	[L/(mol*s)]
AC1	9.2	0.49	8	1.1	8.1	53	8.0
AC2	4.4	0.33	5	1.1	3.5	23	3.5
AC3	0.7	0.12	2	1.1	1.1	8	1.1

On the basis of presented results it is possible to explain the observed higher molecular weights at higher TEA concentration (Figure 21 and Figure 22). Now it seems that the TEA molecule coordinated on the titanium ion could stabilize the active site leading to the increase of the molecular weight of produced polymer.

Moreover, for the investigation of the TEA cocatalyst influence on the microstructure of polymers prepared with different initial TEA concentration some selected polymer samples were also analyzed by ^{13}C-NMR measurement for the determination of the stereosequence distribution. The obtained data are summarized in Table 13 and the dependence of the amount of isotactic *mmmm* pentad on the polymerization time is presented in Figure 27. It is apparent that the polymer produced on the bimetallic active sites, which were created at the high excess of the TEA cocatalyst, exhibits higher stereoregularity at the beginning of polymerization. This observation indicates that the bimetallic sites with coordinated TEA molecule are more stereospecific than the monometallic sites created at low TEA concentration.

Table 13: *Determined stereosequence distribution (mol.-%) in polymers prepared at different TEA concentrations. Polymerization conditions: temperature 30°C; atm. pressure; heptane 180 mL; propene 0.61 mol/L; catalyst amount 11.2 µmol-Ti.*

Initial TEA concentration AC1: $[TEA]_M$ = 0.49 mmol/L; $[TEA]_0$ = 9.4 mmol/L

Exp. No.	Time [s]	Yield [g-PP/mmol-Ti]	*mmmm*	*mmmr*	*rmmr*	*mmrr*	*mrmm+ rmrr*	*rmrm*	*rrrr*	*rrrm*	*mrrm*
AC 65	10	6.1	97.5	0.9	0.1	0.6	0.3	0.1	0.2	0.2	0.2
AC 67	60	18.0	97.1	1.0	0.3	0.6	0.2	0.0	0.3	0.2	0.3
AC 90	120	26.4	96.6	1.0	0.2	0.8	0.3	0.1	0.4	0.3	0.4
AC 128	300	50.5	95.0	1.8	0.2	0.8	0.4	0.0	0.7	0.6	0.6

Initial TEA concentration AC3: $[TEA]_M$ = 0.12 mmol/L; $[TEA]_0$ = 0.7 mmol/L

Exp. No.	Time [s]	Yield [g-PP/mmol-Ti]	*mmmm*	*mmmr*	*rmmr*	*mmrr*	*mrmm+ rmrr*	*rmrm*	*rrrr*	*rrrm*	*mrrm*
AC 164	60	4.7	96.6	1.1	0.2	0.6	0.3	0.0	0.3	0.4	0.4
AC 162	120	7.5	96.7	1.0	0.1	0.6	0.3	0.0	0.4	0.4	0.4
AC 106	240	13.8	96.4	0.9	0.0	0.8	0.3	0.0	0.5	0.5	0.5
AC 139	300	17.9	96.1	1.3	0.1	0.8	0.4	0.1	0.4	0.4	0.6

It was shown in previous Chapter 5.2.1 that the extraction of internal donor by TEA cocatalyst is very limited in the case of di-ester type catalyst and applied conditions. So, the decrease in the amount of *mmmm* pentad, which is more than 3 times faster at high TEA concentration, could be related mainly to the creation of the syndiotactic polypropene sequences (*rrrr*), because as could be seen in Table 13 the difference of stereosequence distribution in the samples prepared at different TEA concentrations is not significant. Also the comparison of time profiles of *mmmm* and *rrrr* pentads in Figure 27 and Figure 28 shows that the syndiotactic *rrrr* pentad exhibits a profile that is the inverse of the isotactic pentad (*mmmm*) dependence. Busico et al. [138] explains the creation of the short syndiotactic sequences in the isotactic blocks on the basis of a reversible interconversion of the active sites (reversible dissociation of dinuclear Ti_2Cl_6 species), which may be shorter than the average growth time of polymer chain. In a present case it appears that the probability of the described interconversion is higher when the TEA molecule is coordinated to the Ti atom. Another explanation also suggested by Busico et al. [88,89] could be in the instability of TEA-Ti active complex undergoing fast dissociation and association and thus, it is changing the nature of the active site resulting in the generation of the higher amount of stereoerrors.

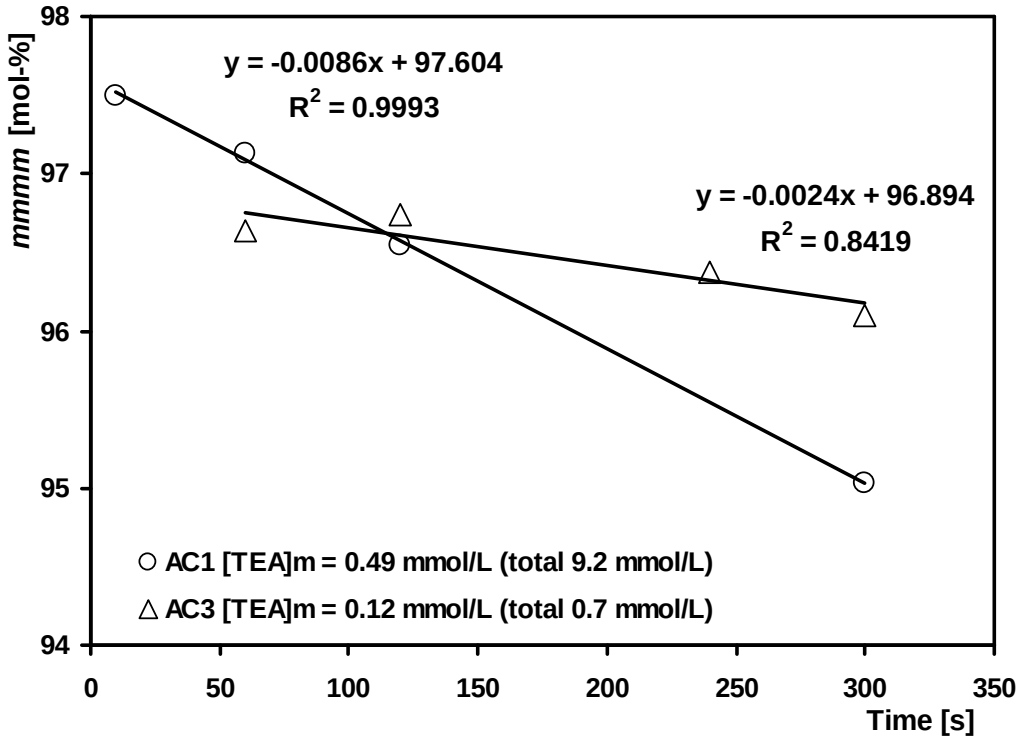

Figure 27: *Dependence of portion of isotactic pentad (mmmm) on polymerization time for two different TEA concentrations.*

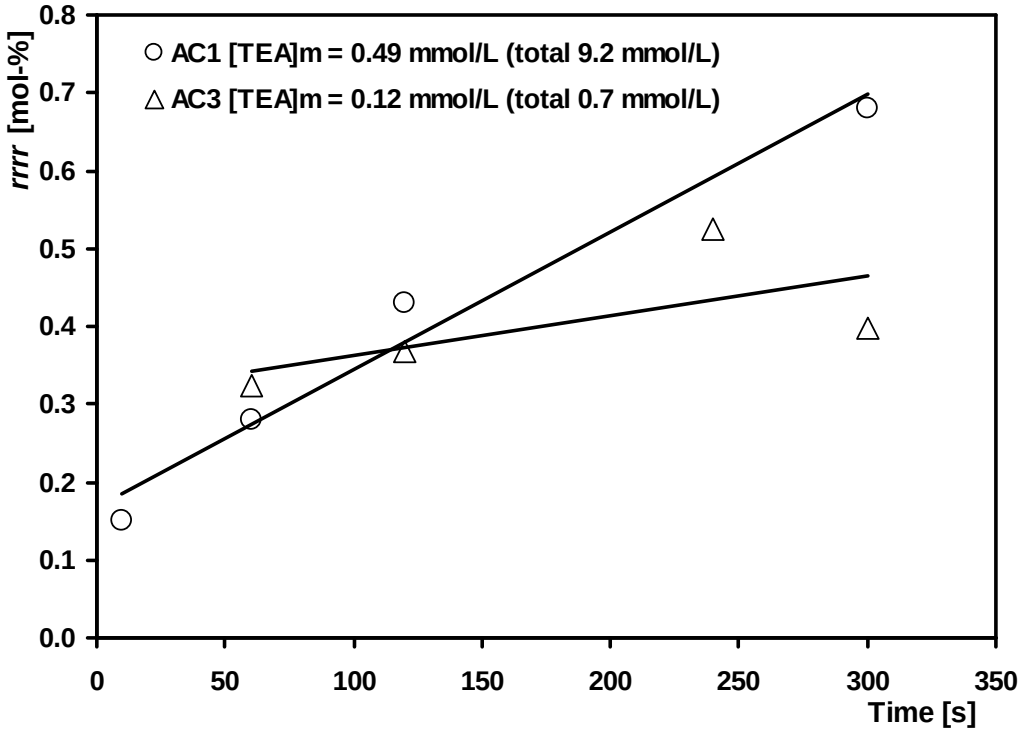

Figure 28: *Dependence of portion of syndiotactic pentad (rrrr) on polymerization time for two different TEA concentrations.*

5.2.4 Effect of Catalyst Prepolymerization in Slurry at Low TEA Concentration

The effect of the short catalyst prepolymerization performed at mild conditions (typically low temperature and pressure), followed by the main polymerization period under conditions closer to the industrial conditions was studied by Samson et al. [133,141]. Experiments performed in gaseous and liquid propene revealed a significant increase in the subsequent polymerization rate in the main polymerization period with the prepolymerized catalyst. It was found that the activity enhancement with the prepolymerized catalyst was more remarkable in the case of the polymerizations in liquid propylene. A similar observation was obtained by Pater et at. [142-144] applying the isothermal and non-isothermal prepolymerization techniques. They observed that the lower polymerization rate in the case of experiments where the prepolymerization step was not applied is a result of a particle overheating in the initial stage of polymerization. Further, they also found a strong influence of the initial polymerization conditions on the final polymer particle morphology.

For the purpose of a deeper investigation of the TEA cocatalyst influence on the active sites properties, the short-time prepolymerization runs at low TEA concentration ($[TEA]_M$ = 0.12 mmol/L; total 0.7 mmol/L) were performed. Then immediately after the prepolymerization time elapsed, the concentration of TEA was enhanced by additional introduction of the defined TEA amount up to the final TEA concentration: $[TEA]_M$ = 0.49 mmol/L; total 9.4 mmol/L. During the investigation, the three different prepolymerization periods (30, 60 and 150 s) were applied. The resulting prepolymerization yields are summarized in Table 14.

Table 14: *Time and yield of prepolymerization at low TEA concentration. Polymerization conditions: temperature 30℃; atm. pressure; heptane 180 mL; pr opene 0.61 mol/L; catalyst amount 11.2 µmol-Ti; initial TEA concentration* $[TEA]_M$ *= 0.12 mmol/L (total 0.7 mmol/L).*

Exp. No.	Prepolym. [s]	Yield of prepolym. [g-PP/g-cat]
AD1	30	1.0
AD2	60	1.4
AD3	150	2.7

The technique of precise short-time experiments was applied for the exact determination of the kinetic profiles, which followed after the introduction of additional TEA amount (Figure 29). It is obvious that the additional TEA introduction causes the fast increase of polymerization rate to the level comparable to the kinetics determined in the short-time experiments performed with high TEA concentration since the first seconds of polymerization (without prepolymerization) in Chapter 5.2.2. Detailed comparison of all kinetic profiles presented in Figure 30 reveals that the kinetics are similar, without noticeable activation period. This finding indicates that TEA access to the catalyst particle is very fast and is not influenced by the polymer layer surrounding the catalyst particle after the 150 s of prepolymerization to the yield 2.7 g-PP/g-cat. Further, the results show that the adverse high initial polymerization rates, observed in experiments performed at high TEA concentrations, could be eliminated by the introduction of the defined cocatalyst amount in two separate injections during the short initial period. As it is shown in Figure 29, such introduction of relatively high TEA amount, but dosed in two separate parts, leads to the same polymerization rate as in the experiments where the whole TEA amount was present since the first seconds of polymerization, but in this case without the high initial polymerization rates.

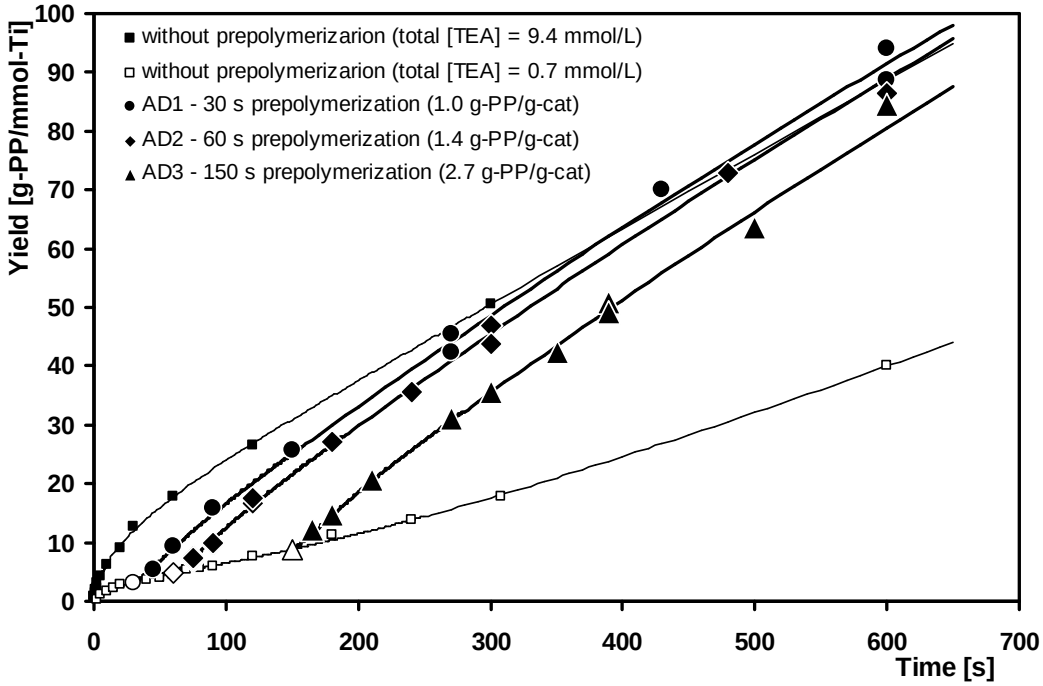

Figure 29: *Kinetic profiles determined by short-time experiments after the 30, 60 and 150 s of prepolymerization at low TEA concentration. The empty points (○,◇,△) indicate the moment of the second TEA amount injection. Polymerization conditions are similar as those in Table 14.*

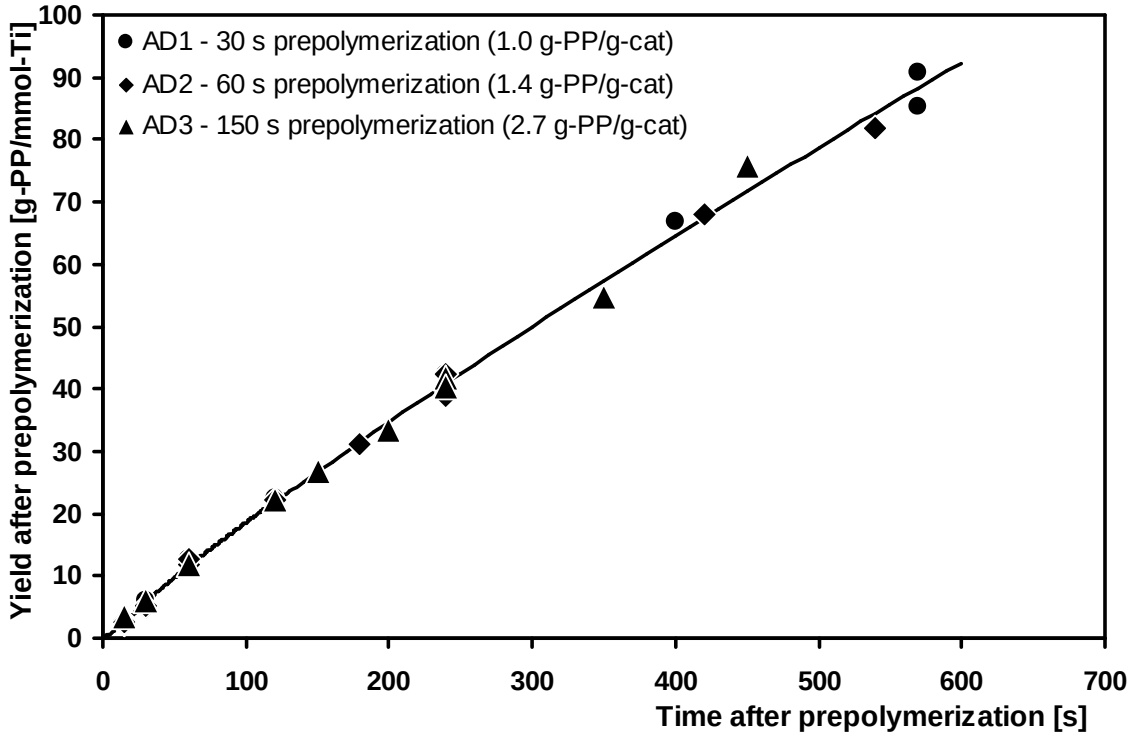

Figure 30: *Comparison of polymerization kinetic profiles subsequently obtained after different prepolymerization periods.*

The selected polymer samples prepolymerized at low TEA concentration for 30, 60 and 150 s were utilized for the GPC/SEC analysis and consequent calculation of the number of macromolecules. Resulting values of M_n, M_w, polydispersity index M_w/M_n and number of macromolecules *N* complemented by the overall polymerization time consisting of the two-stages (prepolymerization at $[TEA]_0$ = 0.7 mmol/L and main polymerization period at $[TEA]_0$ = 9.4 mmol/L) are summarized in Table 15. Then, the corresponding time dependences compared with the experiments performed without the prepolymerization period are expressed in the following figures (Figure 31, Figure 32 and Figure 33).

Table 15: *Values of number-average M_n and weight-average M_w molecular mass, accompanied by calculations of polydispersity index M_w/M_n and number of macromolecules. Initial TEA concentration $[TEA]_M$ = 0.12 mmol/L (total 0.7 mmol/L); final TEA concentration $[TEA]_M$ = 0.49 mmol/L (total 9.4 mmol/L).*

AD1: 30 s of prepolymerization (1.0 g-PP/g-cat)

Exp. No.	Time [s]	Yield [g-PP/mmol-Ti]	M_n*10^{-3} [g/mol]	M_w*10^{-3} [g/mol]	M_w/M_n	*N* [mol/mol-Ti]
AC 157	45	5.4	104	497	4.8	0.051
AC 154	60	9.4	116	549	4.8	0.081
AC 144	90	15.9	111	542	4.9	0.143
AC 153	150	25.6	107	566	5.4	0.242
AC 156	270	42.5	112	568	5.0	0.378

AD2: 60 s of prepolymerization (1.4 g-PP/g-cat)

Exp. No.	Time [s]	Yield [g-PP/mmol-Ti]	M_n*10^{-3} [g/mol]	M_w*10^{-3} [g/mol]	M_w/M_n	*N* [mol/mol-Ti]
AC 147	75	6.9	107	516	4.8	0.064
AC 145	90	9.5	112	538	4.8	0.086
AC 143	120	16.5	91	483	4.8	0.182
AC 146	180	27.0	106	560	5.3	0.254
AC 155	300	43.7	124	588	4.8	0.353

AD3: 150 s of prepolymerization (2.7 g-PP/g-cat)

Exp. No.	Time [s]	Yield [g-PP/mmol-Ti]	M_n*10^{-3} [g/mol]	M_w*10^{-3} [g/mol]	M_w/M_n	*N* [mol/mol-Ti]
AC 174	165	12.2	93	577	6.2	0.132
AC 171	180	14.7	95	571	6.0	0.155
AC 170	210	20.7	97	578	6.0	0.214
AC 173	270	31.1	116	564	4.9	0.268
AC 183	350	42.4	123	559	4.6	0.345

The comparison between the time dependences of M_n and M_w (Figure 31 and Figure 32) of the polymer samples, prepared with enhanced TEA concentration after the defined prepolymerization period, show a rapid increase of M_n value to the level corresponding to the experiments performed with high TEA concentration from the beginning of polymerization. On the contrary, in the case of M_w the value remains unaffected by the introduction of second TEA dose, following the M_w profile of the polymerizations performed at low TEA concentration. It appears that the prepolymerization stabilizes the catalytic system. So the introduction of additional TEA and consequent active sites transformation to the bimetallic form cause only the decrease in the production of the low molecular weight polymer (higher M_n), but does not increase the production of the long chains (constant M_w), which causes the decrease in the polymer polydispersity (narrower MWD). The observed change in the M_w and M_n proportion causes the decrease of the polydispersity index to the level around 5 (Figure 33). The non-prepolymerized samples show a polydispersity index around 6 (Figure 23 in Chapter 5.2.3).

Also, from the presented figures it is apparent that the response of the molecular weight on the additional TEA dose slows down with the prolongation of the prepolymerization time.

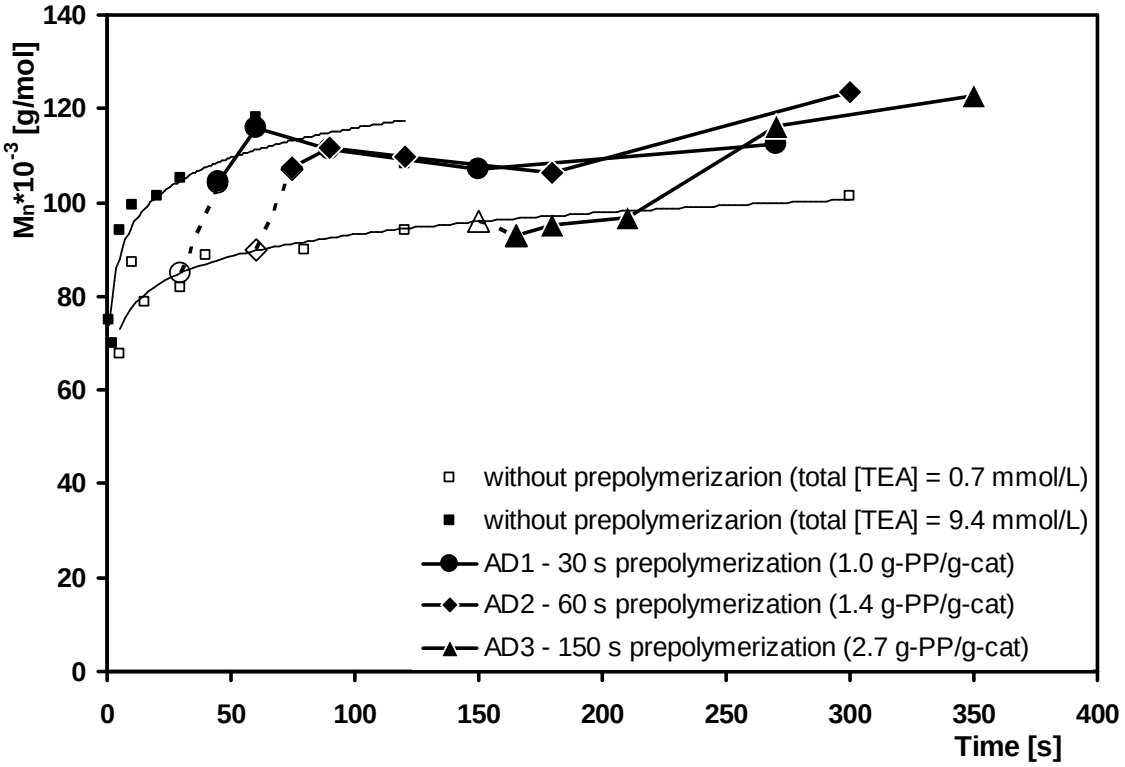

Figure 31: *Dependence of M_n on overall polymerization time for prepolymerization periods 30, 60 and 150 s compared with data determined in experiments without prepolymerization. The empty points* (○,◇,△) *indicate the moment of the second TEA amount injection.*

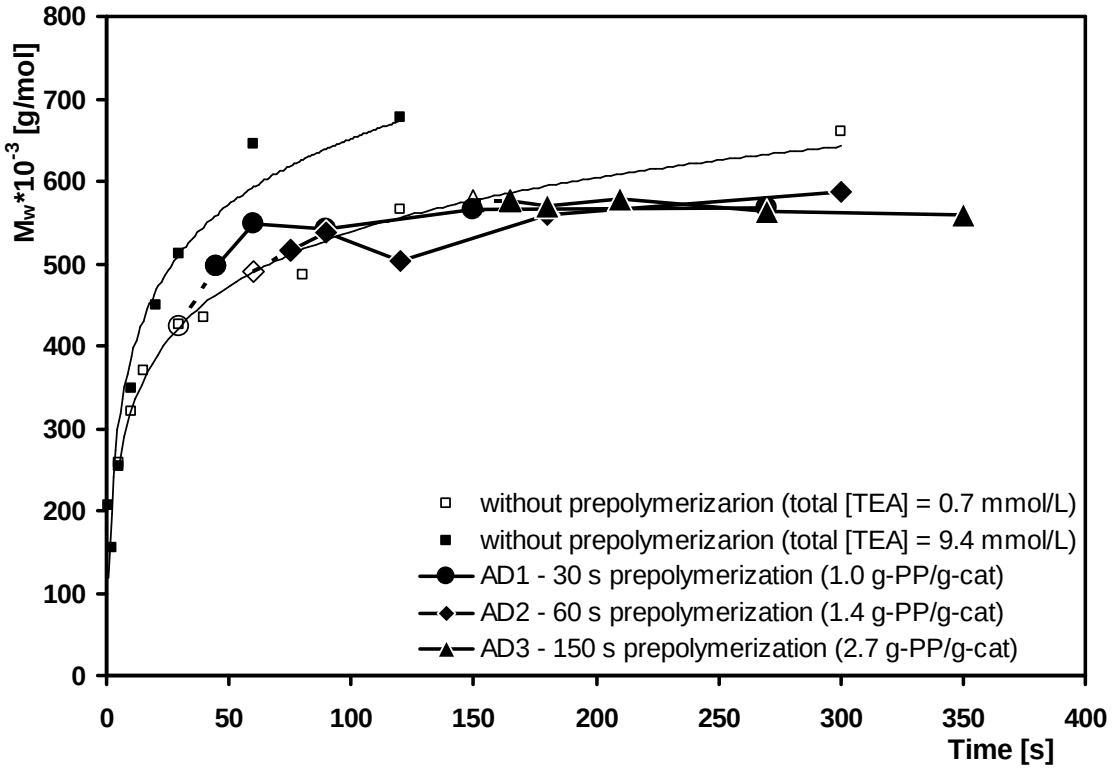

Figure 32: *Dependence of M_w on overall polymerization time for prepolymerization periods 30, 60 and 150 s compared with data determined in experiments without prepolymerization. The empty points* (○,◇,△) *indicate the moment of the second TEA amount injection.*

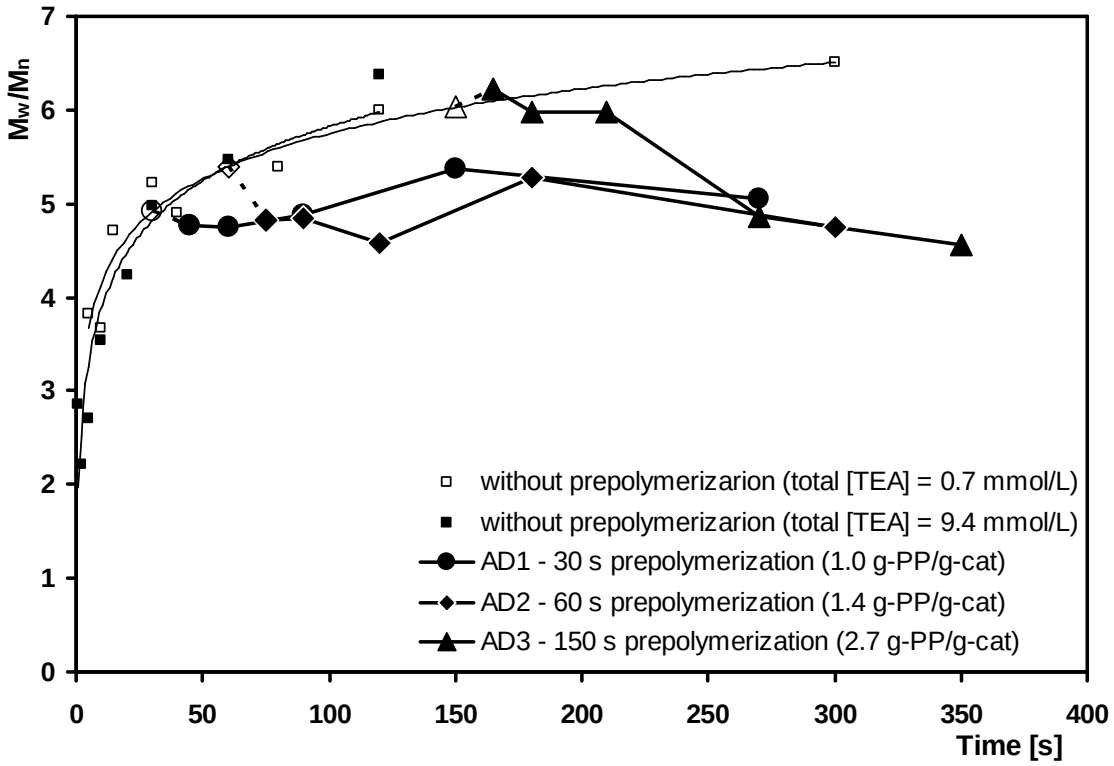

Figure 33: *Dependence of M_w/M_n (polydispersity index) on overall polymerization time for prepolymerization periods 30, 60 and 150 s compared with data determined in experiments without prepolymerization. The empty points* (○,◇,△) *indicate the moment of the second TEA amount injection.*

The dependence of the number of macromolecules *N* on polymerization time (Figure 34) shows a similar profile in comparison with the experimentally determined kinetics presented in Figure 29. This comparability of the polymer yield and number of macromolecules (*N*) time dependencies is more obvious from the Figure 35, where the *N* versus polymer yield dependence exhibits similar overlapping linear behavior without the noticeable influence of the applied prepolymerization procedure and TEA concentration. So, the same conclusion could be postulated as in the case of the TEA concentration study presented in the previous Chapter 5.2.3. No new active sites are formed after the TEA concentration increase. The increase of TEA amount after the prepolymerization at significantly lower TEA concentration does not reveal any remarkable change in the slope of the *N* vs. yield dependence. Thus, the prepolymerization study could be considered as another proof of the postulated presumption that the change in TEA concentration influences proportionally the propagation k_p and transfer k_{tr} rate coefficients, resulting in the constant k_{tr}/k_p ratio and the slope of the *N* vs. yield dependence.

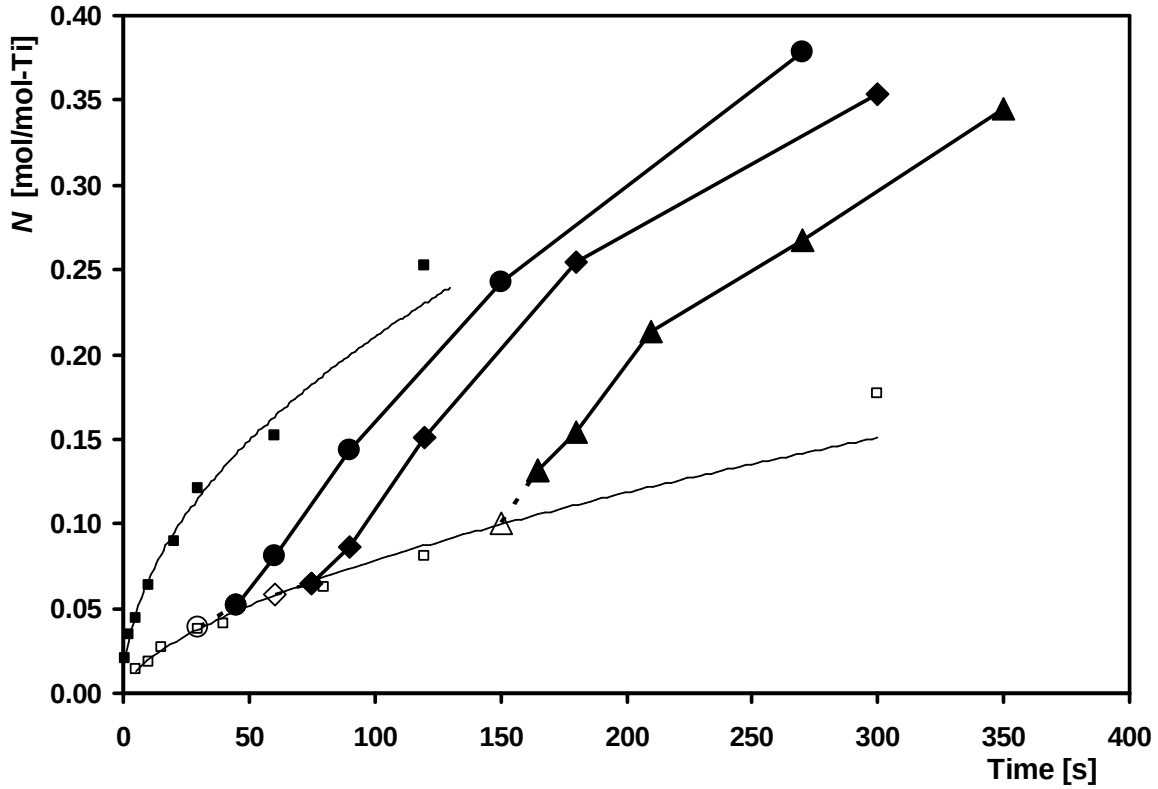

Figure 34: *Dependence of number of macromolecules (N) on overall polymerization time for prepolymerization periods 30, 60 and 150 s compared with data determined in experiments without prepolymerization. The empty points (○,◇,△) indicate the moment of the second TEA amount injection.*

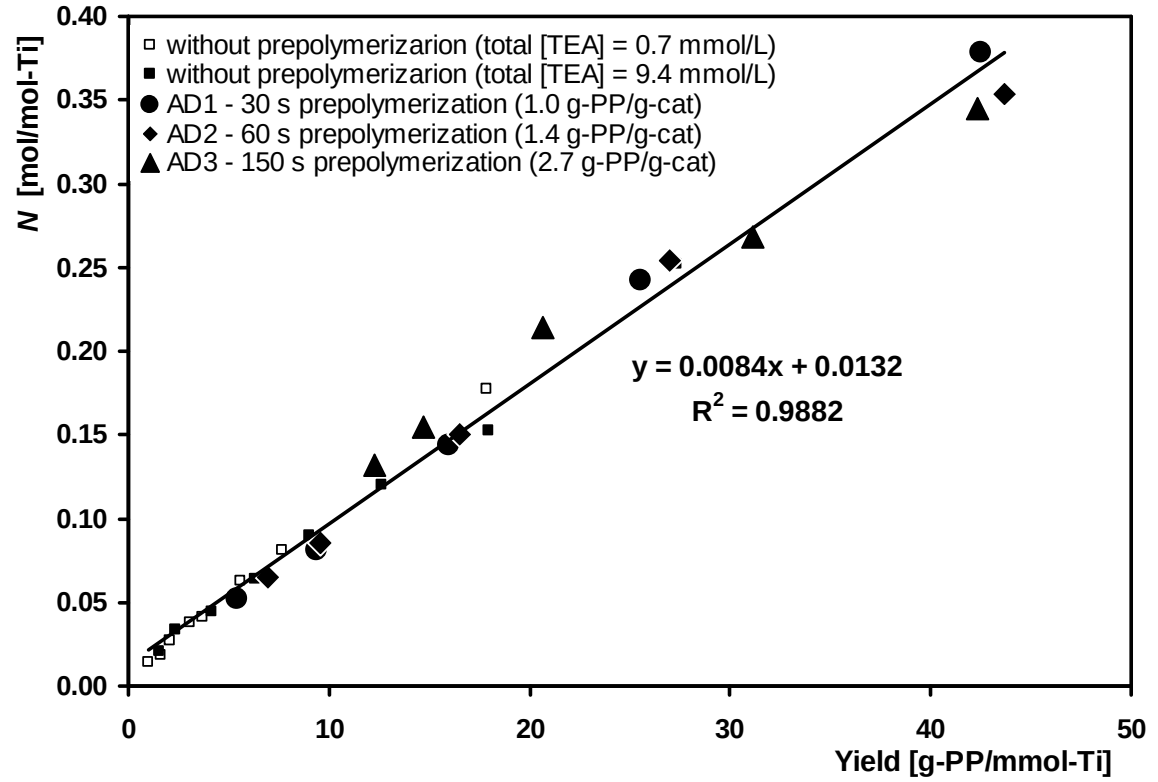

Figure 35: *Dependence of number of macromolecules (N) on the polymer yield for prepolymerization periods 30, 60 and 150 s compared with data determined in experiments without prepolymerization.*

Furthermore, the series of polymer samples with 60 s prepolymerization was analyzed by ^{13}C-NMR for the determination of the stereosequence distributions. The resulting values are presented in Table 16. The time dependence of the content of isotactic pentads (*mmmm*) in Figure 36 exhibits a non-linear profile, revealing the temporary increase of the polymer isotacticity with the introduction of additional TEA amount. The decrease followed in the same rate as it was observed in the experiments performed with high TEA concentration since the beginning of polymerization. This temporary increase in the polymer isotacticity implies that TEA, besides the increase of polymerization rate, improves also the active site stereospecificity. However, as it was described in the previous Chapter 5.2.3, it also enhances the generation of stereoerrors, mainly in the case of the short syndiotactic sequences (*rrrr* pentad).

The change in the nature of the active sites caused by the interaction with TEA cocatalyst is more obvious when the content of isotactic pentads is shown in the dependence on the polymer yield (Figure 37). It is apparent that the introduction of the additional TEA to the catalyst activated at the low TEA concentration causes the fast change in the properties of produced polypropene. The structure of the polymers obtained is comparable to the polypropene samples prepared on the catalyst activated at the high TEA concentration. This observation is another indication that the TEA molecule could be the part of the active site, directly influencing the polymerization reaction (monomer insertion into the growing chain).

Table 16: *Stereosequence distribution (mol.-%) in prepolymerized polypropene samples. Initial TEA concentration $[TEA]_M$ = 0.12 mmol/L (total 0.7 mmol/L); final TEA concentration $[TEA]_M$ = 0.49 mmol/L (total 9.4 mmol/L). Polymerization conditions: temperature 30℃; atm. pressure; heptane 180 mL; propene 0.61 mol/L; catalyst amount 11.2 µmol-Ti.*

AD2: 60 s of prepolymerization (1.4 g-PP/g-cat)

Exp. No.	Time [s]	Yield [g-PP/mmol-Ti]	*mmmm*	*mmmr*	*rmmr*	*mmrr*	*mrmm+ rmrr*	*rmrm*	*rrrr*	*rrrm*	*mrrm*
AD 191	75	7.3	96.7	0.9	0.2	0.6	0.3	0.0	0.4	0.5	0.4
AD 169	120	17.5	97.0	0.8	0.2	0.6	0.3	0.1	0.3	0.4	0.3
AD 146	180	27.0	96.9	0.8	0.1	0.7	0.3	0.0	0.5	0.4	0.4
AD 190	240	35.7	96.0	0.9	0.1	0.8	0.4	0.0	0.6	0.6	0.6
AD 155	300	43.7	95.7	1.1	0.2	0.9	0.4	0.0	0.6	0.6	0.5

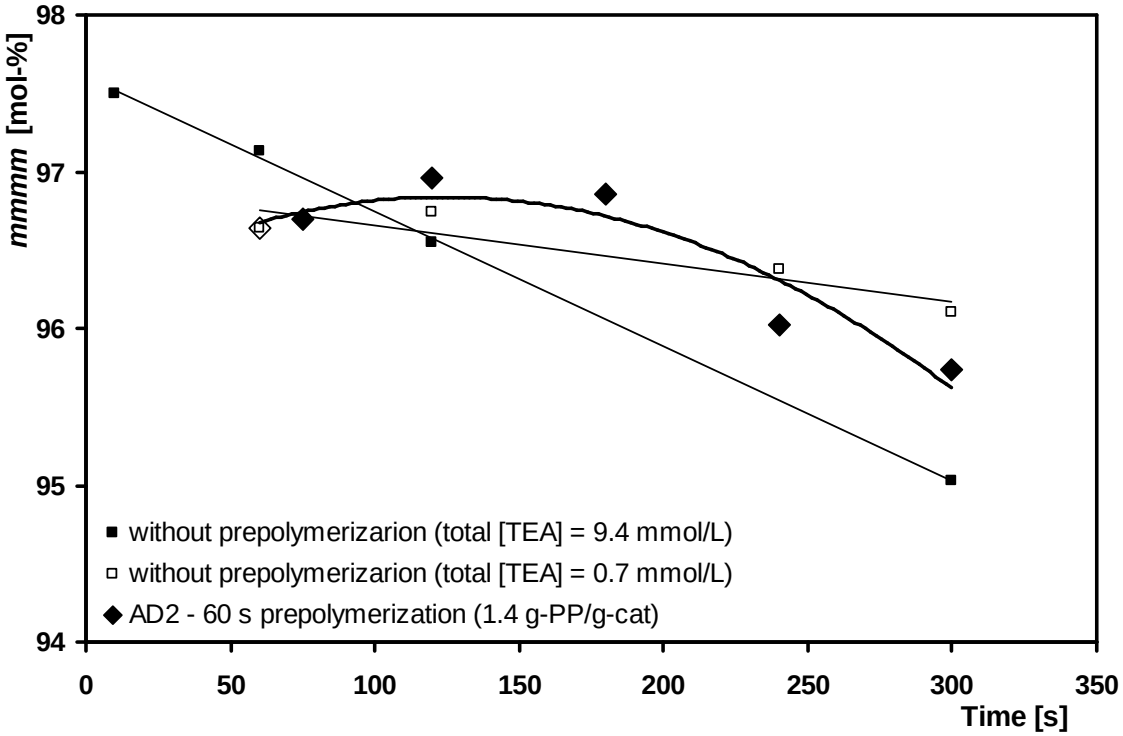

Figure 36: *Dependence of portion of isotactic pentad (mmmm) on polymerization time for polymer samples prepolymerized at low TEA concentration for 60 s and compared with the non--prepolymerized experiments at two different TEA concentrations. The empty point (◇) indicates the moment of the second TEA amount injection.*

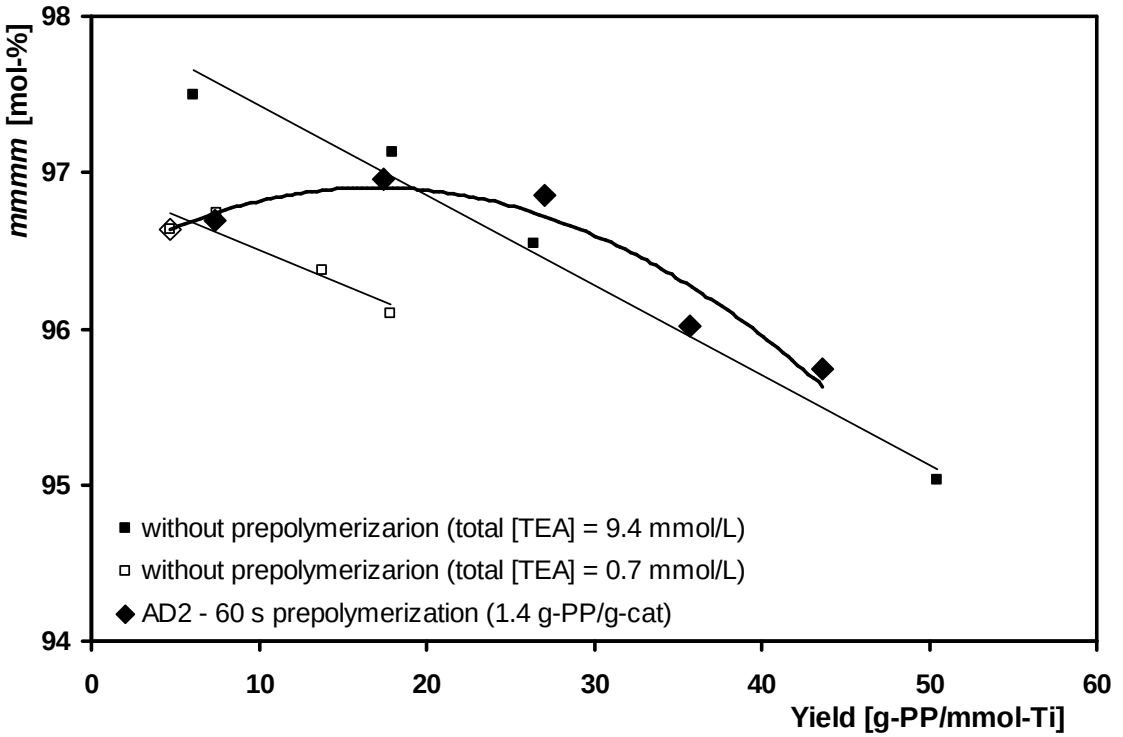

Figure 37: *Dependence of portion of isotactic pentad (mmmm) on polymer yield for samples prepolymerized at low TEA concentration for 60 s and compared with the non-prepolymerized experiments at two different TEA concentrations. The empty point (◇) indicates the moment of the second TEA amount injection.*

5.2.5 Influence of Propene Concentration in Slurry and Gas-phase Experiments

It was formerly proved that the first order mechanism is suitable for the description of the dependence of polymerization rate on the propene concentration, over the broad concentration range, by using $TiCl_3$ and $MgCl_2$-supported $TiCl_4$ heterogeneous catalysts [5,19]. Further, the investigation of the effect of monomer concentration on the polymer MWD distribution was published for example by Chien et al. [137]. They found that the M_n value increase with monomer concentration and polydispersity index remains unaffected by the changes in the monomer concentration.

In the current study, the short-time experiments were performed at three different propene concentrations:

I. M1 = 0.47 mol/L corresponding to the equilibrium concentration of the pure propene saturated in 180 mL of *n*-heptane at 40℃ and atmospheric pressure.
II. M2 = 0.22 mol/L corresponding to the equilibrium concentration of the propene/nitrogen mixture (50 mol.-%) saturated in 180 mL of *n*-heptane at 40℃ and atmospheric pressure. Equilibrium propene/ nitrogen concentration in the solution was calculated on the basis of PKP method [139,140].
III. M3 = 0.04 mol/L concentration of pure propene in the gas phase at 40℃ and atmospheric pressure. Experiments were performed in the fixed-bed reactor. More information about the procedure could be found in Chapter 4.2.

The Table 17 is summarizing the determined values of optimized function parameters describing the evaluated kinetic profiles at different propene concentrations. The resulting kinetics are presented in the original integral form (dependence of the polymer yield on time in Figure 38) fitting the experimentally determined points and corresponding derivative expression of the applied function (dependence of polymerization rate R_p on time in Figure 39).

The kinetic data show that the initial polymerization rate significantly depends on the monomer concentration exhibiting high initial activities, followed by the fast deceleration. However, contrary to the TEA study (controlled by the Langmuir-Hinshelwood mechanism), together with the significant decrease of initial activity, the overall polymerization rate also decreases.

It could be seen in Table 17 that the order of deactivation (parameter *n*) is independent on the applied monomer concentration exhibiting constant value. This implies that the catalyst deactivation by monomer occurs in the same mechanism independently to the monomer concentration. The most probable mechanism of the deactivation of the active sites by monomer is the formation of the “dormant” sites by the irregular monomer 2,1-insertion, because the experiments were carried out without hydrogen and at low temperature [18,32-37].

Furthermore, the comparison of the deactivation order determined in the experiment performed at 30℃ (Table 7 in Chapter 5. 2.2, experiment AC1+BB131) and in the experiment presented in this study carried out at 40℃ (experiment M1 in Table 17), both with pure propene and the same initial TEA concentration, revealed the decrease of the order of deactivation from 2.9 to 2.3 with decreasing polymerization temperature. This observation is in agreement with the results published by Samson et al. [133] proposing the existence of various mechanisms of

catalyst deactivation depending on the polymerization temperature. Unfortunately the direct comparison of other function parameters is not easy, because a different catalyst lot with a slightly lower polymerization rate was applied in the monomer concentration study.

Moreover, the kinetics in Figure 39 comparing the slurry polymerizations (M1 and M2) with the experiments performed in the gas phase (M3) exhibits relatively different kinetic behavior. The low initial polymerization rate and remarkably slower deactivation were determined in the case of gas-phase experiments. The reason for the difference could be in the application of the different experimental techniques. The remarkable difference could be found for example in the catalyst activation by the TEA cocatalyst. While in slurry experiments the catalyst comes into contact with cocatalyst and monomer at the same time, in the case of the gas-phase polymerization the catalyst was initially preactivated by the cocatalyst and dispersed in the salt bed before the monomer introduction.

The dependence of the polymer yield on the monomer concentration after 600 s of polymerization, which could be found in Table 17 and Figure 40 does not exhibit the expected linear decrease to zero with decreasing propene concentration [5,19], if the yields from the slurry and the gas-phase experiments are combined together. After the exclusion of the point belonging to the experiment carried out in the gas-phase, the dependence of the polymer yield on propene concentration in slurry polymerizations shows the expected linear decrease to zero.

As it is further indicated in Figure 40, the experiments performed in the gas phase and slurry exhibit different responses with the propene concentration, which complicates the direct comparison with the runs in *n*-heptane slurry. The experiments with gaseous propene revealed more than 2 times higher activity than could be expected in the polymerizations performed in the slurry (*n*-heptane) at the same monomer concentration (Figure 40). This observation indicates that the different catalyst response on propene concentration could be controlled rather by the concentration of monomer sorbed in the polymer phase surrounding the catalyst particle than by the monomer concentration in the system. This presumption is supported by the propene sorption measurements published by Hutchinson and Ray [145] indicating that the higher polymerization rate observed in the gas phase versus in slurry systems could be explained on the basis of differences in the actual propene concentration on the catalyst surface. They assume that in the case of the slurry experiments the competitive sorption of the solvent and monomer molecules leads to the lower monomer concentration on the catalyst particle surface and consequently to the observed relatively lower polymerization rate in *n*-heptane slurry. On the contrary, in the gas phase, during the sorption into the polymer, monomer could condense, which increases the actual concentration on the catalyst surface and enhances the polymerization rate.

However, as it is demonstrated in Figure 41, the dependence of initial polymerization rate $R_p(0)max$ on monomer concentration exhibits a decreasing profile with decreasing monomer concentration without the influence of applied experimental environment (gas-phase or *n*-heptane slurry). This indicates that the sorption effect described by Hutchinson and Ray [145] is not valid at the beginning of polymerization, when the catalyst particle is not surrounded by a polymer layer and

the initial polymerization rates $R_p(0)max$ correspond mainly to the overall propene concentration in the system.

Recently a similar observation was presented by Bergstra [146,147] comparing the gas-phase and slurry experiments in a case of ethylene polymerization with a heterogeneous metallocene catalyst. He determined that the slurry and gas-phase initial polymerization rates exhibited similar dependence on monomer concentration with the second order dependence at low monomer concentrations, and first order at high concentrations. He explains it on the basis of a modified trigger mechanism (Ystenes [148]), where the incoming monomer, not the complexed monomer, is inserted in the polymer chain.

Table 17: *Comparison of optimized parameters of mathematical function applied for the kinetic profile description at various propene concentrations (parameter k_{ds} is excluded from optimization). The kinetics was determined by the short-time experiments for the first 10 min of polymerization. SD is the value of resulting standard deviation. Experimental conditions in slurry polymerizations (M1 and M2): temperature 40℃; atm. pressure; heptan e 180 mL; initial TEA concentration $[TEA]_M$ = 0.49 mmol/L (total 9.1 mmol/L); catalyst amount 12.2 µmol-Ti. Experimental conditions in gas-phase polymerizations (M3): temperature 40℃; atm. pressure; salt bed amount 20 mL; catalyst amount 4 – 6 µmol-Ti, total TEA amount 0.7 mmol (Al/Ti = 150).*

Exp. No.	[M] [mol/L]	Yield (600 s) [g-PP/mmol-Ti]	$R_p(0)$max [g-PP/(mmol-Ti*h)]	n-order	$R_p(0)$f [g-PP/(mmol-Ti*h)]	K_D [mmol-Ti/m^3]	k_a [1/h]	$R_p(0)$s [g-PP/(mmol-Ti*h)]	k_{ds} [1/h]	SD [g]
M1	0.47	90.7	9540	2.2	9085	10.5	889	455	1.0E-11	0.003
M2	0.22	45.9	2847	2.3	2643	1.3	28.0	204	1.0E-11	0.002
M3	0.04	21.1	418	2.3	283	0.3	1.4	135	1.0E-11	0.006

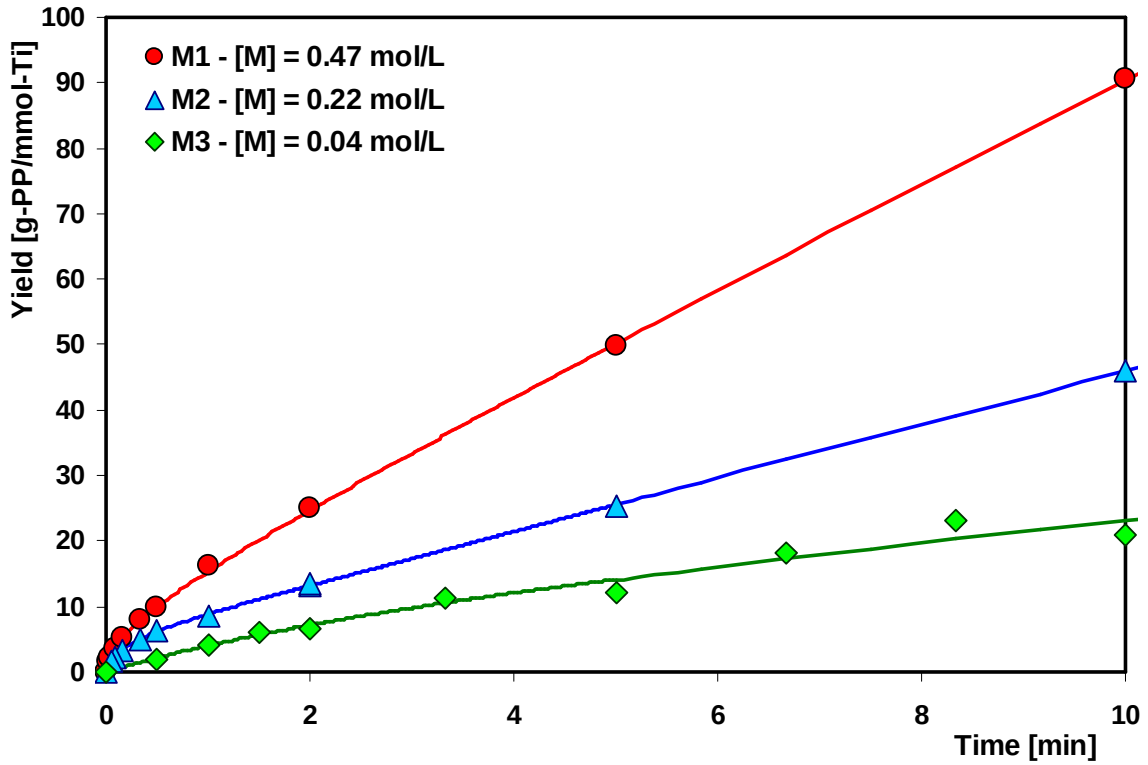

Figure 38: *Kinetic profiles of the first 10 min of polymerization determined by short-time polymerization technique for three different propene concentrations fitted by mathematical kinetic function in integral form. Polymerization conditions are the same as those in Table 17 (M1 and M2 slurry polymerization; M3 gas-phase polymerization).*

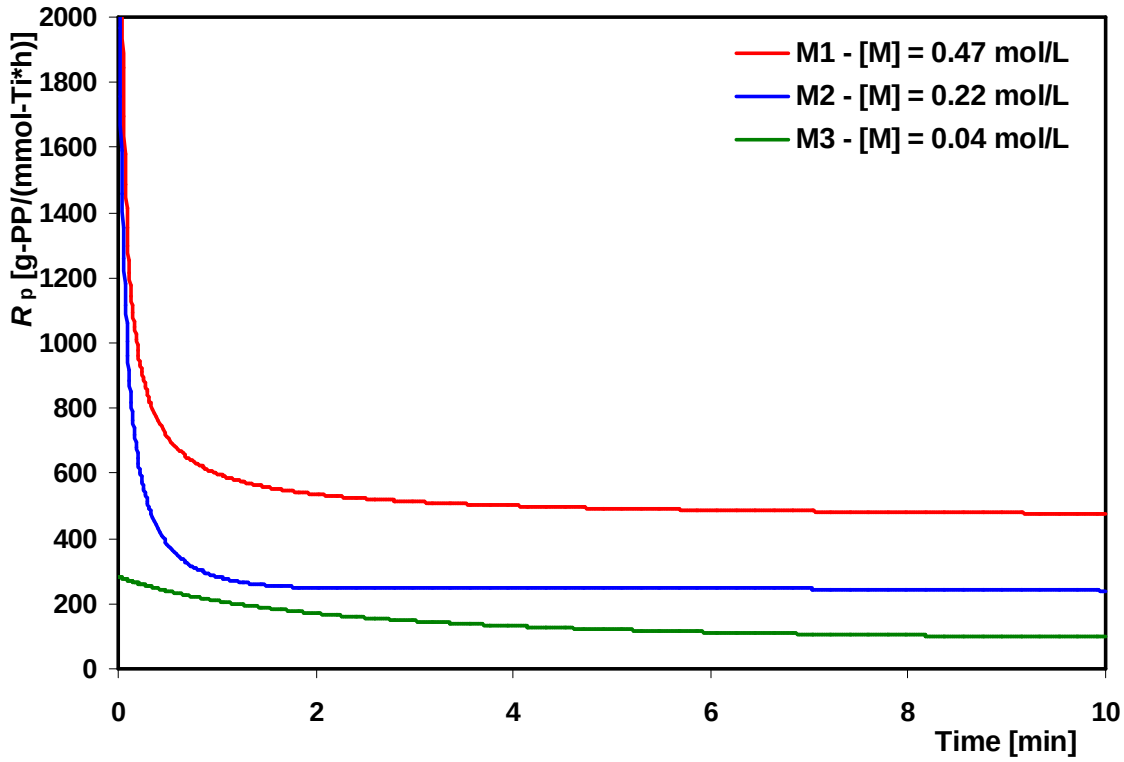

Figure 39: *Derivative expression of optimized mathematical function as dependence of polymerization rate on time for three propene concentrations.*

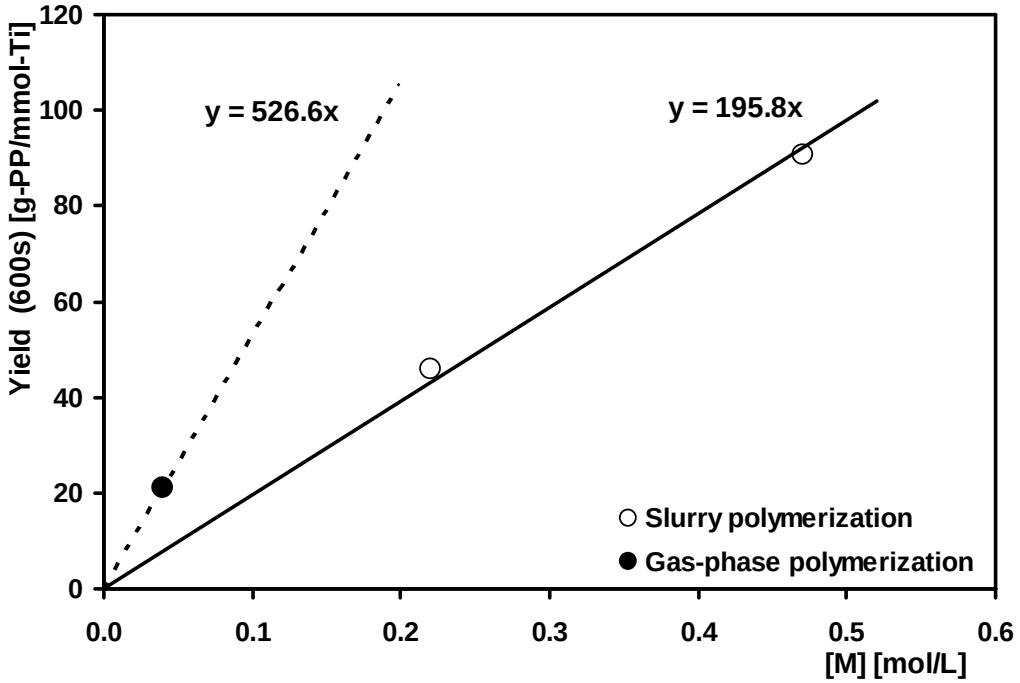

Figure 40: *Dependence of polymer yield after 10 min of polymerization on propene concentration for slurry and gas-phase experiments.*

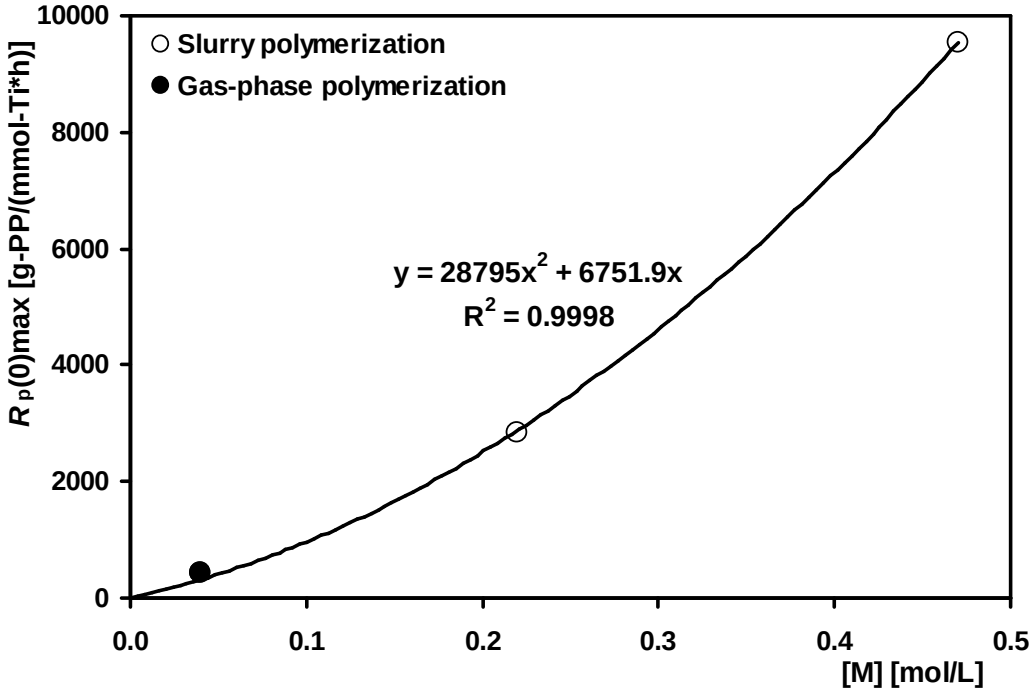

Figure 41: *Dependence of initial polymerization rate on propene concentration.*

The results from the GPC/SEC analyses, obtained on three sets of polymer samples prepared at different propene concentrations, are summarized in Table 18. The following dependences of M_n and M_w on polymerization time, presented in Figure 42 and Figure 43, show a remarkable decrease of the polymer molecular weight with decreasing propene concentration. This observation is similar to the results published formerly by Chien et al. [137]. The resulting M_w/M_n polydispersity index in Figure 44 shows the values around 10. However, the high scatter of experimental data complicates the further investigation of the influence of monomer concentration on the MWD broadening over time.

Table 18: *Values of number-average M_n and weight-average M_w molecular mass, accompanied by calculations of polydispersity index M_w/M_n and number of macromolecules. Polymerization conditions are the same as those in Table 17.*

M1: propene concentration (n-heptane) [M] = 0.47 mol/L

Exp. No.	Time [s]	Yield [g-PP/mmol-Ti]	M_n*10^{-3} [g/mol]	M_w*10^{-3} [g/mol]	M_w/M_n	*N* [mol/mol-Ti]
AC213	1	1.5	49	367	7.5	0.031
AC211	2	2.3	46	430	9.3	0.050
AC208	5	3.6	53	470	8.9	0.068
AC207	10	5.1	48	539	11.2	0.107
AC210	30	9.9	60	569	9.5	0.167
AC206	60	16.1	60	620	10.3	0.267
AC209	120	25.0	61	732	12.1	0.413

M2: propene concentration (n-heptane) [M] = 0.22 mol/L

Exp. No.	Time [s]	Yield [g-PP/mmol-Ti]	M_n*10^{-3} [g/mol]	M_w*10^{-3} [g/mol]	M_w/M_n	*N* [mol/mol-Ti]
AC231	5	2.2	43	374	8.8	0.052
AC226	10	3.3	41	341	8.3	0.080
AC232	20	4.8	49	409	8.4	0.099
AC230	60	8.5	47	463	9.9	0.182
AC227	120	13.5	54	474	8.7	0.249

M3: propene concentration (gas phase) [M] = 0.04 mol/L

Exp. No.	Time [s]	Yield [g-PP/mmol-Ti]	M_n*10^{-3} [g/mol]	M_w*10^{-3} [g/mol]	M_w/M_n	*N* [mol/mol-Ti]
PP49	30	2.6	34	322	9.5	0.076
PP50	60	4.7	30	347	11.5	0.157
PP48	90	6.1	34	263	7.6	0.176
PP39	120	6.7	33	260	7.9	0.202
PP44	200	13.2	35	293	8.4	0.380

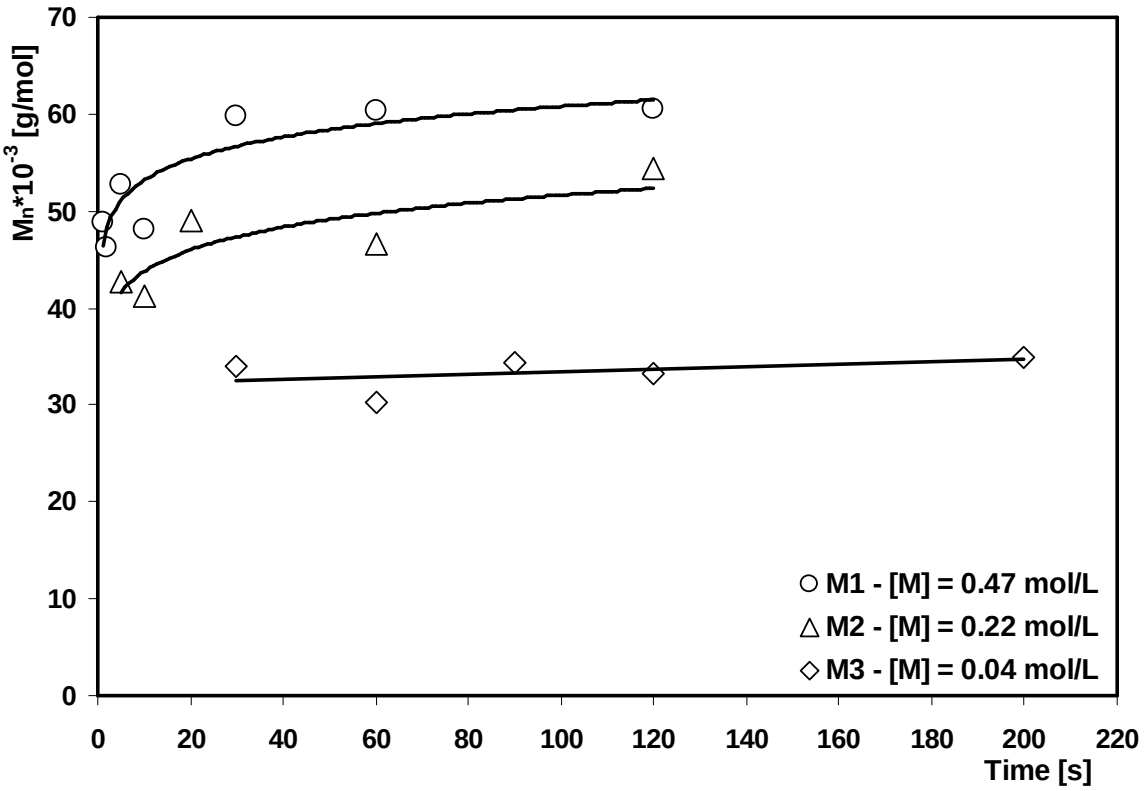

Figure 42: *Dependence of number-average molar mass M_n on polymerization time for three different propene concentrations (M1 and M2 slurry polymerization; M3 gas-phase polymerization).*

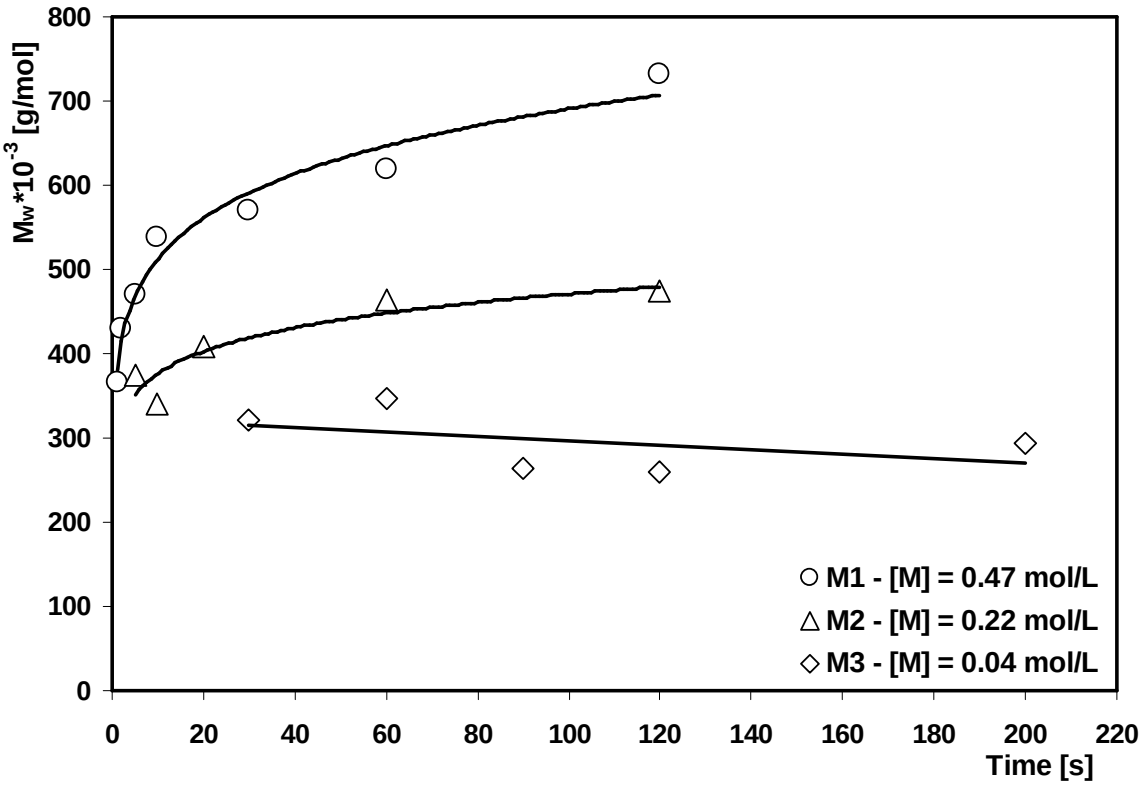

Figure 43: *Dependence of weight-average molar mass M_w on polymerization time for three different propene concentrations (M1 and M2 slurry polymerization; M3 gas-phase polymerization).*

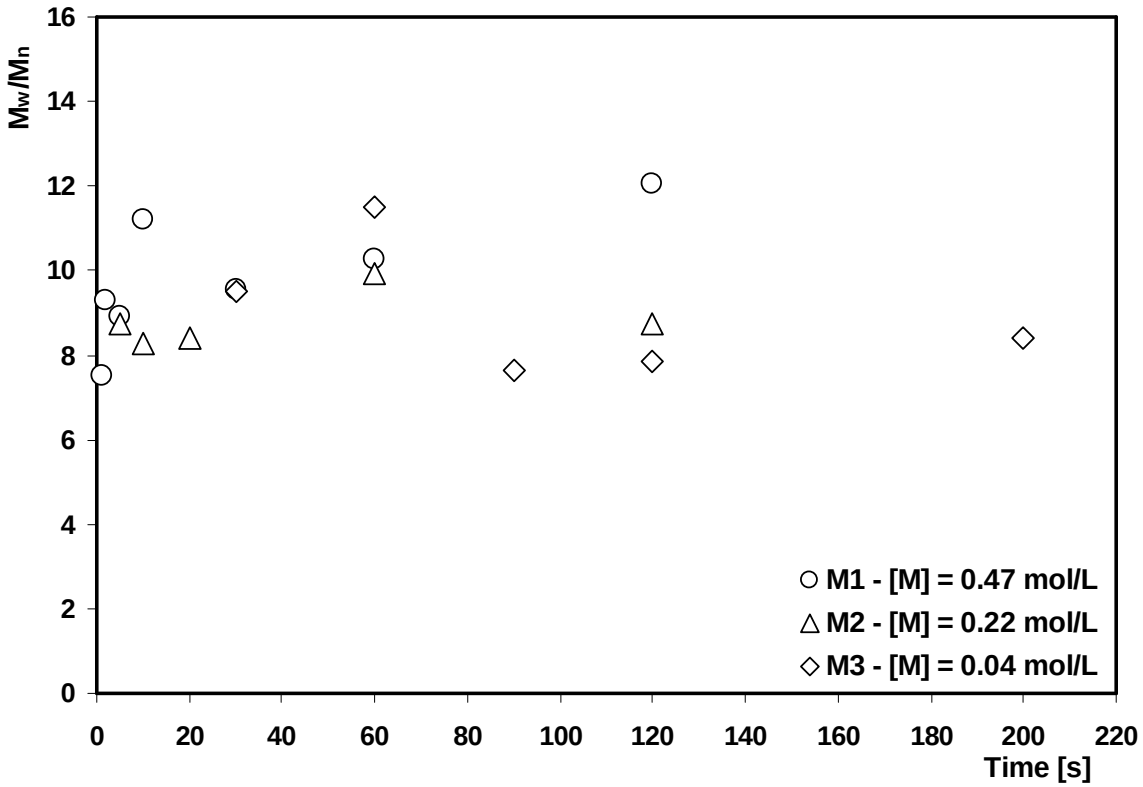

Figure 44: *Dependence of polydispersity index M_w/M_n on polymerization time for three different propene concentrations (M1 and M2 slurry polymerization; M3 gas-phase polymerization).*

Figure 46 shows the influence of monomer concentration on the dependence of number of macromolecules on polymerization time. In the case of the slurry experiments, the time profile of the number of macromolecules corresponds proportionally to the determined kinetics, but in the case of the gas-phase polymerization the number of created macromolecules increases with time significantly faster than it could be assumed from the kinetics (Figure 38). This observation is more apparent from the dependence of the number of macromolecules on the propene concentration shown in Figure 45. It indicates that the intensity of transfer reactions is ca. 5 times higher in the gas-phase than in slurry experiments. These increased chain transfer reactions in the gas-phase experiments could be related to the virtually higher propene concentration in the polymer layer surrounding the catalyst particle (Hutchinson and Ray [145]).

Also, it is obvious from Figure 47 that the non-proportional increase of k_{tr} influences the ratio of transfer and propagation rate k_{tr}/k_p, which leads to the higher slope of the number of macromolecules versus polymer yield. In the case of the slurry experiments, a noticeable change in the slope was not observed, so a similar conclusion as that for the previous studies could be proposed. The decrease in the monomer concentration proportionally influences the transfer and propagation rate exhibiting constant ratio and consequently constant slope in Figure 47 for the slurry experiments. On the basis of the results presented, it is difficult to judge, which component is the dominant transfer agent in these polymerizations. Nevertheless, it is generally accepted that the transfer with monomer is at least one order of magnitude higher than with alkylaluminium cocatalyst [4,5,62,63].

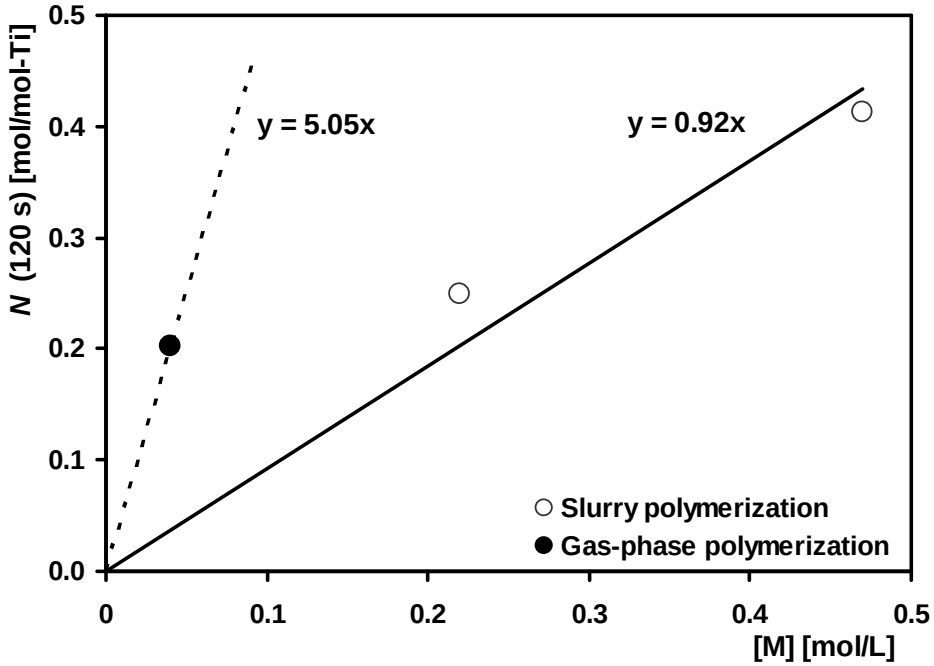

Figure 45: *Influence of propene concentration on the number of macromolecules created after 120 s of polymerization in slurry and gas phase.*

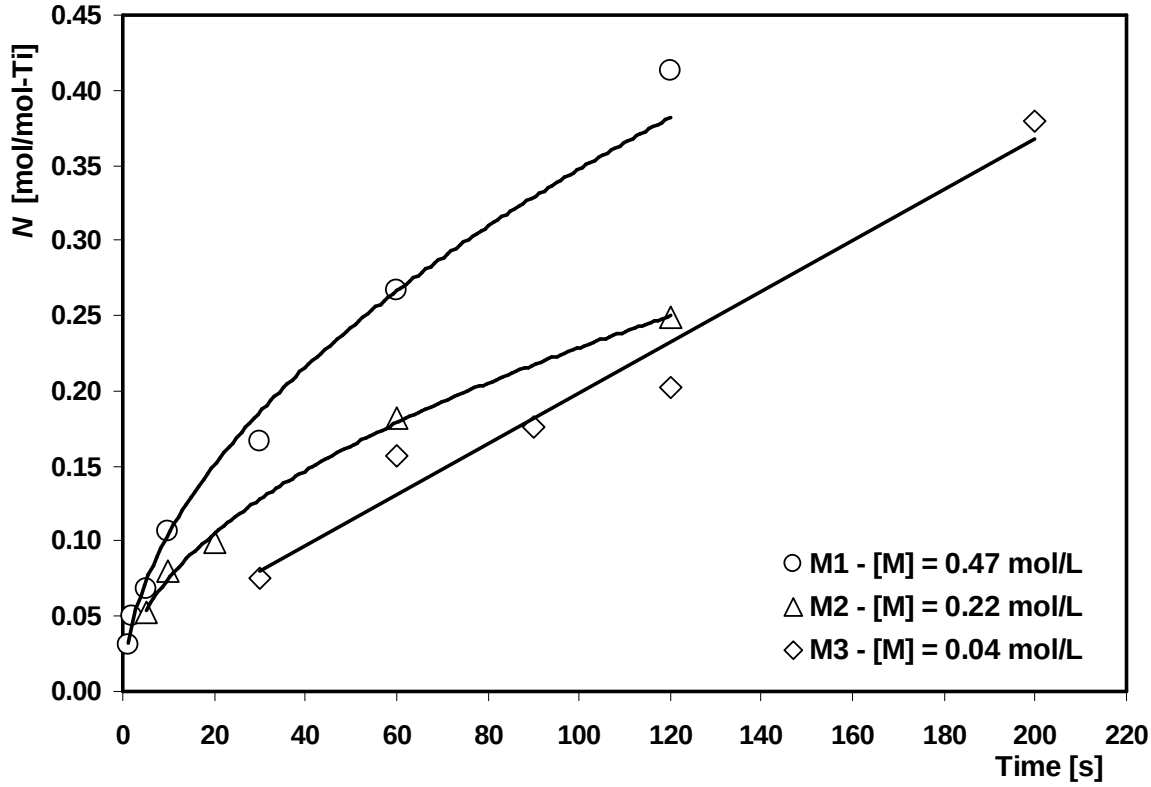

Figure 46: *Dependence of number of macromolecules on polymerization time for three different propene concentrations (M1 and M2 slurry polymerization; M3 gas-phase polymerization).*

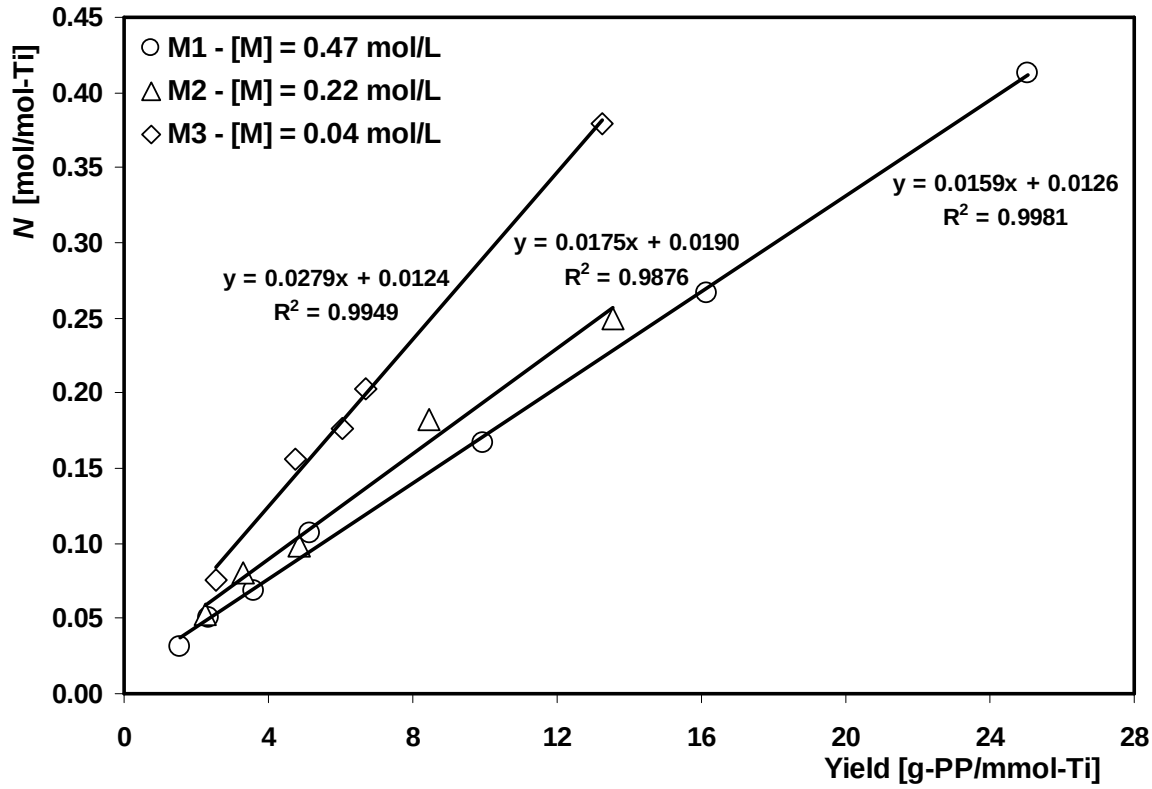

Figure 47: *Dependence of number of macromolecules N on polymer yield for three different propene concentrations (M1 and M2 slurry polymerization; M3 gas-phase polymerization).*

The conformity of the gas phase and slurry techniques demonstrates the utility of both methods. The fixed-bed method, employing the flowing gaseous polymerization medium inside the reactor, exhibited features of accuracy and reproducibility comparable with the slurry short-time experiments. These facts confirmed the homogeneity of the fixed bed conditions, which can be considered as favorable for potential further studies. The small gas-phase volume in respect to gas flow renders the fixed-bed reactor superior for studies based on fast changes of the gas phase composition e.g. preparing well-defined copolymers or bimodal polymers.

6 CONCLUSIONS

The influence of TEA cocatalyst, prepolymerization and monomer concentration on the $MgCl_2$/phthalate/$TiCl_4$ catalyst was investigated in this study. The main interest was focused, first of all, on the catalyst kinetic behavior during the polymerization at low temperature and pressure. For this purpose, the detailed kinetic investigation was performed using two independent techniques for the determination of the catalyst kinetic profiles involving the first seconds of polymerization up to one hour. The subsequent combination with GPC/SEC and ^{13}C-NMR analyses allowed deeper insight into the active site structure and its behavior during the initial and following polymerization periods.

The main conclusions resulting from this investigation could be summarized in the following items:

1. The overall catalyst polymerization rate could be related to the adsorption of monomeric TEA on the catalyst surface, and the dependence of overall polymerization rate on the initial concentration of monomeric TEA could be fitted by the Langmuir-Hinshelwood equation.
2. The ^{13}C-NMR microstructure analysis revealed that the extraction of internal donor by the TEA cocatalyst is very limited in the case of the phthalate catalyst and the applied mild conditions.
3. The initial kinetics from the short-time experiments combined with kinetics assessed via monomer consumption revealed good agreement, showing a significant influence of TEA concentration on the initial polymerization rate.
4. The initial kinetic profiles do not reveal any activation period in the first seconds of polymerization, indicating very fast catalyst activation by the interaction with TEA cocatalyst.
5. The results presented here show that the order of unstable sites deactivation is dependent on the initial concentration of monomeric TEA, increasing from the second to the third order with increasing TEA concentration. The complex order of deactivation that was found indicates that different mechanisms of deactivation could occur at the same time, with the differing intensity depending on the experimental conditions.
6. The increase of initial TEA concentration beyond a certain level enhances only the initial polymerization rate. So the accurate adjustment of initial TEA concentration could be applicable for the exact control of the catalyst behavior in the initial stage of polymerization.
7. At low TEA concentrations, the amount of free monomeric TEA is still sufficient for the activation of all active sites precursors, but is not sufficient to create the bimetallic complexes with higher polymerization rate.
8. It is assumed that the secondary activation observed in the experiments carried out at low TEA concentration can be attributed to the dissociation of TEA dimer, and the transformation of low-activity monometallic sites to bimetallic ones.

9. The initial broadening of the molecular weight distribution corresponds to the decrease in the amount of unstable sites, which are replaced by the stable sites with lower polymerization rate and broader MWD of produced polymer.
10. It was proven that the increased initial TEA concentration did not lead to the creation of new active sites, so the observed increase in the number of macromolecules can be related to the increase of transfer reactions caused by the increased monomeric TEA concentration.
11. The alleged non-existing transfer with TEA observed in the dependence of number of macromolecules on polymer yield could be explained in the terms of presumption that the change of the TEA cocatalyst concentration influences in the same manner the transfer (k_{tr}) and the propagation rate (k_p) coefficients, resulting in their constant ratio and consequent slope of the dependence. The prepolymerization study supports the postulated explanation. A similar phenomenon was observed in the slurry experiments with different monomer concentration.
12. The study performed with varying initial TEA concentration indicates that the propagation rate coefficient for the bimetallic sites is ca. 8 times higher than the k_p coefficient belonging to the monometallic ones.
13. The ^{13}C-NMR analysis revealed that the bimetallic sites with coordinated TEA molecule are more stereospecific than the monometallic sites created at low TEA concentration.
14. The high initial polymerization rates, observed in experiments performed at high TEA concentrations could be eliminated by the introduction of the defined cocatalyst amount in two separate injections during the short initial period.
15. The prepolymerization study confirmed the assumption that the excess TEA molecules further added to the polymerization could become a part of the existing active sites, directly influencing the polymerization reaction.
16. The different catalyst response on propene concentration in the gas phase and slurry is caused, not by the monomer concentration in the system, but rather by the concentration of monomer sorbed in the polymer phase surrounding the catalyst particle.
17. The dependence of the initial polymerization rate on propene concentration indicates that the propene sorption effect is not involved at the beginning of polymerization, when the catalyst particles are not surrounded by polymer layer. It was found that the initial polymerization rate corresponds mainly to the overall propene concentration presented in the system.
18. The intensity of transfer reactions is ca. 5 times higher in the gas-phase than in slurry experiments. The increased chain transfer reactions in the gas-phase experiments could be related to the virtually higher propene concentration in the polymer layer surrounding the catalyst particles. The observed significant difference between the gas-phase and slurry environment indicates the high potential of the fast changes of the reaction conditions for the kinetic studies.
19. The conformity of the gas phase and slurry techniques demonstrates the utility of both methods. The fixed-bed method, employing the flowing gaseous

polymerization medium inside the reactor, exhibited features of accuracy and reproducibility comparable with the slurry short-time experiments. These facts confirmed the homogeneity of the fixed bed conditions which can be considered as favorable for potential further studies. The small gas-phase volume in respect to gas flow renders the fixed-bed reactor superior for studies based on fast changes of the gas phase composition e.g. preparing well--defined copolymers or bimodal polymers.

7 REFERENCES

1 Kashiwa N., J. Polym. Sci. Part A: Polym. Chem. 42, 1 (2004)
2 Rätzsch M., J. Macromol. Sci. – Pure Appl. Chem. 11, 1587 (1999)
3 Seppälä J. V., Auer M., Prog. Polym. Sci. 15, 147 (1990)
4 Dusseault J. J. A., Hsu Ch. C., J. Macromol. Sci. – Rev. Macromol. Chem. Phys. C33, 103 (1993)
5 Albizzati E., Giannini U., Collina G., Noristi L., Resconi L., Polypropylene Handbook Part I., ed. Moore E. P., p. 11, Hanser Publishers, Munich Vienna New York 1996
6 Liu B., Matsuoka H., Terano M., Macromol. Rapid Commun. 22, 1 (2001)
7 Weickert G., 3rd International Workshop on Heterogeneous Ziegler-Natta Catalysts, Japan, 2003.
8 Al-haj Ali M., Betlem B., Roffel B., Weickert G., Macromol. React. Eng. 1, 353 (2007)
9 Di Martino A., Broyer J. P., Spitz R., Weickert G., McKenna T. F., Macromol. Rapid Commun. 26, 215 (2005)
10 Di Martino A., Broyer J. P., Schweich D., de Bellefon C., Weickert G., McKenna T. F., Macromol. React. Eng. 1, 284 (2007)
11 Skoumal M., Cejpek I., Cheng C. P., Macromol. Rapid Commun. 26, 357 (2005)
12 Suzuki E., Tamura M., Doi Y., Keii T., Makromol. Chem. 180, 2235 (1979)
13 Keii T., Terano M., Kimura K., Ishii K., Makromol. Chem., Rapid Commun. 8, 583 (1987)
14 Terano M., Kataoka T., Makromol. Chem., Rapid Commun. 10, 97 (1989)
15 Mori H., Yamahiro M., Terano M., Takahashi M., Matsukawa T., Macromol. Chem. Phys. 201, 289 (2000)
16 Tait P. J. T., Zohuri G. H., Kells A. M., McKenzie, Ziegler Catalysts, ed. Fink G., Mülhaupt R., Brintzinger H. H., p. 343, Springer-Verlag, Berlin Heidelberg 1995
17 Chien J. W. C., Weber S., Hu Y., J. Polym. Sci., Part A, Polym. Chem. 27, 1499 (1989)
18 Shimizu F., Pater J. T. M., van Swaaij P. M., Weickert G., J. Appl. Polym. Sci. 83, 2669 (2002)
19 Keii T., Suzuki E., Tamura M., Murata M., Doi Y., Makromol. Chem. 183, 2285 (1982)
20 Chien J. W. C., Kuo Ch.-I., Ang T., J. Polym. Sci., Polym. Chem. Ed. 23, 723 (1985)
21 Busico V., Corradini P., Ferraro A., Proto A., Makromol. Chem. 187, 1125 (1986)
22 Yoon J.-S., Ray W. H., Ind. Eng. Chem. Res. 26, 415 (1987)
23 Ostrovskii N. M., Kenig F., Chem. Eng. J. 107, 73 (2005)
24 Mori H., Hasebe K., Terano M., Polymer 40, 1389 (1999)
25 Lim S.-Y., Choung S.-J., Appl. Catal. A, General 153, 103 (1997)
26 Murayama N., Liu B., Nakatani H., Terano M., Polym. Int. 53, 723 (2004)
27 Liu B., Murayama N., Terano M., Ind. Eng. Chem. Res. 44, 2382 (2005)
28 Wang Q., Lin Y., Zhang Z., Liu B., Terano M., J. Appl. Polym. Sci. 100, 1978 (2006)
29 Kissin Y. V., Mink R. I., Nowlin T. E., J. Polym. Sci., Part A, Polym. Chem. 37, 4255 (1999)
30 Kissin Y. V., Brandolini A. J., J. Polym. Sci., Part A, Polym. Chem. 37, 4273 (1999)
31 Kissin Y. V., Mink R. I., Nowlin T. E., Brandolini A. J., J. Polym. Sci., Part A, Polym. Chem. 37, 4281 (1999)

32 Tsutsui T., Kashiwa N., Mizuno A., Makromol. Chem., Rapid Commun. 11, 565 (1990)
33 Corradini P., Busico V., Cipullo R., Catalyst Design for Tailor-Made Polyolefins, ed. Soga K., Terano M., Vol. 89, p. 21, Kodansha-Elsevier, Amsterdam London New York Tokyo 1994
34 Busico V., Cipullo R., Corradini P., Makromol. Chem., Rapid Commun. 13, 15 (1992)
35 Chadwick J. C., Miedema A., Sudmeijer O., Macromol. Chem. Phys. 195, 167 (1994)
36 Kissin Y. V., Rishina L. A., J. Polym. Sci., Part A, Polym. Chem. 40, 1353 (2002)
37 Samson J. J. C., Bosman P. J., Weickert G., Westerterp K. R., J. Polym. Sci., Part A, Polym. Chem. 37, 219 (1999)
38 Guyot A., Spitz R., Dassaud J., Gomez C., J. Mol. Catal. 82, 29 (1993)
39 Guyot A., Spitz R., Journaud C., Catalyst Design for Tailor-Made Polyolefins, ed. Soga K., Terano M., Vol. 89, p. 43, Kodansha-Elsevier, Amsterdam London New York Tokyo 1994
40 Kissin Y. V., Isospecific Polymerization of Olefins, p. 1, Springer-Verlag, New York 1985
41 Nirisen Ø., Rytter E., Lindstrøm T. L., Makromol. Chem., Rapid Commun. 7, 103 (1986)
42 Keii T., Catalyst Design for Tailor-Made Polyolefins, ed. Soga K., Terano M., Vol. 89, p. 1, Kodansha-Elsevier, Amsterdam London New York Tokyo 1994
43 Soga K., Shino T., Doi Y., Makromol. Chem. 189, 1531 (1988)
44 Chien J. W. C., Hu Y., J. Polym. Sci., Part A, Polym. Chem. 26, 2973 (1988)
45 Czaja K., Novokshonova L. A., Kovaleva N. J., Macromol. Chem. Phys. 200, 983 (1999)
46 Zakharov V. A., Bukatov G. D., Yermakov Y. I., Adv. Polym. Sci. 51, 61 (1983)
47 Böhm L. L., Polymer 19, 545 (1978)
48 Al-haj Ali M., Ph.D. Thesis, University of Twente, 2006
49 Al-haj Ali M., Betlem B., Roffel B., Weickert G., AIChE Journal 52, 1866 (2006)
50 Mori H., Iguchi H., Hasebe K., Terano M., Macromol. Chem. Phys. 198, 1249 (1997)
51 Kohara T., Shinoyama M., Doi Y., Keii T., Makromol. Chem. 180, 2139 (1979)
52 Xu J., Feng L., Yang S., Macromolecules 30, 2539 (1997)
53 Busico V., Corradini P., De Martino L., Proto A., Savino V., Makromol. Chem. 186, 1279 (1985)
54 Busico V., Corradini P., Transition Metal Catalysed Polymerizations, ed. Quirk R. P., p. 551, Cambridge University Press, Cambridge New York 1989
55 Sacchi M. C., Tritto I., Locatelli P., Prog. Polym. Sci. 16, 331 (1991)
56 Matsuoka H., Liu B., Nakatani H., Nishiyama I., Terano M., Polym. Int. 51, 781 (2002)
57 Sacchi M. C., Forlini F., Tritto I., Locatelli P., Macromol. Symp. 89, 91 (1995)
58 Liu B., Nitta T., Nakatani H., Terano M., Macromol. Chem. Phys. 204, 395 (2003)
59 Marques M. M. V., Nunes C. P., Tait P. J. T., Dias A. R., J. Polym. Sci., Part A, Polym. Chem. 31, 219 (1993)
60 Albizzati E., Giannini U., Morini G., Smith C. A., Ziegler R. C., Ziegler Catalysts, ed. Fink G., Mülhaupt R., Brintzinger H. H., p. 413, Springer-Verlag, Berlin Heidelberg 1995
61 Noristi L., Barbè P. C., Baruzzi G., Makromol. Chem. 192, 1115 (1991)
62 Bukatov G. D., Zakharov V. A., Barabanov A. A., Kin. Catal. 46, 166 (2005)

63 Yaluma A. K., Tait P. J. T., Chadwick J. C., J. Polym. Sci., Part A, Polym. Chem. 44, 1635 (2006)
64 Wang Q., Murayama N., Liu B., Terano M., Macromol. Chem. Phys. 206, 961 (2005)
65 Busico V., Corradini P., De Martino L., Proto A., Albizzati E., Makromol. Chem. 187, 1115 (1986)
66 Barbè P. C., Noristi L., Baruzzi G., Makromol. Chem. 193, 229 (1992)
67 Soga K., Park J. R., Shiono T., Kashiwa N., Makromol. Chem., Rapid Commun. 11, 117 (1990)
68 Bukatov G. D., Zakharov V. A., Macromol. Chem. Phys. 202, 2003 (2001)
69 Matsuoka H., Liu B., Nakatani H., Terano M., Macromol. Rapid Commun. 22, 326 (2001)
70 Liu B., Matsuoka H., Terano M., Macromol. Symp. 165, 3 (2001)
71 Nishiyama I., Liu B., Matsuoka H., Nakatani H., Terano M., Macromol. Symp. 193, 71 (2003)
72 Albizzati E., Dall'Occo T., Galimberti M., Morini G., Catalyst Design for Tailor-Made Polyolefins, ed. Soga K., Terano M., Vol. 89, p. 139, Kodansha-Elsevier, Amsterdam London New York Tokyo 1994
73 Sacchi M. C., Forlini F., Tritto I., Locatelli P., Morini G., Noristi L., Albizzati E., Macromolecules 29, 3341 (1996)
74 Xu D., Liu Z., Zhao J., Han S., Hu Y., Macromol. Rapid Commun. 21, 1046 (2000)
75 Guastalla G., Giannini U., Makromol. Chem., Rapid Commun. 4, 519 (1983)
76 Kissin Y. V., Makromol. Chem., Macromol. Symp. 66, 83 (1993)
77 Mori H., Endo E., Tashino K., Terano M., J. Mol. Catal. A, Chem. 145, 153 (1999)
78 Chadwick J. C., Miedema A., Sudmeijer O., Macromol. Chem. Phys. 195, 167 (1994)
79 Chadwick J. C., van Kessel G. M. M., Sudmeijer O., Macromol. Chem. Phys. 196, 1431 (1995)
80 Bukatov G. D., Goncharov V. S., Zakharov V. A., Macromol. Chem. Phys. 196, 1751 (1995)
81 Kojoh S., Kioka M., Kashiwa N., Itoh M., Mizuno A., Polymer 36, 5015 (1995)
82 Kojoh S., Tsusui T., Kashiwa N., Itoh M., Mizuno A., Polymer 39, 6309 (1998)
83 Mori H., Tashino K., Terano M., Macromol. Rapid Commun. 16, 651 (1995)
84 Mori H., Tashino K., Terano M., Macromol. Chem. Phys. 197, 895 (1996)
85 Mori H., Iizuka T., Tashino K., Terano M., Macromol. Chem. Phys. 198, 2499 (1997)
86 Cossee P., J. Catal. 3, 80 (1964)
87 Kakugo M., Miyatake T., Naito Y., Mizunuma K., Transition Metal Catalysed Polymerizations, ed. Quirk R. P., p. 624, Cambridge University Press, Cambridge New York 1989
88 Busico V., Cipullo R., Monaco G., Talarico G., Vacatello M., Chadwick J. C., Segre A. L., Sudmeijer O., Macromolecules 32, 4173 (1999)
89 Busico V., Cipullo R., Prog. Polym. Sci. 26, 443 (2001)
90 Härkönen M., Seppälä J. V., Salminen H., Polym. J. 27, 256 (1995)
91 Liu B., Nitta T., Nakatani H., Terano M., Macromol. Chem. Phys. 203, 2412 (2002)
92 Nitta T., Liu B., Nakatani H., Terano M., J. Mol. Catal. A, Chem. 180, 25 (2002)
93 Liu B., Nitta T., Nakatani H., Terano M., Macromol. Symp. 213, 7 (2004)
94 Hasan K., Liu B., Terano M., Polym. Bull. 54, 225 (2005)
95 Corradini P., Guerra G., Transition Metal Catalysed Polymerizations, ed. Quirk R. P., p. 533, Cambridge University Press, Cambridge New York 1989

96 Rodrigues L. A. M., van Looy H. M., J. Polym. Sci. 4, 1971 (1966)
97 Tait P. J. T.: Transition Metal Catalyzed Polymerizations, Alkenes and Dienes, Part A, ed. Quirk R. P., p. 115, Harwood Publ., London 1983
98 Mejzlík J., Lesná M., Kratochvíla J., Adv. Polym. Sci. 81, 83 (1987)
99 Mejzlík J., Vozka P., Kratochvíla J., Lesná M.: Transition Metals and Organometallics as Catalysts for Olefin Polymerization, ed. Kaminsky W. Sinn H., p. 79, Springer-Verlag, Berlin Heidelberg 1988
100 Natta G., J. Polym. Sci. 34, 21 (1959)
101 Ayrey G., Mazza R. J., Makromol. Chem. 176, 3353 (1975)
102 Atarashi Y., J. Polym. Sci. A-1, 8, 3359 (1970)
103 Burfield D. R., Makromol. Chem. 183, 2709 (1982)
104 Doi Y., Morinaga A., Keii T., Makromol. Rapid Commun. 1, 193 (1980)
105 Mejzlík J., Lesná M., Majer J., Makromol. Chem. 184, 1975 (1983)
106 Kashiwa N., Yoshitake J., Makromol. Chem., Rapid Commun. 3, 211 (1982)
107 Kashiwa N., Yoshitake J., Polym. Bull. 12, 99 (1984)
108 Chu K.-J., Eur. Polym. J. 34, 577 (1998)
109 Chien J. C. W., J. Amer. Chem. Soc. 81, 86 (1959)
110 Tait P. J. T., Booth B. L., Jejelowo M. O., Makromol. Chem., Rapid Commun. 9, 393 (1988)
111 Tait P. J. T., Zohuri G. H., Kells A. M., Macromol. Symp. 89, 125 (1995)
112 Marques M. M., Tait P. J. T., Mejzlík J., Dias A. R., J. Polym. Sci.,Part A, Polym. Chem. 36, 573 (1998)
113 Ballard D. G. H., Jones E., Wyatt R. J., Murray R. T., Robinson P. A., Polymer 15, 169 (1974)
114 Doi Y., Murata M., Soga K., Makromol. Chem., Rapid Commun. 5, 811 (1984)
115 Bukatov G. D., Shepelev S. H., Zakharov V. A., Sergeev S. A., Yermakov Y. I., Makromol. Chem. 183, 2657 (1982)
116 Bukatov G. D.,Goncharov V. S., Zakharov V. A., Makromol. Chem. 187, 1041 (1986)
117 Shiono T., Ohgizawa M., Soga K., Makromol. Chem. 194, 2075 (1993)
118 Busico V., Guardasole M., Margonelli A., Segre A. L., J. Am. Chem. Soc. 122, 5226 (2000)
119 Vozka P., Mejzlík J., Makromol. Chem. 191, 589 (1990)
120 Vozka P., Mejzlík J., Makromol. Chem. 191, 1519 (1990)
121 Cejpek I., Mejzlík J., Smith P. D., Macromol. Rapid Commun. 15, 829 (1994)
122 Cejpek I., Ph.D. Thesis, VÚMCH Brno, 1992
123 Kissin Y. V., J. Catal. 200, 232 (2001)
124 Gan S.-N., Loi P. S. T., Ng S.-Ch., Burfield D. R., Catalyst Design for Tailor-Made Polyolefins, ed. Soga K., Terano M., Vol. 89, p. 91, Kodansha-Elsevier, Amsterdam London New York Tokyo 1994
125 Caunt A. D., Davies S., Tait P. J. T., Transition Metal Catalysed Polymerizations, ed. Quirk R. P., p. 105, Cambridge University Press, Cambridge New York 1989
126 Kratochvíla J., Mejzlík J., Makromol. Chem. 188, 1781 (1987)
127 Spitz R., Bobichon Ch., Llauro-Darricades M., Guyot A., Duranel L., J. Mol. Catal. 56, 156 (1989)
128 Barbè P. C., Cecchin G., Noristi l., Adv. Polym. Sci. 81, 1 (1987)
129 Marques M. M. V., Nunes C. P., Tait P. J. T., Dias A. R., J. Polym. Sci., Part A, Polym. Chem. 31, 209 (1993)
130 Mole T., Jeffery E. A., Organoaluminium Compounds, p. 93, Elsevier Publishing Company, Amsterdam 1972

131 Smith M. B., J. Phys. Chem. 71, 364 (1967)
132 Černý Z., Heřmánek S., Fusek J., Kříž O., Čásenský B., J. Organometal. Chem. 345, 1 (1988)
133 Samson J. J. C., Weickert G., Heerze A. E., Westerterp K. R., AIChE Journal 44, 1424 (1998)
134 Tarazona A., Koglin E., Buda F., Coussens B. B., Renkema J., van Heel S., Meier R. J., J. Phys. Chem. B 101, 4370 (1997)
135 Grůza J., Unpublished calculations, Polymer Institute Brno (2006)
136 Keii T., Doi Y., Suzuki E., Tamura M., Murata M., Soga K., Makromol. Chem. 185, 1537 (1984)
137 Chien J. C. W., Kuo Ch., J. Polym. Sci., Part A, Polym. Chem. 24, 1779 (1986)
138 Busico V., Cipullo R., Corradini P., De Biasio R., Macromol. Chem. Phys. 196, 491 (1995)
139 Ploecker U., Knapp H., Prausnitz J., Ind. Eng. Chem.17, 324 (1978)
140 Peroutka O., Unpublished calculations, Polymer Institute Brno (2007)
141 Samson J. J. C., van Middelkoop B., Weickert G., Westerterp K. R., AIChE Journal 45, 1548 (1999)
142 Pater J. T. M., Weickert G., Loos J., van Swaaij W. P. M., Chem. Eng. Sci. 56, 4107 (2001)
143 Pater J. T. M., Weickert G., van Swaaij W. P. M., J. Appl. Polym. Sci. 87, 1421 (2003)
144 Pater J. T. M., Weickert G., van Swaaij W. P. M., AIChE Journal 49, 180 (2003)
145 Hutchinson R. A., Ray W. H., J. Appl. Polym. Sci. 41, 51 (1990)
146 Bergstra M. F., Ph.D. Thesis, University of Twente, 2004
147 Bergstra M. F., Weickert G., Macromol. Mat. Eng. 290, 610 (2005)
148 Ystenes M., J. Catal. 129, 338 (1991)

8 LIST OF SYMBOLS AND ABBREVIATIONS

Abbreviations:

AS	– aspecific site
C3	– propene (propylene)
Cat.	– catalyst
CHMDMS	– cyclohexylmethyldimethoxysilane
DCPDMP	– 2,2-dicyclopentyl-1,3-dimethoxypropane
DEAC	– diethylaluminium chloride
DIBDMS	– di-*i*-butyldimethoxysilane
DIBP	– di-*i*-butyl phthalate
DIPDMP	– 2,2-*i*-propyl-1,3-dimethoxypropane
EADC	– ethylaluminium dichloride
EB	– ethyl benzoate
ED	– external donor
ELPP	– elastomeric polypropene
GPC/SEC	– gel permeation chromatography / size exclusion chromatography
HMS-PP	– high melt strength polypropene
ID	– internal donor
IS_1	– poorly-isospecific site
IS_2	– second highest isospecifity site
IS_3	– isospecific site
KIE	– kinetic isotope effect
L1, L2	– ligands
LB	– Lewis base
MPB	– metal-polymer bond
MPT	– methyl-*p*-toluate
MWD	– molecular weight distribution
NMR	– nuclear magnetic resonance
PC	– personal computer
PE	– polyethene (polyethylene)
PLC	– programmable logical controller
PP	– polypropene (polypropylene)
SD	– standard deviation
TEA	– triethylaluminium
TEPS	– triethoxy(phenyl)silane
TIBA	– tri-*i*-butylaluminium
TMA	– trimethylaluminium
TREF	– temperature rising elution fractionation
ZN	– Ziegler-Natta

Symbols:

[A]	– equilibrium concentration of alkylaluminium	[mol/L]
$[A]_D$	– equilibrium concentration of dimeric alkylaluminium	[mol/L]
$[A]_M$	– equilibrium concentration of monomeric alkylaluminium	[mol/L]
C*	– number of active sites	[mol.-%]

C_i^*	– number of i-type active sites	[mol.-%]
$[Cocat.]_0$	– equilibrium concentration of cocatalyst	[mmol/L]
$[Cocat.]_M$	– equilibrium concentration of monomeric cocatalyst	[mmol/L]
k_a	– activation rate constant	[1/h]
k_{ads}	– adsorption rate constant	[L/(mol*s)]
k_{des}	– desorption rate constant	[L/(mol*s)]
k_{di}	– deactivation rate constant of i-type active site	[1/h]
k_{ds}	– deactivation rate constant of stable active sites	[1/h]
k_{df}	– deactivation rate constant of unstable active sites	[1/h]
k_p	– propagation rate constant	[L/(mol*s)]
k_{tr}	– chain transfer rate constant	[1/s]
K_A	– equilibrium adsorption constant for alkylaluminium	[L/mol]
K_M	– equilibrium adsorption constant for monomer	[L/mol]
K_D	– deactivation constant	[mmol-Ti/m^3]
K_{Diss}	– dissociation constant	[mol/L]
m_P	– amount of saturated propene	[g]
m_H	– amount of *n*-heptane	[g]
[M]	– concentration of monomer	[mol/L]
M_0	– molecular weight of monomer	[g/mol]
M_n	– number-average molar mass	[g/mol]
M_w	– weight-average molar mass	[g/mol]
M_w/M_n	– polydispersity index	
$[MPB]_t$	– total concentration of metal-polymer bonds at time *t*	[mol/L]
$[MPB]_{ex}$	– metal-polymer bond equivalent of the exchanged tritium atoms	
n	– order of active site deactivation	
N	– number of macromolecules	[mol/mol-Ti]
$[N_{tr}]_t$	– concentration of transferred aluminum-polymer bonds	[mol/L]
p	– pressure	[mbar]
P_n	– number degree of polymerization	
R_p	– polymerization rate	[g-PP/(mmol-Ti*h)]
R_{pi}	– polymerization rate of i-type of active site	[g-PP/(mmol-Ti*h)]
$R_p(0)f$	– initial polymerization rate of unstable active site	[g-PP/(mmol-Ti*h)]
$R_p(0)s$	– initial polymerization rate of stable active site	[g-PP/(mmol-Ti*h)]
$R_p(0)max$	– initial polymerization rate	[g-PP/(mmol-Ti*h)]
R_pnet	– net polymerization rate	[g-PP/(mmol-Ti*h)]
t	– time	[s]
T	– temperature	[℃]
$[TEA]_M$	– equilibrium concentration of monomeric TEA	[mmol/L]
$[TEA]_0$	– overall concentration of TEA	[mmol/L]
[X]	– concentration of transfer agent	[mol/L]
Y	– polymer yield	[g]

Greek Letters:

η	– viscosity	[Pa.s]
ρ	– density	[g/cm^3]
τ	– average lifetime of growing polymer chain	[s]

ACKNOWLEDGEMENTS

I would like to thank the companies Polymer Institute Brno spol. s r. o. and Polymer Reactor Technology GmbH for their support of my research and opportunity to work with their sophisticated equipments.

Furthermore, I thank the BASF Catalysts LLC company for providing the catalyst for the research and Dutch Polymer Institute for the financial support of the fixed-bed reactor.

I would like to express sincerely thanks to my supervisors Dr. Igor Cejpek and Prof. Günter Weickert for their help, encouraging support and great interest in my work.

I would like to thank the members of my committee for their contribution and time: Prof. L. Böhm, Prof. K.-H. Reichert, Prof. W. P. M. van Swaaij and Prof. J. G. E. Gardeniers.

My thanks belong also to Radek Matuška and Zlata Vrátníčková for providing me with GPC and ^{13}C-NMR analyzes and to Dr. Jan Grůza and Dr. Oldřich Peroutka for calculations, supplementing my experimental work.

I am grateful to Hana Navrátilová and Dr. Robert Nickol for the proofreading of my thesis draft.

Finally I want to thank my family for support and encouragements over the all years of my studies. This work is dedicated mainly to them.

Miroslav Skoumal
Brno, June 2007

ABOUT THE AUTHOR

Miroslav Skoumal was born on 3rd March, 1980 in Brno, Czech Republic (former Czechoslovakia). After his secondary education, finished in 1998, he started to study at Faculty of Chemistry at University of Technology Brno.

During his studies he was specialized on Material and Macromolecular Chemistry and in June 2003 he obtained the master degree, after the successful defence of his diploma thesis: Determination of $MgCl_2$-supported catalyst kinetics during propene polymerization at low pressure and temperature.

Since September 2003 he started his Ph.D. research at Polymer Institute Brno under the supervision of Dr. Igor Cejpek. Consequently in June 2006 he joined the research group of Professor Günter Weickert at University of Twente.